

2017

## **Modulation Of PKR Activity During HIV Infection And Cellular Stress By PACT And TRBP**

Evelyn E. Chukwurah  
*University of South Carolina*

Follow this and additional works at: <https://scholarcommons.sc.edu/etd>



Part of the [Biological Phenomena, Cell Phenomena, and Immunity Commons](#)

---

### **Recommended Citation**

Chukwurah, E. E.(2017). *Modulation Of PKR Activity During HIV Infection And Cellular Stress By PACT And TRBP*. (Doctoral dissertation). Retrieved from <https://scholarcommons.sc.edu/etd/4497>

This Open Access Dissertation is brought to you by Scholar Commons. It has been accepted for inclusion in Theses and Dissertations by an authorized administrator of Scholar Commons. For more information, please contact [digres@mailbox.sc.edu](mailto:digres@mailbox.sc.edu).

MODULATION OF PKR ACTIVITY DURING HIV INFECTION AND CELLULAR  
STRESS BY PACT AND TRBP

by

Evelyn E. Chukwurah

Bachelor of Science  
Lee University, 2010

---

Submitted in Partial Fulfillment of the Requirements

For the Degree of Doctor of Philosophy in

Biological Sciences

College of Arts and Sciences

University of South Carolina

2017

Accepted by:

Rekha Patel, Major Professor

Alan Waldman, Committee Member

Lewis Bowman, Committee Member

David Reisman, Committee Member

Wayne Carver, Committee Member

Cheryl L. Addy, Vice Provost and Dean of the Graduate School

© Copyright by Evelyn E. Chukwurah, 2017  
All Rights Reserved.

## DEDICATION

This work is dedicated to my wonderful family, without whom any of this would have been possible.

## ACKNOWLEDGEMENTS

I would like to thank my advisor, Dr. Rekha Patel, for being a wonderful mentor and friend in every way. I am eternally grateful for her guidance through the years, for her pushing me to be the best scientist and teacher I could be, for her constant encouragement, and for allowing me to try my hands at several endeavors, grow and learn from my mistakes when these didn't turn out as I expected. She has provided an excellent example to me of what I should strive to be as a scientist, a teacher, and a leader.

I would also like to extend my profound thanks to all the members of my graduate committee; Drs. Waldman, Bowman, Carver, and Reisman, who have been extremely supportive of me over the years, have provided essential feedback on all the work I have presented to them, and have lent me a listening ear on everything from science to life in general. I am truly grateful that they all agreed to walk with me on this journey a few years ago.

I am also greatly indebted to my parents and brothers for their unconditional love and support as I have navigated the ups and downs of graduate school. Every single prayer, kind thought or word, care package, call, text message, and funny video has let me know that they have been solidly behind me every step of the way, and I could not have made it very far without them. I love you all very much!

I have been very fortunate to have built a second family here during my time at USC: I was blessed to have had Ms. Mary Naganathan and Mrs. Indhira Handy as my surrogate grandmother and mother, who have in turns comforted, encouraged, supported, and celebrated with me at each milestone. They have always made me feel loved and welcome here, and it has been my privilege to know them over the years!

I have also been very lucky to have so many wonderful friends cheering me on throughout my graduate studies: Drs. Lauren Vaughn and Andy Schumpert who have been everything weird and wonderful one would expect from siblings, Samuel Burnett and Benedicth Ukhueduan who have both proved worthy distractions from no-good-very bad-terrible days and brightened my last few years in graduate school, Drs. Margaret Cirtain, George Handy, Chandrashekhar Patel, and Richard Showman who have always opened their hearts and doors to me and been shoulders to lean on in so many ways!

I would be remiss not to thank Cameron Carlson, Jerry Madukwe, and Abena Amparbeng for their friendship from our days in BIOL 302L, Lee University, and PANASA – I know that it has been my good fortune to have you all beside me on this adventure! I have always been able to trust my small army of undergraduates to help with my thousand and one experiments over the years, and know that I have learned much more from them than they have from me – Thanks Guillermo, Davide, Victoria, and Sunaina for being great students.

I am also grateful to the Graduate School and the Office of the Vice President for Research here at USC for funding from the Presidential and SPARC fellowships.

## ABSTRACT

A crucial component of the cellular response to stress is the attenuation of protein synthesis to allow the cell to dedicate resources for the restoration of homeostasis or towards the induction of apoptotic cell death in case the stressors overwhelm the cell. This process is itself regulated by one of the four eIF2 $\alpha$  kinases of which PKR (Protein Kinase R) is responsible for inhibiting general translation during viral infection, oxidative stress, ER stress, heat shock or serum withdrawal.

During viral infection, PKR is transcriptionally induced by interferon but remains latent until it interacts with dsRNA. This interaction induces a conformational change that activates PKR's catalytic activity, resulting in the phosphorylation of the eukaryotic initiation factor eIF2 $\alpha$  and the cessation of both general and viral protein synthesis. This inhibition of viral protein synthesis is however short-lived, as several viral and host cellular factors are coopted by viruses to neutralize PKR's catalytic activity against viral replication. One such cellular factor is PACT (Protein Activator of PKR), PKR's protein activator during non-viral stress, which interacts strongly with PKR during HIV infection but does not activate its catalytic activity. We investigated the mechanisms behind PACT's inability to activate PKR robustly during HIV infection. Our results show that PACT acts synergistically with the HIV trans-activator, Tat, dsRNA-containing mRNAs, as well as the adenosine deaminase, ADAR1 to form a PKR inhibitory complex to facilitate the translation of viral mRNAs during HIV infection. Most importantly, these results

elucidate a pathway that could be a target of antiviral therapy to promote PKR activation and reduce viral load in infected cells.

During non-viral stress, PKR's activity is regulated negatively by the TAR RNA Binding Protein, TRBP. TRBP regulates PKR activity by interacting with PKR as well as PACT. Stress-induced phosphorylation of PACT at Serine 287 weakens its interaction with TRBP, while increasing PACT's homomeric interactions and heteromeric interactions with PKR. The role, if any, of similar stress-induced post-translational modifications on TRBP's ability to form homomeric interactions and heteromeric interactions with PKR as well as to inhibit PKR have remained unclear. In this light, we investigated whether TRBP is subject to stress-induced phosphorylation and how that might alter TRBP-TRBP and TRBP-PKR interactions as well as TRBP's ability to inhibit PKR. Our results demonstrate that TRBP is phosphorylated by the Mitogen Activated Protein Kinases JNK and ERK in response to oxidative stress, and consequently forms strong homomeric interactions with PKR, resulting in increased inhibition of PKR and better cell recovery during oxidative stress.

PKR, PACT, and TRBP 's homomeric and heteromeric interactions are primarily mediated by the evolutionarily conserved dsRNA binding motif (dsRBM) present in all three proteins as well as in several other dsRNA binding proteins. We investigated the contributions of the two copies of dsRBMs in PACT to PACT's interactions with dsRNA, PACT, TRBP, and PKR. Our results establish that each motif contributes to a varying extent towards PACT's interaction with its known binding partners, and highlight the importance of PACT homodimerization for PKR activation.



## TABLE OF CONTENTS

DEDICATION .....	iii
ACKNOWLEDGEMENTS .....	iv
ABSTRACT .....	vi
LIST OF FIGURES .....	x
LIST OF ABBREVIATIONS .....	xii
CHAPTER 1 – INTRODUCTION .....	1
1.1 THE EIF2A KINASES: MASTER REGULATORS OF PROTEIN SYNTHESIS DURING CELLULAR STRESS .....	2
1.2 THE INTERFERON INDUCED EIF2A KINASE, PKR .....	6
1.3 REGULATION OF PKR ACTIVITY DURING VIRAL AND NON-VIRAL CELLULAR STRESS: DSRNA, HEPARIN, PACT AND TRBP .....	10
1.4 STRUCTURE OF DISSERTATION .....	28
CHAPTER 2 – ADAR1 AND PACT CONTRIBUTE TO EFFICIENT TRANSLATION OF TRANSCRIPTS CONTAINING HIV-1 TRANS-ACTIVATING RESPONSE (TAR) ELEMENT .....	34
2.1 ABSTRACT .....	35
2.2 INTRODUCTION .....	35
2.3 MATERIALS AND METHODS .....	39
2.4 RESULTS .....	45
2.5 DISCUSSION .....	55

CHAPTER 3 – STRESS-INDUCED TRBP PHOSPHORYLATION ENHANCES ITS INTERACTION WITH PKR TO ENHANCE CELLULAR SURVIVAL.....	73
3.1 ABSTRACT.....	74
3.2 INTRODUCTION .....	74
3.3 MATERIALS AND METHODS.....	77
3.4 RESULTS.....	86
3.5 DISCUSSION .....	96
CHAPTER 4 – CONTRIBUTION OF THE TWO DSRBM MOTIFS TO THE DOUBLE-STRANDED RNA BINDING AND PROTEIN INTERACTIONS OF PACT.....	111
4.1 ABSTRACT.....	112
4.2 INTRODUCTION.....	113
4.3 MATERIALS AND METHODS.....	116
4.4 RESULTS.....	121
4.5 DISCUSSION.....	125
CHAPTER 5 – GENERAL DISCUSSION.....	137
REFERENCES .....	141
APPENDIX A: REPRINT PERMISSION FROM THE BIOCHEMICAL JOURNAL (PORTLAND PRESS) .....	169
APPENDIX B: PROOF OF OPEN ACCESS PUBLICATION OF ‘ADAR1 AND PACT CONTRIBUTE TO EFFICIENT TRANSLATION OF TRANSCRIPTS CONTAINING HIV-1 TRANS-ACTIVATING RESPONSE (TAR) ELEMENT’ .....	170

## LIST OF FIGURES

Figure 1.1. Regulation of eukaryotic translation initiation by the eIF2 $\alpha$ kinases.....	31
Figure 1.2. Domain structure and activating stimuli of the four eIF2 $\alpha$ kinases .....	32
Figure 1.3. Domain structure of the dsRNA binding proteins, PKR, PACT, and TRBP .....	33
Figure 2.1. PACT activates Tat enhanced HIV-1 gene expression from an integrated LTR.....	60
Figure 2.2. PACT does not increase the steady-state mRNA levels of HIV-1 LTR-driven $\beta$ -galactosidase.....	62
Figure 2.3. PACT inhibits PKR activation induced by TAR-containing mRNAs.....	63
Figure 2.4. Tat serves a specific function in mediating inhibition of PKR.....	65
Figure 2.5. PACT and Tat are insufficient to inhibit TAR RNA-dependent PKR activation .....	67
Figure 2.6. ADAR1 is essential for an efficient inhibition of PKR.....	68
Figure 2.7. Comparison of TRBP and PACT's PKR inhibitory activity on TAR RNA.....	70
Figure 2.8. Schematic model.....	72
Figure 3.1. TRBP overexpression protects cells from arsenite-induced apoptosis .....	101
Figure 3.2. TRBP is phosphorylated by ERK and JNK in response to arsenite-induced oxidative stress .....	103
Figure 3.3. TRBP phosphorylation inhibits PKR-mediated apoptosis during cell stress.	105
Figure 3.4. The phosphorylated TRBP isoform efficiently reverses PKR's growth inhibition phenotype in yeast. ....	107

Figure 3.5. TRBP phosphorylation strengthens PKR-TRBP interaction and weakens TRBP-TRBP interaction. .... 108

Figure 3.6. A schematic model of PKR-TRBP interaction in response to oxidative stress ..... 110

Figure 4.1. Mutations in conserved amino acids in PACT’s M1 and M2 dsRNA binding motifs (dsRBMs) disrupt PACT’s interaction with dsRNA. .... 130

Figure 4.2. Mutations of specific hydrophobic residues in PACT’s M1 dsRBM disrupt PACT’s interaction with PKR. .... 132

Figure 4.3. Mutations of hydrophobic residues in PACT’s M1 dsRBM disrupt PACT-PACT homodimer interaction..... 133

Figure 4.4. Hydrophobic residue mutations in PACT’s M1 dsRBM disrupt PACT-TRBP heterodimer interaction. .... 134

Figure 4.5. PACT homodimer interaction is required for stress-induced PACT-PACT interaction and PACT-mediated apoptotic induction..... 135

## LIST OF ABBREVIATIONS

3-AT	3-amino-1,2,4-triazole
5'UTR	5' Untranslated Region
ADAR1	Adenosine Deaminase Acting on RNA 1
ATD	Amino Terminal Domain
ATF3	Activating Transcription Factor 3
ATF4	Activating Transcription Factor 4
ATP	Adenosine triphosphate
Bip/Grp78	Binding Immunoglobulin Protein/78 kDa Glucose-Regulated Protein
CAD	Caspase-Activated DNase
CHOP	C/EBP Homologous Protein
CHO	Chinese Hamster Ovary cells
CMV	Cytomegalovirus
CTD	Carboxyl Terminal Domain
DAPI	4,6-Diamidino-2-Phenylindole
DMEM	Dulbecco's Modified Eagle Medium
dsRBD	double-stranded RNA Binding Domain
dsRBM	double-stranded RNA Binding Motif
dsRNA	double-stranded RNA
DTT	Dithiothreitol
EDTA	Ethylenediaminetetraacetic acid

EGFP ..... Enhanced Green Fluorescent Protein

eIF2.....Eukaryotic Initiation Factor 2

eIF2 $\alpha$  ..... Eukaryotic Initiation Factor  $\alpha$  subunit

eIF2B .....eIF2 Guanine Nucleotide Exchange Factor 2B

ER .....Endoplasmic Reticulum

ERK ..... Extracellular signal–Regulated Kinase

GADD34.....Growth Arrest and DNA Damage-inducible Protein 34

GCN2 ..... General Control Non-Derepressible 2

GDP ..... Guanosine diphosphate

GEF ..... Guanine nucleotide Exchange Factor

GFP .....Green Fluorescent Protein

GTP ..... Guanosine triphosphate

HisRS..... Histidyl tRNA Synthetase

HIV-1 ..... Human Immunodeficiency Virus-Type 1

HRI.....Heme Regulated Inhibitor

IFN ..... Interferon

IL-3..... Interleukin 3

IRF1 ..... Interferon Regulatory Factor 1

IRF3 ..... Interferon Regulatory Factor 3

IRF7 ..... Interferon Regulatory Factor 7

ISG ..... Interferon Stimulated Gene

ISR..... Integrated Stress Response

JNK..... c-Jun N-terminal Kinase

K271R mPKR..... Dominant negative murine PKR mutant

K296R PKR ..... Dominant negative PKR mutant  
 KD ..... Kinase Domain  
 KO ..... Knockout  
 LTR ..... Long Terminal Repeat  
 MAPK ..... Mitogen Activated Protein Kinase  
 miRNA ..... micro RNA  
 MDA5 ..... Melanoma Differentiation-Associated protein 5  
 MEFs ..... Mouse Embryonic Fibroblasts  
 NDV ..... Newcastle Disease Virus  
 NF $\kappa$ B ..... Nuclear Factor kappa B  
 PACT ..... Protein Activator of PKR  
 PAMPs ..... Pathogen Associated Molecular Patterns  
 PARP1 ..... Poly-ADP Ribose Polymerase 1  
 PBM ..... PACT Binding Motif  
 PBMCs ..... Peripheral Blood Mononuclear Cells  
 PERK ..... PKR-like ER Resident Kinase  
 PIC ..... Pre-Initiation Complex  
 PKR ..... Protein Kinase R  
 PMSF ..... Phenylmethylsulfonyl fluoride  
 PP1 ..... Protein Phosphatase 1  
 Prbp ..... Protamine RNA Binding Protein  
*Prkra* ..... Protein kinase, interferon-inducible double stranded RNA dependent activator  
 PRR ..... Pathogen Recognition Receptors  
 RASMC ..... Rat primary aortic vascular smooth muscle cells

RAX ..... PKR associated protein X  
 RISC ..... RNA Induced Silencing Complex  
 RIG-I..... Retinoic acid-Inducible Gene 1  
 RLR .....RIG-I Like Receptor  
 RWD ..... RING finger and WD repeat  
 siRNA .....small interfering RNA  
 ssDNA ..... single-stranded DNA  
 TALEN ..... Transcription Activator-Like Effector Nuclease  
 TAR RNA ..... Trans-Activation Recognition Element RNA  
 TRBP ..... TAR RNA Binding Protein  
 uORF ..... Upstream Open Reading Frame  
 UPR..... Unfolded Protein Response  
 VAI ..... Adenovirus-associated RNA I  
 VSMC.....Vascular Smooth Muscular Cells  
 VSV ..... Vesicular Stomatitis Virus  
 WT ..... Wild type  
 Xlrbpa ..... *Xenopus laevis* RNA-Binding Protein A  
 YPD .....Yeast Peptone Dextrose media



## CHAPTER 1

### INTRODUCTION<sup>1</sup>

---

<sup>1</sup>To be adapted into a comprehensive review titled: 'The double-stranded RNA binding proteins PACT, PKR, and TRBP – diverse roles in cellular stress, innate immunity, and RNA interference' Chukwurah, E., and Patel RC. *Manuscript in preparation.*

## 1.1 THE EIF2A KINASES: MASTER REGULATORS OF PROTEIN SYNTHESIS DURING CELLULAR STRESS

Eukaryotic cells encounter a diverse array of stressful conditions and must respond in each situation such that the cells ensure their survival while limiting the deleterious effects of the stressor. These stressful conditions, which range from viral infection to the accumulation of misfolded proteins in the cell's endoplasmic reticulum (ER), elicit a coordinated response in eukaryotic cells termed the Integrated Stress Response (ISR)<sup>1</sup>.

The focal point of the ISR, which is an evolutionarily conserved signaling pathway induced in response to various stress signals, rests on the attenuation of general protein synthesis and the preferential translation of mRNA transcripts encoding proteins essential for ameliorating the stressful conditions<sup>2,3</sup>. The ISR is also responsible for inducing apoptosis if the stressful conditions overwhelm the cell. The entire stress response pathway is initiated by the phosphorylation of the  $\alpha$ -subunit of the eukaryotic initiation factor (eIF2) by one of four dedicated eIF2 $\alpha$  kinases<sup>4-8</sup>.

During the initiation of protein synthesis, eIF2 forms a ternary complex with GTP and the methionyl charged initiator tRNA (Met-tRNA<sub>i</sub>). The ternary complex subsequently associates with the 40S small ribosomal subunit and other initiation factors to form the 43S pre-initiation complex (PIC). The 5'm<sup>7</sup>-G-cap binding initiation factor complex eIF4F facilitates the interaction of the mRNA transcript with the newly formed PIC, and the PIC scans the 5'UTR of the mRNA transcript until it encounters the AUG start codon. At this point, the 60S large ribosomal subunit associates with the

mRNA transcript and the PIC to initiate the translation of the mRNA transcript. This results in the hydrolysis of the eIF2-bound GTP to GDP, and the release of eIF2-GDP from the ribosome so another round of protein translation can commence <sup>1</sup>.

The eIF2 $\alpha$  kinases effectively inhibit protein synthesis by phosphorylating eIF2's  $\alpha$  subunit (eIF2 $\alpha$ ). The eIF2 protein consists of three subunits, eIF2 $\alpha$ , - $\beta$ , and - $\gamma$ . Active eIF2 has a non-phosphorylated eIF2 $\alpha$  and low affinity to the guanine nucleotide exchange factor eIF2B. In that state, eIF2B exchanges GDP to GTP from the eIF2 $\gamma$  subunit, ensuring its active state. Non-phosphorylated eIF2 $\alpha$ , eIF2 $\beta$ , GTP-loaded eIF2 $\gamma$ , methionyl tRNA (Met-tRNA<sub>i</sub>), and eIF5 form the ternary complex. Upon start site recognition, eIF2 and eIF5 dissociate from the complex and translation initiation and elongation ensue. eIF2 $\alpha$  phosphorylation at Serine 51 increases its affinity for eIF2B and eIF5<sup>9</sup>, thereby reducing the guanine nucleotide exchange factor that slows down the formation of the ternary complex, resulting in the attenuation of protein translation initiation (Figure 1.1.) The decreased abundance of the ternary complex consisting of eIF2, GTP, and the methionyl-charged initiator tRNA leads to the preferential translation of mRNAs encoding stress-responsive proteins i.e. the transcription factors ATF4 <sup>10</sup> and CHOP<sup>11,12</sup>, and protein phosphatase regulatory subunit GADD34 <sup>13</sup> due to alterations in translation initiation at multiple upstream open reading frames (uORFs) in the 5' untranslated region (5' UTR) of these mRNAs.

These transcription factors stimulate the expression of proteins which include chaperones, antioxidant proteins, or proapoptotic proteins among others to ensure cellular recovery or induce apoptosis if stress signals are sustained<sup>14-17</sup>. The GADD34

protein interacts with the catalytic subunit of protein phosphatase 1 (PP1) to trigger eIF2 $\alpha$  dephosphorylation and promote ISR termination<sup>13</sup>. The duration and extent of the stress response is regulated by several feedback mechanisms. For instance, ATF4 regulates the transcription of GADD34, which is essential for translational recovery towards survival, and of CHOP<sup>18</sup>, whose accumulation plays a pivotal role in converting the stress response from an adaptive phase to apoptosis when the ISR is overwhelmed. Many laboratories over several years have characterized each of the four eIF2 $\alpha$  kinases and the specific stress signals that lead to their activation and consequent inhibition of general protein synthesis<sup>3</sup>. The specificity of activation of each kinase in response to stress signals is conferred by the presence of varied regulatory domains flanking a common homologous kinase domains. These regulatory domains mediate the kinases' homodimerization, autophosphorylation, activation and eventual phosphorylation of eIF2 $\alpha$  (Figure 1.2.)

General control nonderepressible 2 (GCN2), which has the distinction of being the only eIF2 $\alpha$  kinase conserved in almost all eukaryotes, is activated during amino acid deprivation, and contains, in addition to its kinase domain, regulatory domains consisting of RING finger and WD repeat (RWD), pseudokinase, histidyl tRNA synthetase-like (HisRS-like), and dimerization/ribosome binding domains. These domains together mediate the interaction between GCN2 and uncharged tRNAs, resulting in GCN2 homodimerization, trans-autophosphorylation and eIF2 $\alpha$  phosphorylation<sup>19,7,20,21</sup>.

The PKR-like ER resident kinase (PERK) is activated in response to the accumulation of misfolded proteins in the endoplasmic reticulum (ER) and is essential component of the Unfolded Protein Response (UPR)<sup>22,23</sup>. In line with this function as a sensor of ER stress, PERK contains an ER luminal domain that associates with the ER-resident chaperone Bip/Grp78<sup>24</sup>. Increased association of misfolded proteins with Bip during ER stress causes its dissociation from PERK's luminal domain and results in the dimerization and activation of PERK's C-terminal cytoplasmic kinase domain, and inhibition of protein synthesis.

The Heme Regulated Inhibitor (HRI) kinase is responsive to the presence of heme, which is essential to globin synthesis in erythroid cells. HRI possesses two heme-binding sites; the first of which is in HRI's N-terminus, and the second inserted within HRI's kinase domain. This second heme binding is essential to ensure HRI's activation in response to heme deficiency, as the reversible binding of heme to this site when heme is abundant within the cell prevents HRI activation, resulting in eIF2 $\alpha$  phosphorylation and the cessation of globin synthesis<sup>6,25,26</sup>.

Protein Kinase R (PKR) is the primary eIF2 $\alpha$  kinase activated in response to viral infection in the cell. To that effect, PKR contains evolutionarily conserved double-stranded RNA binding motifs (dsRBMs) which mediate its interactions, not only with dsRNA generated during viral infection, but also with other dsRBM containing proteins. PKR is also activated in response to non-viral cellular stress which includes stress resulting from the accumulation of misfolded proteins in the ER, reactive oxygen species (oxidative stress), heat shock, and serum deprivation. Additionally, various studies have

shown that PKR is also important for the optimal activation of transcription factors in key cellular signaling pathways such as ATF3<sup>27</sup>, IRF1<sup>28</sup>, NF- $\kappa$ B<sup>29,30</sup>, and p53<sup>31</sup> among others<sup>32</sup>.

As such, PKR and PKR-mediated signaling pathways have been implicated in several cellular processes such as mitotic regulation and inflammation through NF- $\kappa$ B signaling and in human pathological conditions ranging from diabetes to several neurological and neurodegenerative diseases<sup>33,34</sup>.

In this chapter, we describe PKR's structure and the mechanisms by which it is activated during viral and non-viral stress through its interaction with dsRNA and the stress-regulated protein, PACT. We also describe the importance of protein-protein interactions and stress-induced post-translational modifications of PACT as well as the dsRNA binding protein, TRBP, in activating or inhibiting PKR's activity during cellular stress.

## 1.2 THE INTERFERON INDUCED EIF2A KINASE, PKR

Cells employ both cytoplasmic and cell-surface pathogen-recognition receptors to recognize a wide range of pathogens and their molecular products. The association of these Pathogen associated molecular patterns (PAMPs)<sup>35,36</sup> with their cognate receptors induces the secretion of cytokines known as interferons (IFNs)<sup>37,38</sup> which bind to receptors on the target cell to induce the expression of genes termed Interferon Stimulated Genes (ISGs). These ISGs encode proteins with potent antiviral activity targeting several aspects of viral replication in host cells<sup>39,40</sup>.

Separate groups of researchers independently observed that synthesis of both host and viral proteins in IFN-treated reovirus<sup>41</sup>, or encephalomyocarditis virus<sup>42</sup> infected cells as well as in IFN and dsRNA-treated cells were significantly diminished. These observations added inhibition of protein synthesis to the growing list of IFN-induced antiviral activities, and raised questions about the identity of the specific IFN-induced translational inhibitor. Previous studies performed with HRI, then a recently characterized eIF2 $\alpha$  kinase in rabbit reticulocytes, led researchers to believe that this IFN-induced factor was an eIF2 $\alpha$  kinase particularly sensitive to the presence of dsRNA<sup>19</sup>.

Autoradiographs of  $\gamma$ -<sup>32</sup>P ATP labelled proteins from dsRNA and IFN treated cells showed bands at ~67 kDa and ~35 kDa respectively that increased in intensity with increasing dsRNA concentrations indicative of protein phosphorylation. Further experiments confirmed that the increased intensities of the 67 kDa (PKR) and 35 kDa (eIF2 $\alpha$ ) bands were due to increased PKR autophosphorylation and subsequent eIF2 $\alpha$  phosphorylation, while northern and western blot analyses showed steady increases in PKR mRNA transcript and protein levels with IFN- $\alpha$  exposure<sup>43</sup>. These findings demonstrated that PKR is the IFN-induced eIF2 $\alpha$  kinase responsible for the inhibition of viral mRNA translation.

### 1.2.1 PKR's DOMAIN STRUCTURE: DSRNA BINDING MOTIFS AND EIF2 ALPHA KINASE DOMAIN

PKR, like the other eIF2 $\alpha$  kinases, is a serine-threonine kinase responsible for phosphorylating eIF2 $\alpha$  on Serine 51. A direct comparison of PKR's 551 amino acid sequence with those of other eIF2 $\alpha$  kinases as seen in Figure 1.2 places PKR's kinase catalytic domain at its C-terminus (residues 165 – 551). This was confirmed by experiments using a mutant PKR protein in which the C-terminus had been deleted; while the expression of full length PKR in *Saccharomyces cerevisiae* induced an inhibitory growth phenotype, the mutant protein was unable to produce a similar effect on the yeast cells' growth. This mutant protein also retained its dsRNA binding properties, indicating that PKR's regulatory dsRNA binding domain was located at its N terminus (residues 1-64).

Further characterization of PKR's N-terminal dsRNAs binding domain (dsRBD) indicated that this domain was comprised of two tandem dsRNA binding motifs; dsRBM1 (residues 10 -72) and dsRBM2 (residues 100 -165), separated by a flexible 20-amino acid long linker sequence<sup>44</sup>. Like dsRBMs in other dsRNA binding proteins, PKR's dsRBMs have been shown to possess an  $\alpha$ - $\beta$ - $\beta$ - $\beta$ - $\alpha$  fold with the  $\alpha$ -helices lying on one face of a three-stranded antiparallel  $\beta$ -sheet.

These  $\alpha$ -helices are amphipathic in nature as they are primarily made up of basic and hydrophobic residues on opposite sides of the helices. Some of the basic amino acids in these helices were shown to be important for dsRNA binding, as targeted mutations of several of those residues (K60, K61, K64, and K69) were shown to disrupt PKR binding to



dsRNA through a poly I:C agarose binding assay, with some mutations directly affecting PKR activation<sup>45-47</sup>. Together with the random coiled 20-amino acid linker, these basic amino acid residues have been proposed to wrap around the target dsRNA and establish essential electrostatic interactions with the 2'-OH groups and negatively charged phosphate backbone of the dsRNA to ensure optimal PKR-dsRNA binding, resulting in efficient PKR activation<sup>48</sup>.

The amphipathic  $\alpha$ -helical structures in PKR and other proteins have been shown to play key roles in the proteins' dimerization, and accordingly mediate PKR's dimerization through mutational analysis. Mutations of hydrophobic residues in PACT's  $\alpha$ -helices necessary for PKR dimerization destroyed PKR's ability to phosphorylate eIF2 $\alpha$  and inhibit yeast growth, demonstrating that PKR dimerization is important for PKR's full enzymatic activity<sup>49</sup>.

On the other hand, structural analysis of PKR's C-terminal kinase domain showed that it consisted of an ATP binding pocket flanked on either side by an N-terminal and C-terminal lobe. Mechanistic studies of dsRNA-PKR binding show that dsRNA binding to PKR induces a conformational change in PKR that exposes the ATP binding pocket such that PKR can trans-autophosphorylate itself<sup>50,51</sup>, become activated and then phosphorylate eIF2 $\alpha$  on Serine 51.

## 1.3 REGULATION OF PKR ACTIVITY DURING VIRAL AND NON-VIRAL CELLULAR STRESS: DSRNA, HEPARIN, PACT AND TRBP

### 1.3.1 PKR ACTIVATION BY DSRNA AND HEPARIN

dsRNA remained the most well-characterized and recognized PKR activator until studies demonstrating PKR activation in response to other cellular conditions without dsRNA spurred the search for other cellular PKR activators. Due to the nature of PKR's interaction with polyanionic dsRNA, researchers used *in vitro* kinase activity assays to test the ability of other polyanionic molecules such as dextran sulfate and chondroitin sulfate to activate PKR in the absence of dsRNA<sup>52</sup>. All the compounds that were tested induced PKR activation, but the highest PKR activity was observed when the assay was performed using the polyanionic glycosaminoglycan, heparin<sup>46,52,53</sup>. Heparin is a polysaccharide synthesized and secreted by mast cells and basophils and made up of alternating sulfated glucosamine with glucuronic or sulfated iduronic acid units.

Based on previous findings that showed strong PKR activation by heparin *in vitro*, researchers investigated heparin's ability to activate PKR *in vivo* and the effects of this event on VSMC proliferation<sup>54</sup>. They found a significant increase in PKR activation in heparin-treated VSMCs correlative with increased PKR-heparin interaction, and noted that the absence of PKR, observed with cell cycle analysis of PKR null (PKR<sup>-/-</sup>) and wild type (PKR<sup>+/+</sup>) MEFs, was sufficient to negate the anti-proliferative effects of heparin treatment<sup>54</sup>. These results were recapitulated in rat primary aortic vascular smooth muscle cells (RASMCs) transfected with the dominant negative PKR mutant, K296R PKR,

where inhibition of PKR partially rescued the G1-to-S transition block<sup>55</sup>. Taken together, these results established PKR as a key effector of heparin's anti-proliferative activity.

Based on the comparable properties of heparin and dsRNA, it was expected that the mechanism by which heparin induced PKR activation would also involve interaction with PKR's N-terminal dsRBMs. Intriguingly, researchers observed that *in vitro* kinase assays performed with N-terminal PKR deletion mutants and wt PKR showed comparable levels of PKR autophosphorylation and eIF2 $\alpha$  phosphorylation with heparin<sup>56</sup>. Later work also demonstrated that pre-incubation of PKR with heparin blocked subsequent PKR activation by dsRNA and heparin did not out-compete the adenovirus VAI dsRNA for binding to PKR<sup>57</sup>. All these findings suggested that heparin associated with PKR at a different site than the expected dsRBD, and conformational changes induced by heparin precluded the activation of PKR's kinase activity by dsRNA interaction with PKR's dsRBD. More importantly, these findings clearly indicated that heparin induces PKR activation by an alternative mechanism involving heparin's interaction with PKR's C-terminal kinase domain.

Deletion mapping of PKR's heparin interaction domains showed that two regions designated ATD (residues 279 - 318) and CTD (412 - 479) within PKR's C-terminal kinase domain were crucial to heparin-PKR interaction and heparin-induced PKR activation<sup>56</sup>. Further characterization of the heparin interacting domains revealed the presence of a positively charged binding cleft conducive to heparin binding<sup>57</sup>, and provided evidence for a mechanism of PKR activation in which heparin associates with PKR monomers and induces a conformational change to facilitate dimerization and PKR activation.

### 1.3.2 PKR ACTIVATION BY PACT

The specific circumstances required for PKR's activation by heparin led researchers to continue to search for other cellular activators that could account for PKR activation in other non-viral cellular contexts.

PACT (Protein Activator of PKR), a 313-amino acid long protein, was identified as a PKR interacting protein in a yeast two-hybrid screen of a human cDNA library using the trans-dominant negative PKR mutant K296R as bait<sup>58</sup>. A murine PACT homolog, RAX (PKR-associated protein X), was also similarly identified in a mouse cDNA library screen using the catalytically inactive murine PKR homolog (K271R mPKR) as bait<sup>59</sup>.

A comparison of PACT/RAX's amino acid sequence to that of PKR and other dsRNA binding proteins showed that PACT also contained three evolutionarily conserved dsRBMs (Figure 1.3)

PACT's first two dsRBMs showed the strongest sequence conservation to PKR's N-terminal dsRBD and the first two dsRBMs found in TRBP (TAR RNA Binding Protein), TRBP's murine homolog Prbp (Protamine RNA-binding Protein) and the *Xenopus* dsRBP Xlrpba (*Xenopus laevis* RNA-binding Protein A). PACT/RAX's ability to recognize and bind dsRNA were independently confirmed through dsRNA binding assays that showed their preferential binding to synthetic dsRNA (poly I:C) over dsDNA or ssDNA<sup>58,59</sup>.

To determine the functional importance of PACT's interaction with PKR for PKR's catalytic activity, investigators performed *in vitro* PKR activity assays using purified recombinant PACT and immunoprecipitated PKR. Similar to results obtained with previously characterized PKR activators, the addition of increasing amounts of PACT

resulted in a corresponding increase in PKR's kinase activity, after which higher PACT concentrations resulted in PKR inhibition<sup>58</sup>.

Further evidence that PACT could efficiently activate PKR in the absence of dsRNA was provided by *in vitro* kinase assays performed with recombinant PACT purified to remove associated dsRNA and *in vivo* yeast growth inhibition assays<sup>58</sup>. In the former set of experiments, the results demonstrated that PACT strongly activated PKR in the absence of dsRNA and could even activate PKR point mutants defective in activation by dsRNA (K150A PKR, and A158D PKR), indicating that PKR association with dsRNA was inconsequential to PACT-mediated PKR activation.

The latter set of experiments supported results from the first set of experiments, as investigators observed a marked reduction of yeast growth in cells co-expressing PACT and wt PKR. Like the previous results, PACT was still able to enhance PKR-mediated yeast growth inhibition in yeast cells expressing the dsRNA-binding defective PKR point mutants, showing that this activation was independent of dsRNA binding. The results from these experiments showed that PACT retained its ability to strongly activate PKR in the absence of dsRNA or PKR's dsRNA binding ability, establishing PACT as a PKR-interacting protein that could activate PKR in response to non-viral cell stress. Considering the evidence pointing towards PACT as a potential cellular activator of PKR, it became necessary to identify the specific cellular conditions that required PACT for efficient PKR activation *in vivo*, as well as the domains of PACT necessary for mediating its interaction with PKR and PKR's consequent activation.

*PACT ACTIVATION OF PKR DURING NON-VIRAL CELLULAR STRESS: DSRBM-MEDIATED INTERACTIONS AND REQUIREMENT OF STRESS-INDUCED PACT PHOSPHORYLATION FOR EFFICIENT PKR ACTIVATION.*

To investigate PACT's role in enhancing PKR activation *in vivo*, mammalian cells were transiently transfected with PACT and subsequently assessed for changes in translation, PKR autophosphorylation, and eIF2 $\alpha$  phosphorylation. Results indicated that PACT overexpression significantly enhanced PKR activation and consequently eIF2 $\alpha$  phosphorylation, resulting in a ~2-fold increase in protein translation inhibition compared to cells expressing an empty vector<sup>58</sup>. Cells overexpressing PACT/RAX also demonstrated an increased sensitivity to cellular stress and apoptosis<sup>59,60</sup> resulting from serum starvation, exposure to hydrogen peroxide, sodium arsenite and inflammatory cytokines<sup>59-61</sup>. In contrast, PACT overexpression in PKR<sup>-/-</sup> MEFs had a marginal effect on stress-induced apoptosis<sup>60</sup>, indicating that PACT primarily exerted its effects on PKR in response to stressful cellular conditions.

These results were recapitulated in PACT<sup>-/-</sup> and PKR<sup>-/-</sup> MEFs treated with tunicamycin, a reagent which induces the unfolded protein response and ER stress in cells by inhibiting N-linked glycosylation of nascent proteins<sup>62</sup>. Reconstitution of PACT or PKR restored tunicamycin-induced apoptosis, eIF2 $\alpha$  phosphorylation, as well as downstream induction of CHOP expression, implicating PACT in PKR's response to ER stress<sup>62</sup>. Taken together, these findings provided conclusive evidence that PACT is responsible for the efficient activation of PKR in response to a diverse range of non-viral cellular stressors.

## *PACT INTERACTION WITH PKR – DSRNA BINDING MOTIF MEDIATED INTERACTIONS*

Co-immunoprecipitation assays with *in vitro* synthesized PACT and PKR or PKR's N-terminal dsRNA binding domain showed that PACT directly interacted with PKR, and specifically with PKR's dsRBD, as no direct interaction was observed between PKR's C-terminal kinase domain and PACT<sup>58</sup>.

With noted similarities between two of PACT's dsRBMs and PKR's own dsRBMs, experiments were performed to determine which of PACT's three dsRBMs were absolute requirements for PKR interaction and activation were by successively deleting each PACT dsRNA binding motif. Co-immunoprecipitation assays with full length PKR and the various PACT deletion mutants demonstrated that while each individual motif was unable to co-immunoprecipitate PKR, the PACT mutant lacking the M3 motif retained PACT's ability to interact with PKR<sup>63,64</sup>, demonstrating that PACT's M1 and M2 cooperated with each other to ensure PACT's interaction with PKR.

Having determined that PACT's interaction with PKR is primarily mediated by the M1 and M2 motifs, *in vitro* translation inhibition assays and apoptosis assays in cells transfected with the PACT deletion mutants were subsequently performed to characterize the contribution of each motif to PKR activation. While the PACT deletion mutants lacking the M1 and M2 motifs showed similar levels of enhanced PKR-mediated translation inhibition of a luciferase reporter and induction of apoptosis, removal of PACT's M3 motif completely abolished both effects. *In vitro* kinase assays performed with these mutants showed also that the M3 motif alone induced PKR activation strongly, which the other two motifs were unable to do. However, when cells were

transfected with a PACT M3 deletion expression construct, this PACT mutant was unable to activate PKR *in vivo*, suggesting that while the M3 motif is essential for PACT's activation, the M1 and M2 motifs contribute *in vivo* to PACT's ability to activate PKR<sup>63</sup>.

This suggestion was borne out by independent experiments performed with chimeric proteins consisting of PACT's M3 motif and PKR's dsRBD or TRBP's two dsRNA binding motifs<sup>65</sup>. While both proteins' dsRBDs had previously been shown to inhibit PKR activity, the addition of PACT's M3 motif to each domain led to PKR activation, indicating that the M3 motif confers PKR activation abilities to PACT and PACT-PKR heterodimerization conferred by PACT's first two dsRBMs is important to ensure PACT's activation of PKR *in vivo*.

Interestingly, while *in vivo* co-immunoprecipitation assays showed strong interaction between PACT/RAX and PKR in stressed cells, the interaction between PACT and PKR is markedly reduced although not completely absent. This indicated that specific stress-induced changes such as posttranslational modifications may be responsible for the stronger *in vivo* interactions.

#### *ROLE OF STRESS-INDUCED PACT PHOSPHORYLATION IN EFFICIENT PKR ACTIVATION DURING NON-VIRAL CELLULAR STRESS*

Initial insights into the regulation of PKR activity via stress-induced PACT phosphorylation were provided by two different studies; in the first study, the authors observed a stress-dependent rapid enhancement of RAX-PKR interaction that correlated with an increase in eIF2 $\alpha$  phosphorylation in IL-3 dependent cells deprived of IL-3 or



treated with thapsigargin, sodium arsenite, or hydrogen peroxide<sup>59</sup>. Anti-RAX immunoblotting performed after isoelectric focusing of protein extracts from the examined cells revealed the presence of a banding pattern consistent with stress-induced RAX phosphorylation<sup>59</sup>. In the second study, investigators exposed cells to sodium arsenite or hydrogen peroxide to activate PKR, and observed a similar stress-dependent increase in PACT-PKR association over the course of treatment<sup>60</sup>. *In vivo* <sup>32</sup>P-orthophosphate labeling of PACT in the treated cells also showed that the observed increase in PACT-PKR interaction coincided with increased PACT phosphorylation<sup>60</sup>. Interestingly, both studies demonstrated that PACT/RAX phosphorylation preceded eIF2 $\alpha$  phosphorylation in response to cellular stress induced by IL-3 deprivation or treatment with hydrogen peroxide, sodium arsenite or thapsigargin. These results led both sets of investigators to conclude that stress-induced PACT/RAX phosphorylation increased the interaction between PACT and PKR to enhance PKR activation and consequently PKR-mediated eIF2 $\alpha$  phosphorylation in response to non-viral cellular stress.

Given that PACT's M3 motif had been demonstrated to be crucial for PKR activation and increased PACT-PKR heterodimerization and PKR activation is always accompanied by stress-induced phosphorylation of PACT, Li and colleagues set about identifying candidate serine residues in PACT's M3 motif that could be phosphorylated in response to stress<sup>66</sup>. Alanine-scanning mutagenesis identified four of these residues (S246, S265, S279, S287) of which two (S246, S287) were unable to induce PKR activation and consequently apoptosis. Substitution of threonine or aspartic acid for

alanine in the S246A and S287A mutants restored their ability to induce apoptosis in transfected cells and activate as well as bind PKR.

Results from further biochemical analysis of purified PACT from stress and unstressed cells revealed the presence of three differentially phosphorylated PACT isoforms. Researchers observed that PACT was either unphosphorylated or partially phosphorylated when purified from unstressed cells, and exposure of these cells to stress resulted in a significant increase in a fully phosphorylated PACT isoform.

Intriguingly, the researchers also observed that the S246A PACT mutant exhibited only the unphosphorylated PACT isoform while the S287A PACT mutant exhibited both the unphosphorylated and partially phosphorylated PACT isoforms before and after stress. These results established that PACT is constitutively phosphorylated at S246 in the absence of stress, and becomes phosphorylated at S287 in response to stress signals leading to the observed increased interaction between PACT and PKR and subsequent PKR activation.

#### *ROLE OF PACT HOMODIMERISATION IN EFFICIENT PKR ACTIVATION DURING NON-VIRAL CELLULAR STRESS*

Since PKR dimerization had already been shown to be important to PKR activation, it was unclear as to whether PACT's ability to activate PKR was equally dependent on its ability to dimerize, and if stress-induced PACT phosphorylation had any role in inducing this dimerization. Yeast two-hybrid assays were subsequently performed to identify the PACT motifs required for PACT-PACT dimerization, and results

showed that while PACT's M1 and M2 motifs could interact with each other (M1-M1, M1-M2, M2-M2), PACT's M3 motif was only able to interact with itself (M3-M3). As PACT's M3 motif had already been shown to contain two phosphorylation sites (S246, S287) crucial to PACT's activation of PKR, the specificity of the M3-M3 motif interaction strongly suggested that M3-M3 motif interaction could be enhanced during stress to enhance PACT-PACT interaction and consequently, PACT-PKR interaction and PKR activation. Increased homomeric PACT-PACT interactions in response to stress signals were supported by yeast two-hybrid experiments with phosphorylation-mimetic (PACT S246 S287D) and phosphorylation-defective (S246A S287D) PACT point mutants<sup>67</sup>.

The importance of the observed PACT homodimer formation in PACT-mediated PKR activation in response to stress was clearly demonstrated in experiments with a dimerization-deficient PACT mutant (L99E PACT) which retained its ability to interact with PKR. While wt PACT, dsRNA, and heparin robustly activated PKR, L99E PACT was unable to activate PKR efficiently, indicating that PACT dimerization was necessary for efficient PACT-mediated PKR activation<sup>68</sup>.

While the studies with PACT phosphorylation-defective and mimetic mutants underscored the importance of stress induced PACT-PACT and PACT-PKR interaction and reduced PACT-TRBP mediated through residues in PACT's M3 motif, the individual contributions of PACT's M1 and M2 motifs to PACT's ability to interact with dsRNA as well as with itself, PKR and TRBP have remained unclear and have been elucidated in Chapter 4 of my dissertation.

## *PACT AND PKR DURING VIRAL INFECTION*

In addition to its established role in the PKR-mediated stress response pathway, PACT has also been shown to be involved in a steadily increasing number of key cellular pathways, such as small RNA biogenesis<sup>69-72</sup> during RNA interference via interaction with the Dicer protein and the cellular innate immune response to viral infection via interaction with pattern recognition receptors RIG-I and MDA-5<sup>73,74</sup>.

A possible antiviral function for PACT was first presented in a study in which siRNA PACT/RAX-depleted MEFs were infected with vesicular stomatitis virus (VSV). These VSV-infected cells exhibited significantly increased viral titers and viral protein synthesis as well as decreased eIF2 $\alpha$  phosphorylation levels compared to the wildtype cells<sup>61</sup>. These results suggested then that in addition to its role as a PKR activator during non-viral stress, PACT could also enhance PKR's antiviral activity or possess an inherent antiviral function independent of PKR activation. A subsequent study involving L929 cells infected with the Newcastle disease virus (NDV) demonstrated that PACT expression could in fact stimulate IRF3 and IRF7 activity in these cells in a PKR independent manner, resulting in IFN- $\beta$  expression and increased IFN- $\beta$  enhancer reporter activity<sup>75</sup>. PACT was also shown to be directly involved in enhancing the RLR-mediated response to viral infection by interacting directly with the cytoplasmic RNA sensor, RIG-I, during Sendai virus infection<sup>73</sup>. PACT's interaction with RIG-I's CTD stimulated RIG-I's ATPase activity and facilitated the production of IFN in the Sendai-virus infected cells as indicated by decreased viral plaque formation with PACT and RIG-I co-expression<sup>73</sup>.

As a well-characterized activator of PKR in response to cellular stress, it was interesting to study PACT's ability to activate PKR during HIV infection. A 2013 study of PACT's role during HIV infection revealed a significant increase in PACT-PKR interaction as well as between PACT, PKR, and another dsRNA binding protein, ADAR1, coincidental with a decrease in PKR activity over the course of viral infection<sup>76</sup>. An ISG product, ADAR1 (Adenosine Deaminase Acting on RNA 1) is an RNA-editing enzyme that catalyzes the deamination of adenosine to inosine in dsRNA substrates, which in turn leads to the destabilization of RNA secondary structure or the erroneous incorporation of amino acids detrimental to viral protein structure and function<sup>77</sup>. Thus, ADAR1 can work in an anti-viral manner, but HIV specifically seemed to target ADAR1 to inactivate its anti-viral functions and replicate efficiently<sup>78</sup>. siRNA mediated knockdown of either PACT or ADAR1 in HIV infected cells was sufficient to restore PKR-mediated viral replication inhibition, suggesting that both proteins act synergistically to enhance viral replication, and more importantly, it was suggested that PACT could in fact inhibit PKR's activity in HIV-infected cells<sup>76</sup>. Questions however remained from this study about the mechanisms underlying this dramatic change in PACT's ability to activate PKR. Chapter 2 of my dissertation aims to fill this gap and elucidates the mechanism of ADAR1 – mediated inactivation of PACT-induced PKR activation during HIV replication<sup>79</sup>.

### 1.3.2 PKR INHIBITION BY TRBP

As a key effector of IFN's antiviral activities, PKR is the target of several viral strategies to limit its inhibition of viral protein synthesis in infected cells. While many of

these strategies rely on viral factors that may sequester potentially PKR-activating dsRNAs<sup>80,81</sup>, act as decoy substrates<sup>80,82</sup>, or directly interact with PKR<sup>83</sup>, some strategies involve the recruitment of cellular host proteins to enhance viral replication, transcription, and translation by inhibiting PKR<sup>84–86</sup>.

One such protein is the TAR RNA Binding Protein (TRBP) which was initially identified as a HIV TAR RNA binding protein in a HeLa cDNA expression library screen with a TAR RNA probe<sup>87</sup>. TRBP was subsequently shown to enhance the expression of reporter genes driven by the HIV-1 LTR, as well as the translation of TAR RNA containing mRNAs by destabilizing the secondary structure of the dsRNA to allow for greater translation efficiency. These findings, together with the observation that knockdown of TRBP expression resulted in dramatically decreased HIV-1 LTR driven gene expression and viral protein production during active HIV-1 replication<sup>88</sup> and viral replication in astrocytes which express low levels of TRBP was markedly limited<sup>89</sup>, confirmed that TRBP is indeed a cellular protein co-opted by the HIV-1 virus to ensure its replication.

TRBP has also been shown to be involved in miRNA biogenesis and RNA induced silencing through its interaction with Dicer and the RNA induced silencing complex (RISC)<sup>90,91</sup>. Mass spectrometric analysis of proteins coimmunoprecipitated with human Dicer showed an interaction with TRBP, which was also independent of the presence of dsRNA<sup>90</sup>. While the initial studies characterizing TRBP's interaction with Dicer and functional importance to miRNA processing showed that TRBP depletion had deleterious effects on miRNA silencing efficiency, subsequent studies have raised skepticism about the role, if any, that TRBP plays in RNA induced silencing, and if that

role is simply non-essential<sup>92</sup>. Questions have also been raised about PACT, which is 40% similar to TRBP, and whether it serves a redundant function to TRBP and similarly interacts with Dicer<sup>92</sup>. Some reports indicate that PACT associates with Dicer to facilitate miRNA production<sup>93,70</sup>, while a more recent study shows that TALEN-mediated knockout of PACT expression has no functional effect on Dicer's activity or miRNA biogenesis, and any interaction between PACT and Dicer that was previously observed was attributable to the fact that the studies were conducted under conditions where PACT was excessively overexpressed<sup>92</sup>.

Sequence alignment of TRBP with the amino acid sequences of members of the double-stranded RNA binding protein family (of which PKR is a member) showed that TRBP contained three conserved dsRNA binding motifs like PKR's cellular activator, PACT (Figure 1.3). Since TRBP and PACT had been shown to interact with the TAR RNA to different effects on TAR mRNA translation<sup>94</sup> and both proteins have similar interacting partners (i.e. PKR, Dicer), several laboratories sought to uncover the potential regulation of PKR's activities during viral replication and cellular stress by TRBP.

#### *TRBP INHIBITION OF PKR DURING HIV-1 INFECTION*

During viral infection, IFNs transcriptionally induce the expression of PKR which remains latent within the cell until it is activated by dsRNA binding. This results in the inhibition of viral protein synthesis, and consequently, the abrogation of viral replication. To determine if TRBP could prevent the translational inhibition imposed by IFN-induced PKR during HIV infection, Benkirane et al infected cells with a chimeric HIV-

1 virus expressing TRBP, and assayed for changes in viral replication compared to the cells infected with wild type HIV-1 virus after IFN $\alpha$  treatment<sup>95</sup>. While the cells infected with the wild-type HIV-1 virus demonstrated a dose-dependent reduction in viral replication with IFN $\alpha$  treatment, the cells infected with the HIV-1 virus expressing TRBP were completely resistant to IFN $\alpha$ , suggesting that TRBP was involved in limiting IFN's anti-viral activities in infected cells.

Comparative analysis of HIV protein synthesis in HeLa cells expressing the HIV genome and transfected with PKR or PKR and TRBP showed that while PKR evidently reduced the expression of HIV encoded proteins, TRBP significantly blunted PKR's inhibition of HIV protein synthesis. Direct detection of viral replication by HIV reverse transcriptase activity in infected cells transfected with PKR, or co-transfected with PKR and TRBP showed that TRBP expression boosted viral replication as compared to the cells infected only with the HIV virus, demonstrating that TRBP directly inhibited PKR activity to enhance viral replication and protein synthesis. Researchers also observed that a TRBP mutant devoid of dsRNA-binding inhibited PKR's activity at similar levels with wt TRBP, indicating that this inhibitory activity was independent of TRBP's dsRNA binding. The interaction of PKR and TRBP was also shown to be independent of dsRNA interaction, as cellular extracts completely depleted of dsRNA still demonstrated strong PKR-TRBP interaction, even when the interaction between a dsRNA binding defective PKR mutant and TRBP was tested. This inhibition of PKR by TRBP in the absence of dsRNA strongly indicated that TRBP could potentially regulate PKR's activity during non-viral cellular conditions.



### *TRBP INHIBITS PKR'S CATALYTIC ACTIVITY BY INTERACTION WITH PACT*

Since PACT had been shown to be primarily responsible for activating PKR in response to cellular stress, investigators sought to uncover if TRBP could regulate PKR's activity through its interaction with its cellular activator, PACT. Co-immunoprecipitation assays with PACT and TRBP in the complete absence of RNA showed that both proteins could heterodimerize independently of dsRNA<sup>96,58</sup>, and subsequent yeast two-hybrid experiments demonstrated that each protein's M1, M2 and M3 motifs could interact with the corresponding protein's motifs. The effect of such a strong PACT-TRBP interaction on PKR activity was tested by knocking down TRBP expression in cells transfected with PACT. PACT overexpression, which normally results in PKR activation (as detected by phospho-PKR in western blot analysis) was absent in cells expressing TRBP, whereas stable knockdown of TRBP restored this activity, indicating that TRBP primarily served to inhibit PKR activity by heterodimerizing with PACT<sup>97</sup>.

Since it had been previously established that PACT interacts with and activates PKR in response to stress signals, it was predicted that PACT would dissociate from TRBP in response to stress signals to allow for PACT's association with PKR. This idea was supported by results from co-immunoprecipitation experiments to assay for changes in PACT-TRBP interaction in response to hydrogen peroxide and sodium arsenite induced oxidative stress which showed that PACT-TRBP interaction is disrupted in response to stress<sup>98,67</sup>.

Stress-induced PACT phosphorylation at S287 dramatically increases PACT-PACT homomeric interactions as well as PKR-PACT heteromeric interaction, so experiments

were performed to test if this phosphorylation event was the trigger for the decrease in PACT-TRBP heteromeric interaction in response to stress<sup>67</sup>. As such, yeast two-hybrid experiments were performed with TRBP and phosphorylation mimetic PACT (S246D S287D) yeast expression constructs and followed by *in vitro* and *in vivo* co-immunoprecipitation assays with S246D S287D PACT and TRBP. In all three experiments, researchers observed a dramatic reduction in 246D 287D PACT interaction with TRBP as compared to wt PACT, showing conclusively that stress-induced PACT phosphorylation increased PACT-PACT and ultimately PACT-PKR interaction and PKR activation by weakening PACT-TRBP interaction<sup>67</sup>. The functional importance of a weakened PACT-TRBP interaction on PKR mediated apoptosis was demonstrated by analysis of induction of cell death after PACT (S246D S287D, wt) and TRBP co-transfection into HeLa cells<sup>67</sup>. While co-expression of TRBP and wt PACT was sufficient to rescue apoptosis induced by PACT transfection, TRBP was completely unable to rescue apoptosis induced by transfection of the S246D S287D phosphorylation mimetic mutant<sup>67</sup>.

Taken together, the results from these studies showed that TRBP prevents aberrant PKR activation by forming heterodimers with PACT and upon the receipt of stress signals due to PACT's phosphorylation, dissociates from PACT to allow for PACT's timely activation of PKR's kinase activity.

#### *TRBP PHOSPHORYLATION REGULATES PKR ACTIVITY*

In addition to its role as a PKR inhibitor during HIV infection and cellular stress, a recent study indicated that TRBP may also regulate PKR activity during the cell cycle<sup>92</sup>. In

one study, investigators noted that mitotic cells showed increased PKR phosphorylation levels that correlated with increased phosphorylated JNK and eIF2 $\alpha$  levels<sup>92,99</sup>. eIF2 $\alpha$ , of course, is a well characterized substrate of PKR, and JNK is a Mitogen Activated Protein Kinase (MAPK) whose efficient activation has been shown in several studies to depend on PKR activation<sup>32</sup>. This increased PKR phosphorylation during mitosis was shown to be independent of PACT<sup>92</sup>, and raised questions about TRBP's role, if any, in modulating PKR's activity during mitosis.

These questions were answered by the cell cycle analysis of TRBP knockout (TRBP KO) and wildtype cells<sup>92</sup>; evaluation of both sets of cells showed that the levels of phosphorylated PKR and eIF2 $\alpha$  were significantly elevated and the duration of the G2/M phase was longer in TRBP KO cells as compared to the wildtype cells. These results, in addition to a previous finding that PKR overexpression in Chinese Hamster ovary (CHO) cells induces a similar delay in transition to the G1 phase<sup>99</sup>, suggested that TRBP could modulate PKR's activity during the cell cycle, and consequently affect the cell cycle transition from the M to the G1 phase.

The western blot analysis of cellular extracts from cells arrested in the G1, S, and M phases did not show changes in TRBP expression during the cell-cycle, but showed changes in TRBP phosphorylation<sup>92</sup>. TRBP was hyperphosphorylated during M phase and the hyperphosphorylated TRBP isoform was subsequently shown to interact more strongly with PKR compared to the unphosphorylated S phase TRBP isoform. The phosphorylated TRBP inhibited PKR's activation and eIF2 $\alpha$  phosphorylation much strongly than the unphosphorylated isoform. In an intriguing turn, the kinase

responsible for TRBP's phosphorylation during mitosis was revealed to be JNK, which is itself phosphorylated by PKR activated by nuclear dsRNAs during mitosis as the nuclear membrane disappears. Thus, PKR is involved in a negative feedback loop that promotes its own inhibition during the cell cycle by facilitating TRBP hyperphosphorylation through JNK activation<sup>92</sup>.

Another study also suggested that JNK-mediated TRBP phosphorylation plays a role in activating PKR during obesity and propagating inflammation in obese animals<sup>100</sup>, thereby implicating sustained PKR activation in metabolic disease. These results are controversial, as another report showed that PKR has no functional role in regulation of obesity-induced metabolic regulation<sup>101</sup>. The observed effects in the first study were deemed to be specific only to the animals used in that study.

Since TRBP phosphorylation has been shown to inhibit PKR's activity during mitosis, it is interesting to investigate if, like PACT, TRBP is also phosphorylated in response to cellular stress and if this phosphorylation event alters the heteromeric interactions between TRBP and PACT/ PKR to dampen the negative effects of sustained PKR activation during cellular stress. These aspects were explored in chapter 3 of my dissertation.

## 1.4 STRUCTURE OF DISSERTATION

In **Chapter 2** of this dissertation, we report the findings of our investigation into the mechanisms underlying PACT's inability to activate PKR efficiently despite an increase in PACT protein levels during active HIV infection. Using a HIV LTR  $\beta$ -

galactosidase reporter cell line, we found that PACT, like TRBP, enhances the expression of the LTR-driven reporter in a virally encoded transcription factor (Tat)-dependent manner at a translational level. Our results establish that PACT, in synergy with Tat, enhances the translation of HIV TAR-RNA containing transcripts by directly inhibiting PKR activation. We also demonstrate that the dsRNA binding protein ADAR1 as well as HIV TAR-RNA are required factors that inactivate PACT-mediated PKR activation. A complex of PACT-Tat-ADAR1 (and possibly TRBP) formed on TAR-RNA keeps PACT inactive for PKR activation and facilitates translation of HIV encoded transcripts<sup>79</sup>.

In **Chapter 3**, we examine the roles that stress-induced TRBP phosphorylation plays in regulating PKR activation in response to oxidative stress. Using a tetracycline-inducible TRBP overexpressing HeLa cell line, we demonstrate that TRBP is phosphorylated in response to sodium arsenite-induced oxidative stress by the MAPKs, ERK and JNK, and the time-course of this phosphorylation event directly coincides with a steady decline in PKR and eIF2 $\alpha$  phosphorylation and results in a reduction of PKR-mediated cellular apoptosis. We also show that the observed decrease in PKR activation is due to enhanced ability of the phosphorylated TRBP to inhibit PKR. This was further confirmed by assaying the effect of phosphorylation-mimetic TRBP mutants on the growth inhibition of yeast cells expressing catalytically active PKR. Finally, protein interaction studies lead us to conclude that TRBP phosphorylation during oxidative stress significantly weakens TRBP-TRBP homomeric interactions, which in turn results in increased TRBP-PKR heteromeric interactions and diminished PKR activity. These findings provide us with a model for the attenuation of sustained PKR activation and

induction of cellular apoptosis through increased inhibitory interactions between PKR and phosphorylated TRBP.

In **Chapter 4**, we further assess the effects of mutations of conserved hydrophobic residues in PACT's M1 and M2 motifs on PACT's dsRNA binding and interactions with PACT, TRBP, and PKR. By generating a dsRNA-binding and homodimerization- defective phosphorylation mimetic point mutant (L99E DD), we gained insight into how defective homodimerization affects stress-induced PACT-PACT interaction and PACT-mediated apoptotic induction. These findings together elucidate the contributions of each of PACT's dsRNA binding motifs to efficient PACT-PACT, PACT-TRBP, and PACT-PKR interaction and highlight the importance of PACT-PACT homodimer formation to efficient PKR activation in response to cellular stress.

In **Chapter 5**, we provide general conclusions about the studies presented.

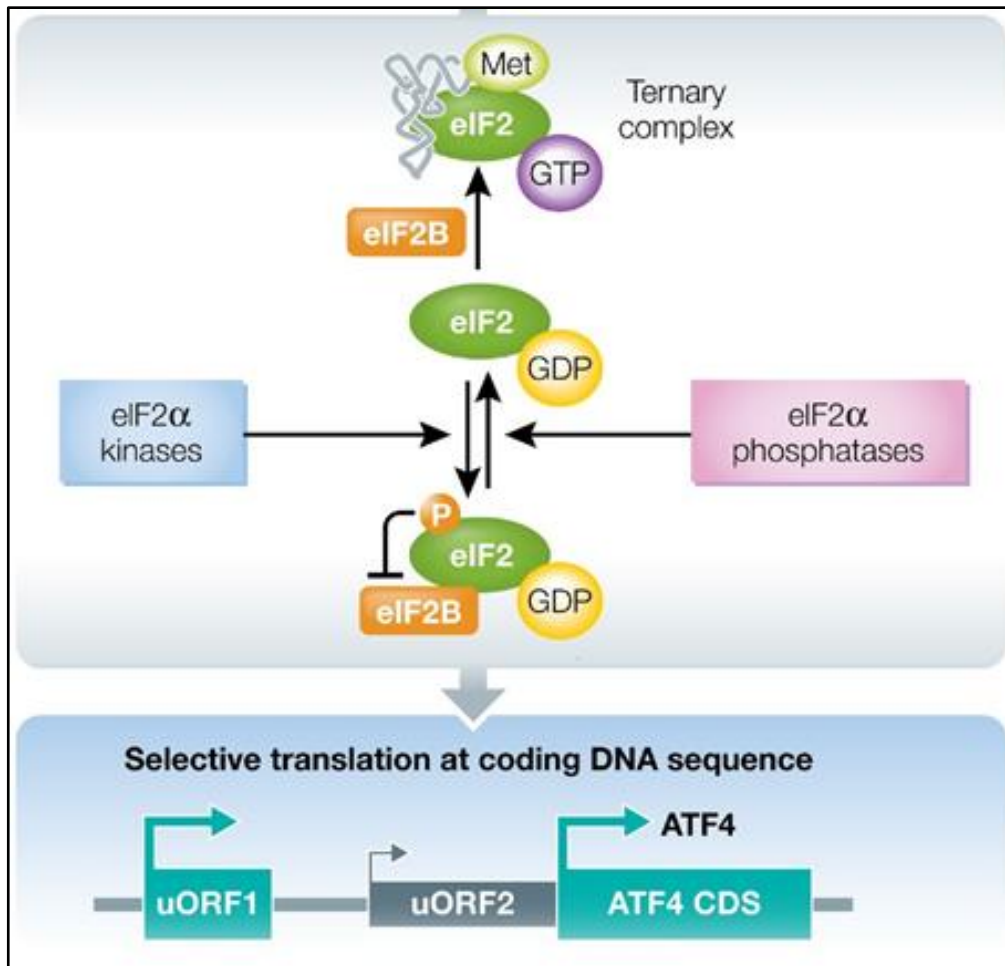


**Figure 1.1: Regulation of eukaryotic translation initiation by the eIF2 $\alpha$  kinases.**

The eukaryotic factor eIF2 (made up of  $\alpha$ ,  $\beta$ , and  $\gamma$  subunits) associates with GTP and the methionyl-charged initiator tRNA to form a ternary complex. This complex then associates with the 40S small ribosomal subunit to form a 40S pre-initiation complex, which in turn binds the mRNA transcript as well as other initiation factors. The onset of translation due to the binding of the 60S large ribosomal subunit is accompanied by the hydrolysis of GTP to GDP. Another initiation factor, eIF2B which is the dedicated eIF2 GTP exchange factor (GEF), exchanges the hydrolyzed GDP for GTP so another round of translation initiation can begin. However, the phosphorylation of eIF2's  $\alpha$  subunit on Serine 51 by one of the four eIF2 $\alpha$  kinases during cellular stress prevents the exchange factor activity of eIF2B without preventing its association with eIF2 $\alpha$  via eIF2 $\beta$ . This results in the blockage of active eIF2B as it stays complexed with eIF2 $\alpha$  effectively shutting off protein synthesis, as eIF2B is present in limited quantities within the cell. The resulting decline in ternary complex formation leads to the cessation of general protein synthesis<sup>1</sup>.

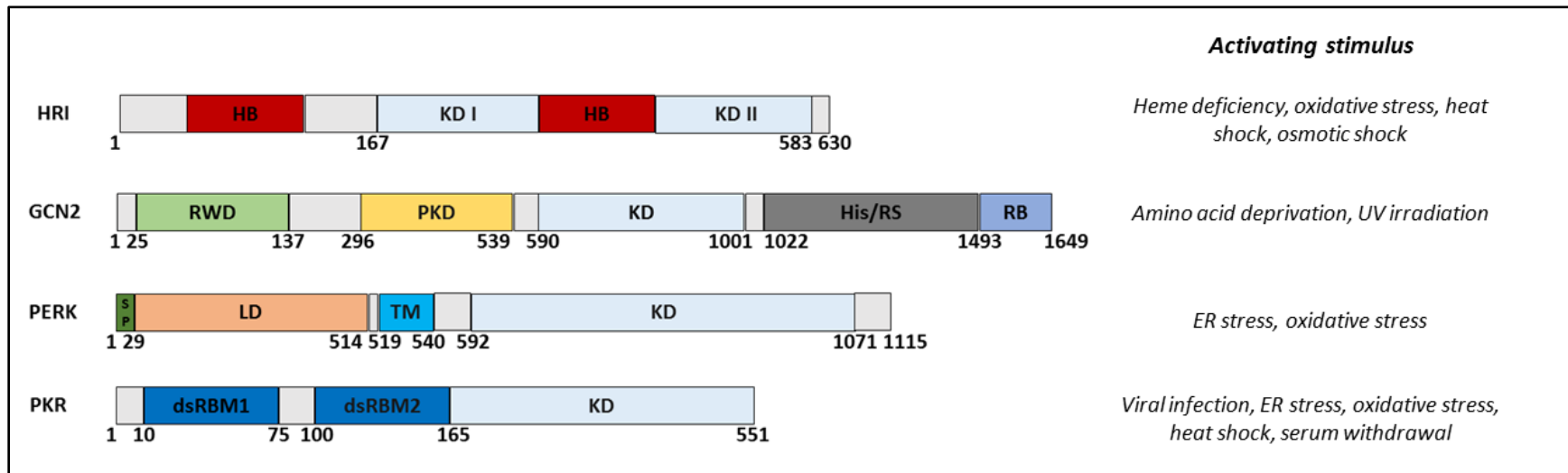


**Figure 1.2: Domain structure and activating stimuli of the four eIF2 $\alpha$  kinases.** Each of the four eIF2 $\alpha$  kinases is activated by a diverse range of cellular stress signals and contain, in addition to a kinase domain, distinct regulatory domains. HRI possesses two heme binding domains (HB; depicted in red) one of which is inserted within HRI's kinase domain (KD I & II; depicted in light blue). GCN2 has an N-terminal RING finger and WD repeat domain (RWD; depicted in green), a pseudokinase domain (PKD; depicted in orange), a kinase domain (KD; depicted in light blue), a histidyl tRNA synthetase-like (HisRS-like) domain (His/RS; depicted in grey), and a C-terminal ribosome binding and dimerization domain (RB; depicted in purple). PERK, the ER resident eIF2 $\alpha$  kinase, contains an N-terminal signal peptide (SP; depicted in green), and ER luminal domain (LD; depicted in orange), a transmembrane domain (TM; depicted in blue), and a cytoplasmic domain which envelopes its kinase domain (KD; depicted in light blue). PKR, the interferon induced eIF2 $\alpha$  kinase, contains two N-terminal double-stranded RNA binding motifs (dsRBM1 and dsRBM2; depicted in navy blue) in addition to its C-terminal kinase domain (KD; depicted in light blue).



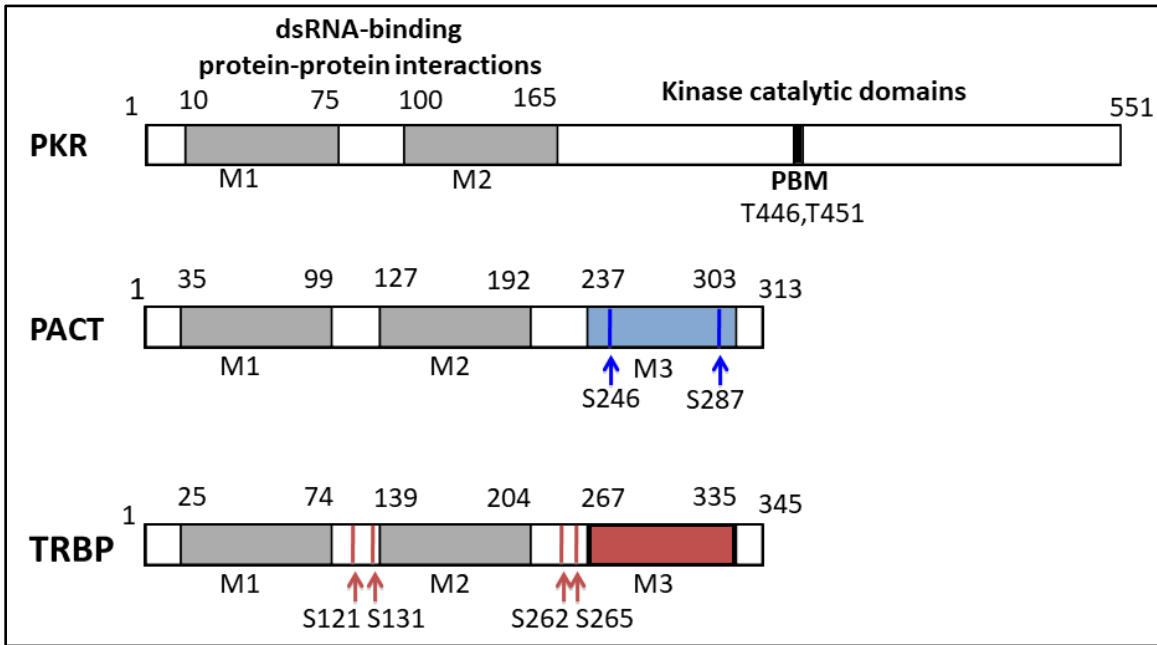


**Figure 1.3: Domain structure of the dsRNA binding proteins, PKR, PACT, and TRBP:** All three dsRNA binding proteins contains multiple copies of the conserved dsRNA binding motifs. PKR possesses two dsRBMs (M1 and M2; depicted in grey) which mediate PKR's interactions with dsRNA as well as with other dsRBM containing proteins. PKR also has a C-terminal kinase catalytic domain containing a region important for PACT interaction (denoted by PBM). Two threonine residues (T446, and T451) are the sites of PKR trans-autophosphorylation required for PKR activation and phosphorylation of eIF2 $\alpha$  on Serine 51. PACT, PKR's cellular activator contains three dsRNA binding motifs (M1, M2, M3; depicted here in grey and light blue). Blue arrows depict the serine residues (S246, S287) identified as stress-induced phosphorylation sites necessary for increased PACT interaction with PKR and PKR activation. TRBP, an inhibitor of PKR's activator during cellular stress and HIV infection, contains three dsRNA binding motifs like those of PACT (M1, M2, and M3 depicted here in grey and red). Red arrows depict serine residues (S121, S131, S262, S265) identified as MAPK (JNK/ERK) phosphorylation sites. PACT and TRBP's respective M3 motifs confer each protein with their activities as pertains to PKR activity.

## CHAPTER 2

# ADAR1 AND PACT CONTRIBUTE TO EFFICIENT TRANSLATION OF TRANSCRIPTS CONTAINING HIV-1 TRANS-ACTIVATING RESPONSE (TAR) ELEMENT<sup>2</sup>

---

<sup>2</sup> Chukwurah, E., Handy, I., and Patel R.C. 2017 *Biochemical Journal* 474: 1241-1257  
Reprinted here with permission of publisher.

## 2.1. ABSTRACT

Human immunodeficiency virus type 1 (HIV-1) has evolved various measures to counter the host cell's innate antiviral response during the course of infection. Interferon (IFN) stimulated gene products are produced following HIV-1 infection to limit viral replication, but viral proteins and RNA counteract their effect. One such mechanism is specifically directed against the IFN-induced Protein Kinase PKR, which is centrally important to the cellular antiviral response. In the presence of viral RNAs, PKR is activated and phosphorylates the translation initiation factor eIF2 $\alpha$ . This shuts down the synthesis of both host and viral proteins, allowing the cell to mount an effective antiviral response. PACT (protein activator of PKR) is a cellular protein activator of PKR, primarily functioning to activate PKR in response to cellular stress.

Recent studies have indicated that during HIV -1 infection, PACT's normal cellular function is compromised and that PACT is unable to activate PKR. Using various reporter systems and *in vitro* kinase assays, we establish in this report that interactions between PACT, ADAR1 and HIV-1-encoded Tat protein diminish the activation of PKR in response to HIV-1 infection. Our results highlight an important pathway by which HIV-1 transcripts subvert the host cell's antiviral activities to enhance their translation.

## 2.2: INTRODUCTION

Cells infected with a virus employ a variety of mechanisms to counteract the negative impact of viral replication and promote cell survival<sup>102</sup>. The innate immune response to a viral infection is mediated by external and internal sensor molecules,

which recognize the viral components as “non-self” and trigger mechanisms leading to the production of interferons (IFNs)<sup>103</sup>. IFNs are secreted anti-viral cytokines that bind to receptors in a paracrine and autocrine manner on cells to trigger signaling cascades culminating in the expression of IFN-stimulated genes (ISGs)<sup>77</sup>. Most ISGs have antiviral functions, although some ISGs with both antiviral and proviral functions have been recently described<sup>78,104,105</sup>. Viral and cellular factors regulate ISGs to promote or limit viral replication respectively and this regulatory interplay between the virus and the host cell is crucial in determining the outcome of a viral infection. Retroviruses such as the Human Immunodeficiency Virus type 1 (HIV-1) produce viral factors that interact with various cellular proteins, including ISGs. As a result, the virus subverts their antiviral properties or co-opts them from their regular cellular activities to facilitate efficient viral replication within the infected host cell<sup>106,107</sup>.

One of the ISG products is PKR (protein kinase, RNA-activated), a protein kinase that plays a central role in regulating the outcome of a viral infection<sup>108–110</sup>. In virally infected cells PKR is activated by binding to dsRNA, a product of several viral infections, including HIV-1<sup>34,83</sup>. The interaction between PKR and dsRNA induces a conformational change that is essential for PKR’s catalytic activation<sup>111</sup>. PKR then phosphorylates the translation initiation factor eIF2 $\alpha$  on Serine 51, resulting in a decline of general protein synthesis, and consequent cessation of viral protein synthesis<sup>112,113</sup>. In order to counteract PKR’s antiviral actions, viruses have developed measures that include dsRNA sequestration, decoy substrates and direct interaction of virally encoded inhibitory proteins with PKR<sup>114,115</sup>. One of the host proteins that inhibits PKR activation during HIV-

1 replication is the TAR RNA Binding Protein (TRBP), which was first identified due to its strong binding affinity for the Trans-activation response element (TAR) RNA found in the 5' end of all HIV-1 mRNA transcripts<sup>87,116</sup>. In eukaryotic mRNAs, the 5' untranslated region (UTR) is critical for ribosome recruitment to the mRNA, start codon choice, and control of translation efficiency. This dual inhibitory effect of TAR on translation has promoted development of viral countermeasures in order to achieve efficient viral replication. During HIV-1 infection, TRBP inhibits PKR activation by sequestration of the activating TAR RNA and by direct interaction with PKR's two dsRBMs<sup>95,117,118</sup>. Although TRBP is an effective inhibitor of PKR, HIV-1 has evolved additional mechanisms to more effectively block PKR activity and successfully replicate in infected cells<sup>109,119</sup>.

In the absence of viral infections, basal levels of PKR are present in all cells<sup>108</sup>. In uninfected cells PKR regulates responses to oxidative stress, endoplasmic reticulum (ER) stress and serum starvation<sup>97,120</sup>. Under these conditions, a cellular Protein Activator of PKR (PACT) regulates PKR activation<sup>121,122</sup>. PACT is constitutively phosphorylated on Serine 246, and is phosphorylated on Serine 287 in response to stress, resulting in increased homodimerization and PACT-PKR heterodimerization<sup>58,60,67</sup>. PACT activates PKR and general protein synthesis is halted, allowing the cell to mount an effective response to the stressor, or undergo apoptosis if the stressful conditions cannot be overcome. This stress response pathway is negatively regulated by TRBP, as TRBP interacts efficiently with PACT in the absence of stress. PACT's phosphorylation at Serine 287 in response to cellular stress decreases its interaction with TRBP and consequently PACT-PACT and PACT-PKR interactions increase to activate PKR<sup>66,67</sup>. Thus, TRBP

negatively regulates PKR activation during a virus infection, as well as during cellular stress<sup>68</sup>.

Recent studies established that PACT's function as a PKR activator is suppressed during HIV-1 infection and PACT is unable to activate PKR in HIV-1 infected cells<sup>98,109,119</sup>. During the course of HIV-1 infection, there is a transient increase in PKR activation followed by a gradual decrease, which indicates the presence of a viral mechanism to subvert sustained PKR activation. A significant increase in the interactions between PACT, PKR and ADAR1 (Adenosine Deaminase Acting on RNA 1) is observed, and it strongly correlates with decreased PKR activation and increased viral protein production<sup>98</sup>. ADAR1 p150 isoform is an ISG encoded, RNA editing enzyme that catalyzes the deamination of adenosine to inosine in viral and cellular dsRNA substrates<sup>76,123</sup>. This often results in the destabilization of RNA secondary structures or incorporation of amino acids detrimental to viral protein structure and function<sup>78,105,124</sup>. In this study, we further characterized the molecular mechanisms involved in mediating PACT's proviral effects during HIV-1 replication. Our findings indicate that PACT increases HIV-1 gene expression at the translational level via inhibition of PKR activation by acting in concert with a HIV-1 encoded protein Tat and a cellular protein ADAR1 to bring about sustained PKR inhibition and efficient translation of TAR-containing mRNAs. This study underscores the essential role of Tat protein in this inhibitory complex and indicates that Tat enhances the translation of HIV-1 mRNAs in addition to its canonical transactivation function during transcription<sup>125</sup> and its PKR inhibitory role by acting as a pseudosubstrate<sup>126</sup>. Our study also highlights the importance of ADAR1 in this

multiprotein complex as a key component that mediates PKR inhibition during HIV-1 infection. As all HIV-1 mRNAs contain the TAR structure at their 5' end, these results shed light on how these mRNAs are efficiently translated in virally infected cells.

## 2.3 MATERIALS AND METHODS

### 2.3.1 CELL LINES AND ANTIBODIES

HeLa MAGI-CCR5 cells<sup>127</sup> were obtained through the NIH AIDS Reagent Program. HeLa-MAGI-CCR5 cells, PKR  $-/-$  murine embryonic fibroblasts (MEFs)<sup>80</sup>, HEK-293T (ATCC CRL-11268) and HeLa (ATCC CRM-CCL-2) cells were cultured in Dulbecco's modified Eagle's medium (DMEM) containing 10% Fetal Bovine Serum and penicillin/streptomycin. The following antibodies were used: Anti-Flag monoclonal M2 (Sigma), anti-PKR (human) monoclonal (71/10, R&D Systems), anti-V5 (Invitrogen), anti-Myc (Santa Cruz).

### 2.3.2 PLASMIDS

The CMV-TAR-Luciferase/pGL3 basic plasmid was constructed as follows: The TAR sequence was inserted as an oligonucleotide in the *HindIII-BamHI* sites of pcDNA3-EGFP (Addgene). An 818 bp region containing the CMV promoter followed by TAR was excised from the TAR pcDNA3-EGFP plasmid described previously and inserted into the pGL3 basic vector (Promega) at the *SmaI-XhoI* site upstream of the luciferase coding sequence. The corresponding CMV-Luciferase pGL3 basic plasmid devoid of TAR was constructed as follows: A 753 bp region was excised from the pcDNA3-EGFP plasmid and

inserted into the *SmaI-XhoI* site upstream of the luciferase coding sequence. The mutant CMV-TAR-Luciferase/pGL3 basic was constructed by inserting the mutated TAR oligonucleotide into the *HindIII-BamHI* sites of pCDNA3-EGFP. The 818 bp region containing the CMV promoter and mutant TAR sequence was subsequently excised from the pCDNA3-EGFP expression construct and inserted into the pGL3 Basic vector at the *SmaI-XhoI* site upstream of the luciferase coding sequence. PACT and TRBP expression constructs were as described previously<sup>60,62</sup>. The Tat/pCDNA3 expression construct was a gift from Dr. Ashok Chauhan<sup>128</sup>, while the pCMV-Rev and pCDNA3.1-ADAR1-p150-V5 expression constructs were previously described<sup>128,129</sup>. To generate MycTat/pCDNA 3.1<sup>-</sup>, the Tat insert from Tat/pCDNA3 was subcloned into pcDNA 3.1<sup>-</sup> in order to put a Myc tag at its amino terminus. pCMV2-Flag-PACT was also previously described<sup>62</sup>. These constructs were a gift from Dr. Anne Gatignol (McGill University).

### 2.3.3 $\beta$ -GALACTOSIDASE ASSAY

HeLa-MAGI-CCR5 cells were transfected with indicated amounts of the Tat/pCDNA3, Flag PACT/pCMV2, Flag TRBP/pCDNA 3.1<sup>-</sup> or only pcDNA 3.1<sup>-</sup> expression constructs.  $\beta$ -galactosidase activity was assayed 24 hours after transfection using the Galacto-Star Assay System (ThermoFisher Scientific).



#### 2.3.4 SEMI-QUANTITATIVE REVERSE TRANSCRIPTASE PCR

Total RNA was isolated from HeLa-MAGI-CCR5 cells transfected with indicated amounts of the Tat/pcDNA 3, Flag PACT/pcMV2, Flag TRBP/pcDNA 3.1<sup>-</sup> or pcDNA 3.1<sup>-</sup> expression constructs. After 2 washes with ice cold PBS, 250  $\mu$ l of RNAzol B was added and total RNA was isolated as per the manufacturer's instructions. cDNA was synthesized at 42°C for 1 hour using random hexamer primers, 1  $\mu$ g total RNA, M-MuLV Reverse Transcriptase, 500  $\mu$ M dNTPs, and RNase inhibitor RNAsin (Promega). For each PCR, 2  $\mu$ l of cDNA and 50 pmoles of forward and reverse primers designed to amplify a 166 bp region of the  $\beta$ -galactosidase transcript or a 500 bp region of the  $\beta$ -actin transcript were used with the Promega GoTaq Polymerase Kit. The following conditions were used for PCR: 95°C for 5 min (initial denaturation), denaturation at 95°C for 30 s, annealing at 45°C for 30 s, and extension at 72°C for 30 s for 20, 25, or 30 cycles.

#### 2.3.5 REAL-TIME PCR

RNA was isolated from PKR<sup>-/-</sup> MEFS transfected with either the CMV-TAR-Luciferase pGL3 Basic or CMV Luciferase pGL3 Basic plasmids and the indicated combinations of Flag wt PKR/pcDNA 3.1<sup>-</sup>, Tat/pcDNA 3, and Flag PACT/pCMV2 expression constructs using RNAzol B as per the manufacturer's instructions. DNase treatment was performed to remove plasmid DNA from isolated RNA using the DNA-free™ DNase Removal Kit (Ambion).

cDNA was synthesized as described above using random hexamer primers. Real time PCR reactions were performed with serial dilutions of cDNA to ensure efficiency.

Reactions were performed in triplicate in a total reaction of 20  $\mu$ l and included 4  $\mu$ l cDNA, 250 nM firefly luciferase or  $\beta$ -actin primers, and SensiFAST™ SYBR® No-ROX Kit (Bioline). All reactions were run on a BioRad CFX96 Real Time System C1000 Thermal cycler machine with the following conditions: 95°C for 30 s, 95°C for 5 s, 53°C for 30 s (steps were repeated for 35 cycles), 60°C for 5 s, and then 95°C for 5 s. We used the BioRad CFX Manager software to generate standard curves to compare luciferase expression in each sample. 2 separate RNA isolations from transfected PKR<sup>-/-</sup> MEFs were used for analysis.

#### 2.3.6 TRANSFECTIONS FOR LUCIFERASE REPORTER ASSAYS AND REAL-TIME PCR ANALYSIS

All transfections were carried out in triplicate for each sample using indicated cell types cultured in six-well plates using Effectene (Qiagen) transfection reagent and 500 ng of total DNA per well. One nanogram of pRL-null (Promega) plasmid was co-transfected for normalization of the transfection efficiencies. Cell extracts were prepared at indicated time points and firefly and Renilla luciferase activities were measured with Dual Luciferase Reporter Assay system (Promega).

#### 2.3.7 PKR KINASE ACTIVITY ASSAY

PKR activity assays were performed using an anti-PKR monoclonal antibody (71/10, R&D systems). HeLaM cells were maintained in DMEM containing 10% fetal bovine serum. The cells were harvested when they were at 70% confluence. Cells were

washed in ice-cold PBS and collected by centrifugation at 600 *g* for 5 min. Cell extracts were prepared in lysis buffer [20 mM Tris-HCl pH 7.5, 5 mM MgCl<sub>2</sub>, 50 mM KCl, 400mM NaCl, 2 mM dithiothreitol (DTT), 1% Triton-X 100, 100 U/ml aprotinin, 0.2 mM phenylmethylsulfonyl fluoride (PMSF) and 20% glycerol]. A 100 µg aliquot of total protein was immunoprecipitated using the anti-PKR monoclonal antibody (71/10) in high salt buffer [20 mM Tris-HCl pH 7.5, 50 mM KCl, 400 mM NaCl, 1mM EDTA, 1 mM DTT, 1% Triton-X 100, 100 U/ml aprotinin, 0.2 mM PMSF, 20% glycerol] at 4°C for 30 min on a rotating wheel. A 20 µl aliquot of Protein A-agarose beads was then added and incubated for 1h. The Protein-A agarose beads were washed four times in 500 µl of high-salt buffer and twice in activity buffer [20 mM Tris-HCl pH 7.5, 50 mM KCl, 2 mM MgCl<sub>2</sub>, 2 mM MnCl<sub>2</sub>, 0.1 mM PMSF, 5% glycerol]. The PKR assay was performed with PKR still attached to the beads in activity buffer containing 0.1 mM ATP and 1 µCi of [<sup>32</sup>P] ATP at 30°C for 10 min. PKR was activated using synthesized TAR RNA (IDT DNA Technologies) and the effect of PACT, Tat, ADAR1, and TRBP on TAR-activated PKR was assayed by the subsequent addition of increasing amounts of pure recombinant PACT or pure recombinant TRBP (4, 40, 400 pg and 4 ng) in the presence of recombinant Tat and increasing amounts of recombinant ADAR1 (1.5, 15, and 150 ng). Labeled proteins were analyzed by SDS-PAGE on a 12% gel followed by autoradiography.

### 2.3.8 CO-IMMUNOPRECIPITATION ASSAY

*In vitro* translated, <sup>35</sup>S-labeled ADAR1 and flag epitope-tagged PACT and TRBP proteins were synthesized using the TNT T7 coupled reticulocyte system from Promega. A 5 µl of

<sup>35</sup>S-labeled proteins were mixed in indicated combinations and incubated with 20 µl of anti-flag mAb–agarose (Sigma) in 200 µl of immunoprecipitation (IP) buffer [20 mM Tris–HCl pH 7.5, 150 mM (or 300 mM) NaCl, 1 mM DTT, 100 U/ml aprotinin, 0.2 mM PMSF, 20% glycerol and 1% Triton X-100] at RT for 30 min on a rotating wheel. The beads were washed in 500 µl of IP buffer four times and the washed beads were then boiled in Laemmli buffer [150 mM Tris–HCl pH 6.8, 5% SDS, 5% β-mercaptoethanol and 20% glycerol] for 2 min and eluted proteins were analyzed by SDS–PAGE on a 12% gel followed by phosphorimager analysis for quantification.

#### 2.3.9 YEAST TWO-HYBRID INTERACTION ASSAY

To compare the strength of TRBP-ADAR1 with PACT-ADAR1 interactions, ADAR1 was expressed as a GAL4 DNA-activation domain fusion protein from the pGADT7 vector, and TRBP and PACT were expressed as GAL4 DNA-binding domain fusion proteins from the pGBKT7 vector. ADAR1 pGADT7 /TRBP pGBKT7 and ADAR1 pGADT7/ PACT pGBKT7 were co-transformed into AH109 yeast cells (Clontech), and the transformed yeast cells were plated on double dropout SD (synthetic defined) minimal medium lacking tryptophan and leucine. In order to check for the transformants' ability to grow on triple dropout media, transformed yeast cells were grown to an OD<sub>600</sub> of 2 in liquid growth medium. A 500 µl aliquot of each culture was pelleted and resuspended in an appropriate amount of distilled water to yield an OD<sub>600</sub> of 10. Serial dilutions were then made to yield OD<sub>600</sub> values of 1, 0.1, and 0.01. A 10 µl aliquot of each dilution was

then spotted onto triple dropout SD minimal media lacking histidine, tryptophan, and leucine in. Plates were incubated at 30°C for 3 days.

#### 2.3.10 QUANTIFICATION AND STATISTICS

Radioactive bands were scanned for the TRBP-ADAR1 and PACT-ADAR1 co-immunoprecipitation assays (Typhoon FLA7000) and were quantified using the GE Life Sciences ImageQuant TL software. To determine the statistical significance of the results of the co-immunoprecipitation assay and the  $\beta$ -galactosidase and luciferase assays, a two-tailed Student's *t*-test was performed, assuming equal variance. Each figure legend indicates *P*-values as denoted by brackets and special characters. Note that our  $\alpha$ -level was *P* = 0.05.

## 2.4 RESULTS

### 2.4.1 PACT ENHANCES HIV-1 GENE EXPRESSION FROM A TAT-INDUCED INTEGRATED LONG TERMINAL REPEAT

Our previous work indicated that PACT enhances expression from a HIV-1 promoter in transfected HeLa cells as well as viral replication in HIV-1 infected cells<sup>62,98</sup>. Thus, in this context, PACT exhibited a proviral function similar to the PKR inhibitor TRBP. To determine if PACT can enhance HIV-1 long terminal repeat (LTR)- driven gene expression in the context of latently infected cells, we first compared the effects of TRBP and PACT when HIV-1 LTR is integrated into the host chromosome. HeLa-MAGI-CCR5

cells contain a stably integrated  $\beta$ -galactosidase coding region expressed under the control of the HIV-1 LTR, whose transcription is dependent on HIV-1 Tat protein<sup>86,130–133</sup>.

We first verified that increasing amounts of Tat expression vector (blue bars) resulted in a dose-dependent increase in  $\beta$ -galactosidase activity (Figure 2.1 A) compared to the absence of Tat (black bar). Having confirmed that the cells are responsive to Tat, we next evaluated the effect of PACT in comparison to TRBP. The addition of PACT (green bars) or TRBP (red bars) expression constructs further stimulated Tat-trans-activated HIV-1 LTR-driven  $\beta$ -galactosidase activity (Figure 2.1B).

Furthermore, the addition of increasing amounts of Tat expression plasmid (blue bars) in the presence of a constant amount of PACT (green bars) or TRBP (red bars) led to increased  $\beta$ -galactosidase activity in a dose-dependent manner (Figure 2.1C). In contrast, in the absence of Tat, neither PACT (green bars) nor TRBP (red bars) had any effect on HIV-1 LTR driven expression (Figure 2.1D). These results indicate that similar to TRBP, PACT activates expression from HIV-1 LTR when integrated in the host chromosome and that this effect is dependent on the presence of the viral Tat protein.

#### 2.4.2 PACT DOES NOT AFFECT THE STEADY-STATE TRANSCRIPT LEVELS OF HIV-1 LTR-DRIVEN GENES

To characterize PACT's activating effect on HIV-1 LTR-driven gene expression as either transcriptional or post-transcriptional, we performed semi-quantitative RT-PCR analysis to assess changes in  $\beta$ -galactosidase mRNA levels in HeLa-MAGI-CCR5 cells transfected with Tat and PACT or TRBP expression plasmids relative to  $\beta$ -actin mRNA

levels (Figure 2.2). As expected, we observed that the expression of Tat increased  $\beta$ -galactosidase mRNA levels (lanes 4-6) when compared with empty vector transfected HeLa-MAGI-CCR5 cells (lanes 1-3). As seen in lanes 7-9, there was no increase in  $\beta$ -galactosidase mRNA levels between HeLa-MAGI-CCR5 cells transfected with Tat alone (lanes 4-6) and HeLa-MAGI-CCR5 cells transfected with Tat alone (lanes 4-6) and HeLa-MAGI-CCR5 cells transfected with Tat and TRBP (lanes 7-9) or Tat and PACT (lanes 10-12).

These results show that the enhancing effect of PACT on  $\beta$ -galactosidase activity in HeLa-MAGI-CCR5 cells was not a result of increased levels of  $\beta$ -galactosidase mRNA, but resulted from a post-transcriptional mechanism. As all mRNAs produced from HIV-1 LTR promoter driven reporters contain a TAR structure in their 5'-UTRs, these results indicate that PACT acts at a post-transcriptional level on TAR-containing mRNAs.

#### 2.4.3 TAT AND PACT INHIBIT PKR ACTIVATION INDUCED BY TAR CONTAINING MRNAS

The translation of HIV-1 mRNAs is diminished by the TAR RNA secondary structure in their 5'-UTRs and also by TAR-mediated PKR activation<sup>106,134,135</sup>. This effect is partially compensated for by the cellular proteins TRBP and ADAR1<sup>86,118,129,136,137</sup> as well as by the viral protein Tat<sup>126</sup>.

However, Tat also acts as a potent transcriptional trans-activator for HIV-1 LTR-driven genes, and in order to specifically study Tat's post-transcriptional effects, we used a system that is not affected at the transcriptional level by Tat. For this purpose, we designed an expression construct CMV-TAR-LUC, in which the TAR RNA was placed

directly upstream of the firefly luciferase open reading frame expressed from a CMV promoter. A CMV-Luciferase expression construct (CMV-LUC) was designed as a control without TAR. By producing TAR-containing transcripts from the CMV promoter which is nonresponsive to Tat's transcriptional transactivation, we could specifically assess Tat's post-transcriptional effects mediated by PKR activation.

To examine the activity of PACT and Tat on PKR-induced inhibition of translation, PKR<sup>-/-</sup> MEFs were co-transfected with either CMV-TAR-LUC/pGL3 Basic or CMV-Luciferase/pGL3 Basic along with PACT and Tat expression plasmids, and luciferase activity was assessed. As seen in Figure 2.3A, co-transfection of PKR with CMV-TAR-LUC (white bars) or CMV-LUC (black bars) reduced luciferase activity as previously reported and in agreement with PKR's effect on translation of plasmid-encoded transcripts<sup>62,98,118,129</sup>. Furthermore, co-transfection of Tat with PKR rescued the PKR-mediated reduction of luciferase activity only when TAR was present, indicating that Tat can relieve the translational block imposed by PKR on TAR-containing mRNAs. Surprisingly, PACT also counteracted TAR-induced PKR translational inhibition, whereas it maintained PKR-mediated translational inhibition of plasmid-derived luciferase mRNA in the absence of TAR, suggesting that the presence of TAR is required for both PACT and Tat's inhibitory effect on PKR. In addition, when expressed together, PACT and Tat showed a further significant increase of luciferase expression with CMV-TAR-LUC, but not with CMV-LUC.

These results indicate that PACT inhibits PKR activation on TAR-containing mRNAs, in contrast with its well-characterized PKR-activating function<sup>61,121,122,138,139</sup>. Furthermore,



this PKR-inhibitory activity of PACT can only occur in the presence of TAR- containing mRNA transcripts (compare black bars with white bars) and is significantly enhanced in the presence of Tat. These results suggest that during active production of HIV-1 viral proteins, PACT acts in concert with Tat and TAR RNA to counteract PKR- mediated inhibition of viral mRNA translation.

To ensure that the Tat-dependent, PACT-mediated inhibition of PKR was not a result of changes in TAR-firefly luciferase mRNA or firefly luciferase mRNA transcript levels, we performed qRT-PCR analysis to quantify firefly luciferase mRNA levels in total RNA isolated from the PKR<sup>-/-</sup> MEFs transfected with the constructs indicated in Figure 2.3A. There were no significant differences in firefly luciferase mRNA levels in the various samples (Figure 2.3B), demonstrating that PACT's Tat-dependent effect on luciferase expression is at translational level, most probably by counteracting PKR activation.

#### 2.4.4 TAT-TAR INTERACTION IS ESSENTIAL FOR PACT'S PKR INHIBITORY ACTIVITY

As we observed that Tat and PACT work synergistically to increase translation of TAR containing mRNAs, we wanted to determine if Tat's ability to bind to the TAR RNA was essential for this function. To test this, we generated a CMV-TARm-LUC construct in which the TARm RNA will not bind Tat but would still activate PKR<sup>59</sup>. PKR co-transfection with this construct dramatically reduced the firefly luciferase activity (Figure 2.4A). However, co-transfection of Tat or PACT had no effect on PKR-mediated inhibition of the luciferase activity. These results show that Tat's ability to interact with TAR-containing

mRNAs is essential for the concerted PKR inhibitory effect of Tat and PACT on TAR-containing mRNAs.

To test that the PKR inhibitory effect was specific to Tat-PACT combination, we performed the same transfection experiments with CMV-TAR-Luc and Rev, which is an HIV-1 viral protein that binds to a different RNA structured element in viral mRNAs known as the Rev response element<sup>211-213</sup>. Co-transfection of PKR reduced the luciferase activity as shown in Figure 2.3A, but that of PACT or/and Rev had no effect on luciferase activity (figure 2.4B). These results confirm that PACT's PKR inhibitory activity on TAR-containing mRNAs specifically required Tat and its TAR RNA-binding activity is essential for this function.

#### 2.4.5 ADDITIONAL CELLULAR FACTORS ARE ESSENTIAL TO INHIBIT TAR RNA-MEDIATED PKR ACTIVATION

Based on the above results, the combination of the TAR RNA, PACT, and Tat seems to induce strong inhibition of PKR activation in cell culture. To determine if these components are sufficient to provide complete PKR inactivation, we performed *in vitro* kinase activity assays using PKR immunoprecipitated from HeLa cells to recapitulate the mechanism *in vitro*. We first confirmed that PKR is activated robustly by TAR RNA similar to the synthetic dsRNA polyI:C, with a bell-shaped activation curve with no activation at low and high concentrations of TAR RNA (Figure 2.5A), as previously observed<sup>214,94,215</sup>. We then assessed PACT's ability to inhibit or activate PKR activation caused by TAR RNA in the absence (Figure 2.5B, lanes 3-6) or presence (Figure 2.5B, Lanes 7-10) of Tat. PACT

remained a PKR activator in the presence of TAR-RNA (Figure 2.5B, lanes 3-6). In the presence of Tat, a very modest inhibition of PKR activity with the highest amount of PACT was observed (Figure 2.5B, Lane 10), indicating that PACT and Tat cannot recapitulate PKR inhibition *in vitro* and that additional components present in the mammalian cells are required for the observed inhibition of PKR activation on TAR-containing mRNAs.

#### 2.4.6 THE RNA-EDITING PROTEIN ADAR1 IS ESSENTIAL FOR THE COMPLETE INHIBITION OF TAR-ACTIVATED PKR BY TAT AND PACT

We previously reported that another double stranded RNA binding protein, ADAR1, directly interacts with PKR and PACT during HIV-1 infection to form a PKR-inhibitory complex<sup>98,119,129</sup>. Thus, we investigated if ADAR1 can inhibit TAR-activated PKR when present together with Tat and PACT. Using an *in vitro* kinase assay, we observed that ADAR1 can inhibit PKR activation efficiently in a dose-dependent manner (Figure 2.6, lanes 2-4).

Under these conditions, 150 ng of ADAR1 was required for complete inhibition of PKR activity (lane 2), whereas 15 ng and 1.5 ng of ADAR1 showed partial (lane 3) and no inhibition (lane 4), respectively. The addition of PACT did not improve or compromise the PKR inhibitory function of ADAR1 (lanes 6-8). We then tested the effect of HIV-1 Tat protein on PKR activity as our results in Figure 3 suggested that Tat is required for PKR inhibition. When Tat was present, we observed a complete inhibition of PKR activity at all concentrations of ADAR1 (lanes 9-12). Thus, the Tat protein seems to significantly

enhance the PKR inhibitory actions of ADAR1; 100-fold less ADAR1 (lane 12, 1.5 ng ADAR1) was sufficient to inhibit PKR activity in the presence of Tat, when compared with the conditions where Tat was absent (lane 6, 150 ng ADAR1). Also, Tat when present with ADAR1 does not enhance ADAR1's PKR inhibitory actions when compared with the inhibition observed with ADAR1 alone (lanes 14-16) when PACT is absent.

These results show that Tat, PACT, and ADAR1 act in concert to inhibit PKR and suggest that an inhibitory complex formed with Tat, PACT, and ADAR1 is essential for efficient PKR inhibition on TAR containing HIV-1 mRNAs. Tat by itself (data not shown) or with PACT (Figure 2.5) does not inhibit PKR activity. To further confirm that Tat enhances the PKR inhibitory activity of ADAR1 and PACT, we compared the effect of lower concentrations of ADAR1 in the presence and absence of Tat. As seen in Figure 2.6B, in the absence of Tat, 1.5 ng of ADAR1 showed complete inhibition of PKR activity (lane 2), and 150 and 15 pg ADAR1 showed no PKR inhibition (lanes 3 and 4, respectively). In the presence of Tat, 1.5 ng ADAR1 showed complete inhibition (lane 6) and 150 pg of ADAR1 showed partial inhibition of PKR activity (lane 7). These results demonstrate that Tat enhances the PKR inhibitory actions of ADAR1 in the presence of PACT, and that Tat may function to recruit PACT and ADAR1 to the complex after binding to TAR in HIV-1 encoded transcripts.

#### 2.4.7 A COMPARISON OF PKR INHIBITORY ACTIVITY OF ADAR1 IN THE PRESENCE OF PACT OR TRBP

As TRBP is known to inhibit PKR under various conditions including HIV infection, we wished to compare the relative efficiency of PACT and TRBP to inhibit TAR RNA-activated PKR in the presence of Tat and ADAR1. As seen in Figure 2.7A, we observed that similar to PACT, ADAR1 can inhibit PKR activation efficiently in a dose-dependent manner in the presence of TRBP and Tat (lanes 4-6). Under these conditions, 150 ng ADAR1 was required for a complete inhibition of PKR activity (lane 4). Unlike PACT (which activates PKR in the absence of ADAR1), TRBP shows significant inhibition of PKR even in the absence of ADAR1 (lane 3), and this inhibition is further enhanced by the addition of ADAR1 (lanes 4-6).

Comparing the relative efficiency of TRBP and PACT to inhibit PKR, 100-fold less ADAR1 is required in the presence of PACT (lanes 9-11) when compared to conditions where TRBP was used (lanes 4-6) instead of PACT. Thus, PACT significantly enhances the PKR inhibitory actions of ADAR1 when compared with TRBP (lanes 4-6 and 9-11). These results show that Tat, PACT, and ADAR1 act in concert to inhibit PKR more efficiently than Tat, TRBP, and ADAR1. One possible mechanism for PACT's enhanced ability to increase ADAR1's effective inhibition of PKR could result from its higher affinity for ADAR1. Therefore, we compared the relative strengths of PACT-ADAR1 and TRBP-ADAR1 interactions using a co-immunoprecipitation assay. We used an *in vitro* rabbit reticulocyte translation system to generate <sup>35</sup>S-methionine labeled ADAR1, PACT, and TRBP proteins. As seen in Figure 2.7B, both PACT and TRBP can co-immunoprecipitate

ADAR1 at 150 mM (lanes 4-6) and 300 mM (lanes 7-9) salt concentrations. However, at both salt concentrations, PACT interacts significantly more efficiently with ADAR1 when compared with TRBP (Figure 2.7C). At 150 mM salt concentration, PACT pulled down 12.3% of ADAR1, whereas TRBP could only pull down 3.2% of ADAR1. At 300 mM salt concentration, PACT pulled down 7.3% of ADAR1 and TRBP pulled down only 1.1% of ADAR1.

To compare the PACT-ADAR1 and TRBP-ADAR1 interactions further, we utilized a yeast two-hybrid assay (Figure 2.7D). We have used this system extensively to demonstrate that stress-induced phosphorylation of PACT results in changes in the affinity of its interaction with TRBP and PKR<sup>60,67,140</sup>. Thus, the yeast two-hybrid system is sensitive enough to detect changes in relative affinities between these proteins and measures direct interaction between two proteins. As seen in Figure 2.7D, in comparison with TRBP, PACT shows significantly stronger interaction with ADAR1. These results further suggest that ADAR1 functions as a more efficient inhibitor of TAR RNA-activated PKR in the presence of PACT than in presence of TRBP, either because PACT recruits ADAR1 with higher efficiency to TAR containing mRNAs or because ADAR1 forms a more stable PKR inhibitory complex with PACT. In HIV-infected cells, it is possible that both TRBP and PACT serve redundant roles to form complexes with Tat, ADAR1 and TAR RNA but PACT functions more efficiently to bring about PKR inhibition.

## 2.5 DISCUSSION

In HIV-1 infected patients type I IFNs are produced by plasmacytoid dendritic cells and exert both antiviral and immunomodulatory activities<sup>141</sup>. However, this IFN response is insufficient to clear the virus from infected cells<sup>142,143</sup>. The inability of IFNs to clear the virus is not due to a lack of cellular response to IFN since the ISGs are induced in infected peripheral blood mononuclear cells (PBMCs) when in culture and show inhibition of HIV-1 replication<sup>98</sup>. Thus, the absence of a robust IFN antiviral response in patients is due to a block in the antiviral actions of ISGs. PKR is one of the ISGs whose regulation has been studied extensively in the context of many viral infections including HIV-1. PKR overexpression results in its activation that effectively restricts HIV-1 replication<sup>117,129,144–146</sup>. In addition, a knockdown of PKR using siRNAs or overexpression of a trans-dominant negative PKR mutant results in increased HIV-1 replication in cell culture<sup>137</sup>. In spite of this, the virus replicates efficiently in patient cells, suggesting that PKR activity is heavily limited during the course of a natural infection<sup>129</sup>.

Our previous work showed that PKR activation takes place only transiently after HIV-1 infection of PBMCs or of lymphocytic cell lines with either X4 or R5 HIV-1 strains, suggesting that PKR activation is rapidly inhibited by the presence of HIV-1, which removes a barrier to replication<sup>129</sup>. During the course of HIV-1 infection, PKR is activated by the TAR RNA and inhibited by TRBP, ADAR1 and the viral Tat proteins. Of these inhibitors, the HIV-1 protein Tat inhibits PKR by acting as a substrate competitor<sup>81,82,126</sup> whereas TRBP and ADAR1 inhibit PKR activity by direct interaction. TRBP also sequesters the activator dsRNA and PACT molecules by a direct interaction with them<sup>95,117</sup>. ADAR1

was previously identified as an important contributor for effective PKR inhibition and has emerged as exhibiting both antiviral and proviral functions<sup>78,109</sup>. ADAR1 catalyzes the deamination of adenosine in RNAs with dsRNA regions, thereby causing a destabilization of RNA duplexes and genetic recoding<sup>123</sup>. Thus, ADAR1 functions as a suppressor of dsRNA-mediated antiviral responses, which include activation of PKR and IFN regulatory factor IRF3, the transcription factor for IFN genes<sup>78</sup>. The p150 isoform of ADAR1 is an ISG, present both in the cytoplasm and nucleus, as while the p110 isoform is constitutively expressed and is predominantly present in the nucleus<sup>147</sup>.

The results presented here demonstrate that TAR-mediated PKR activation is also suppressed by a complex of PACT, ADAR1, and the viral protein Tat. Thus, in addition to its well-established functions in the nucleus and in transcription of HIV-1 proviral genome, Tat plays an important function in enhancing HIV-1 mRNA translation in the cytoplasm. Furthermore, in this complex, PACT is unable to activate PKR and that ADAR1 and Tat are essential for repressing PACT's canonical PKR activating role. Neither Rev nor a mutated TAR can inhibit PKR activation, thus suggesting that TAR RNA serves as a scaffold to recruit and stabilize many RNA-binding proteins, and PACT's PKR-activating ability is inactivated by the recruitment of ADAR1 to this complex. It is possible that Tat binds to TAR first to recruit PACT, which in turn is able to efficiently bring ADAR1 to the complex. Our previous data established that PACT and ADAR1 interact directly<sup>98</sup> and our current results show that Tat has an essential function in this complex. Overall, our results suggest that during HIV-1 infection, cytoplasmic Tat may bind to the TAR RNA to simultaneously recruit PACT and ADAR1 to serve a PKR



inhibitory role. This complex serves a crucial role in enhancing translation of viral proteins needed for efficient viral replication as PKR is known to bind to the stem region of TAR RNA<sup>148</sup>.

In addition to its classical transcriptional trans-activation role in the nucleus, Tat's cytoplasmic functions during HIV-1 replication have been reported before in other studies<sup>149,150</sup>. Tat protein counteracts the effect of TAR to stimulate translation of the viral mRNAs by enhancing the activity of RNA helicase DDX3<sup>151–154</sup>. Tat also showed a stimulatory effect on global protein synthesis by competing with eIF2 $\alpha$  for phosphorylation by PKR or by inhibiting PKR activity, independently of the presence of TAR [reviewed in reference<sup>119</sup>]. Our work introduces one more regulatory layer for Tat's central role in HIV-1 replication. As represented in Figure 2.8, our results establish that for efficient translation of TAR-containing mRNAs, the interaction between TAR and Tat is essential to promote the formation of a PKR inhibitory complex that contains PACT and ADAR1. Using a mutated TAR region that does not bind Tat but can activate PKR efficiently, we demonstrate that PKR-mediated translational downregulation was not overcome in the absence of TAR-Tat interaction (Figure 2.4).

As a part of this multiprotein complex, PACT is unable to activate PKR and ADAR1 strongly represses PKR activity (Figure 2.6). ADAR1 has been shown to inhibit PKR activity and reduce eIF2 $\alpha$  phosphorylation efficiently to play a proviral role during the replication of several DNA and RNA viruses<sup>78,105</sup>. Overexpression of either the full-length ADAR1 p150 protein or the region with the RNA- and Z-DNA binding domains alone inhibited PKR autophosphorylation and eIF2 $\alpha$  phosphorylation<sup>129,155</sup>. A stable

knockdown of ADAR1 expression causes enhanced PKR autophosphorylation and eIF2 $\alpha$  phosphorylation following infection with measles virus or vesicular stomatitis virus<sup>156,157</sup>. In ADAR1 containing cells, PKR autophosphorylation is suppressed following a viral infection, but in ADAR1-deficient cells it is enhanced because of the lack of editing-mediated destabilization of dsRNA, lack of sequestration of dsRNA by ADAR1 and also due to a lack of formation of inactive heterodimeric ADAR1:PKR complexes<sup>78</sup>.

Furthermore, a depletion of ADAR1 by RNAi in human cells or by genetic knockout in mouse MEFs leads to enhanced apoptosis and cytotoxicity following infection with RNA viruses from the Paramyxoviridae and the Rhabdoviridae families as well as the *polyoma* DNA virus<sup>156–159</sup>. Using an overexpression screening strategy in which more than 380 human ISGs were tested for their antiviral activity against many medically important viruses, ADAR1 emerged as the most potent *proviral* ISG, which enhanced the replication of HIV-1, West Nile virus, Chikungunya virus, Venezuelan equine encephalitis virus, and yellow fever virus<sup>160</sup>. In case of HIV-1 infection, our results demonstrate that ADAR1 is important to suppress PKR activation by TAR RNA to allow for efficient synthesis of viral proteins as only Tat, PACT, and TAR RNA cannot block PKR activation efficiently in the absence of ADAR1 (Fig. 2.6).

Several viruses have been shown to inactivate PACT function in the infected cells as PACT is involved both in activating PKR to suppress viral protein synthesis and in IFN production via RIG-I like receptors (RLRs)<sup>161</sup>. Middle East Respiratory Syndrome Coronavirus 4a protein<sup>162</sup>, Herpes Simplex Virus US 11 protein<sup>163,164</sup>, Ebola virus VP35 protein<sup>165</sup>, Influenza virus NS1 protein<sup>166</sup>, and orf virus ov20.2 protein<sup>167</sup> have been

shown to inactivate PACT. Overall, our results show that the suppression of PACT activity to effectively inactivate PKR in HIV-1 producing cells is the result of the combined activity of the recruited ADAR1 that mediates PKR kinase inhibition, and Tat most likely stabilizes the complex formed by PKR, PACT and ADAR1. Any effect that Tat may have on PACT's function in the RLR mediated IFN production remains to be explored in future.

The results presented here shed light on how efficient translation of TAR-containing HIV-1 encoded RNAs takes place by suppressing PKR activation. The present work also presents us with new paradigms for testing possible ways to suppress HIV-1 viral protein synthesis. For example, if the formation of the inhibitory complex could be prevented by use of peptides that may block interaction between various components of this complex, we may be able to keep PKR activated in virally infected cells to prevent or at least partially block viral replication.

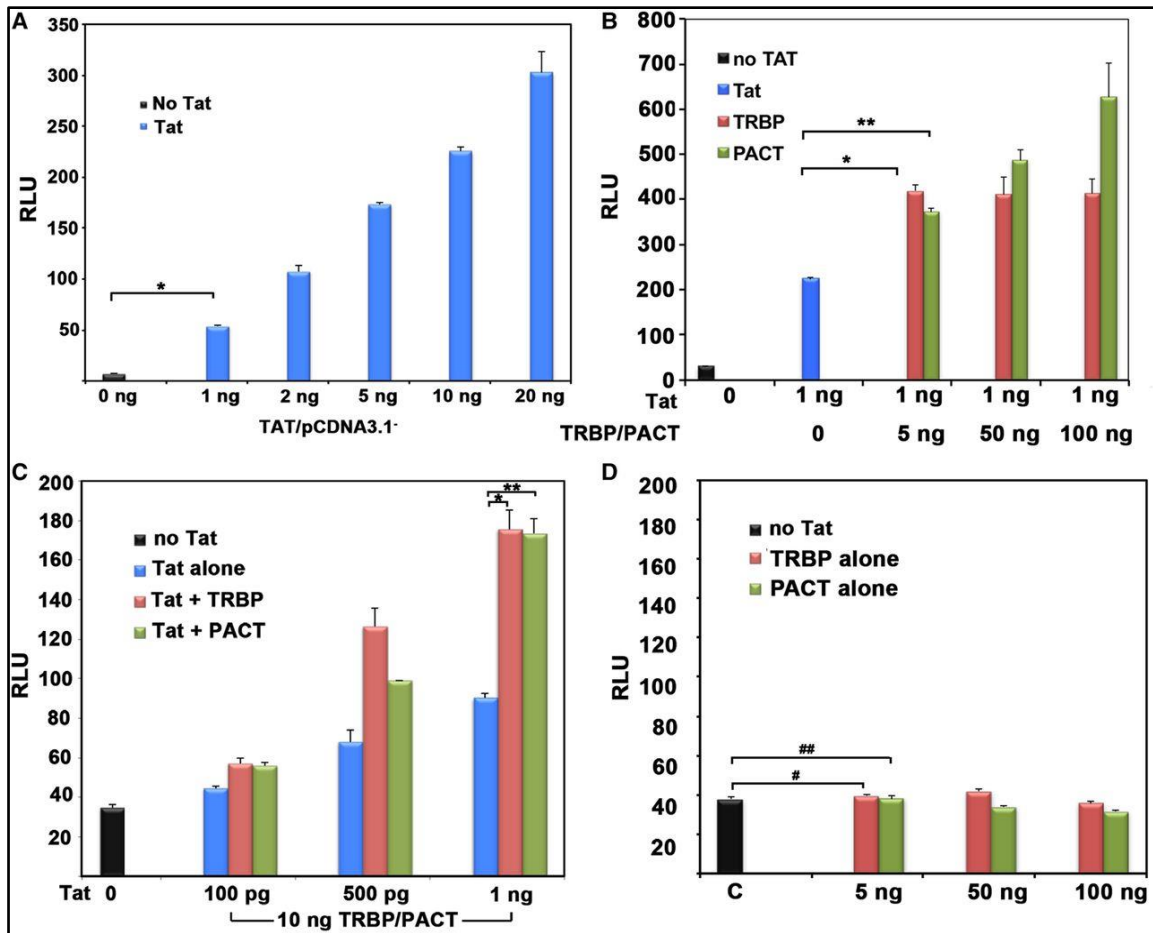


**Figure 2.1: PACT activates Tat-enhanced HIV-1 gene expression from an integrated LTR (A). Requirement and dose response curve for Tat for HIV-1 LTR driven expression.**

HeLa-MAGI-CCR5 cells were transfected with 0 (black bar) or increasing amounts of Tat/pcDNA 3 (blue bars) as indicated.

$\beta$ -Galactosidase activity was assayed 24 hours after transfection. Error bars indicate standard deviation calculated from three independent experiments. The *P*-value (0.0000038) calculated using statistical analyses indicated significant difference between the RLU values indicated by the bracket marked as '\*'.

**(B and C) PACT and TRBP both enhance HIV-1 LTR driven expression. (B)** HeLa-MAGI-CCR5 cells were transfected with 0 (black bar), or 1ng Tat/pcDNA 3 (Blue bar) with increasing amounts of Flag TRBP/pcDNA 3.1<sup>-</sup> (Red bars) or Flag PACT/pCMV2 (Green bars) as indicated. The *P*-values (0.0045 and 0.0044) calculated using statistical analyses indicated significant difference between the RLU values indicated by the brackets marked as '\*' and '\*\*' respectively. **(C)** HeLa-MAGI-CCR5 cells were transfected with 0 ng, (black bar), increasing amounts of Tat/pcDNA 3 (blue bars) and with 10ng of Flag TRBP/pcDNA 3.1<sup>-</sup> (red bars) or with Flag PACT/pCMV2 (green bars).  $\beta$ -Galactosidase activity was assayed 24 hours post-transfection. Error bars indicate standard deviation calculated from three independent experiments. The *P*-values (0.0011 and 0.0004)

**Figure 2.1 (continued)** calculated using statistical analyses indicated significant difference between the RLU values indicated by the brackets marked as ‘\*’ and ‘\*\*\*’ respectively.

**D. PACT and TRBP have no effect on HIV-1 LTR driven expression in the absence of Tat.**

HeLa-MAGI-CCR5 cells were transfected with 0 (black bar), or increasing amounts of Flag TRBP/pcDNA 3.1- (red bars), or Flag PACT/pCMV2 (green bars).  $\beta$ -Galactosidase activity was assayed 24 hours post-transfection. All transfections were compensated to the same amount of DNA with pcDNA 3.1. Error bars indicate standard deviation calculated from three independent experiments. The *P*-values (0.3863 and 0.9124) calculated using statistical analyses indicated no significant difference between the RLU values indicated by the brackets marked as ‘#’ and ‘##’ respectively.

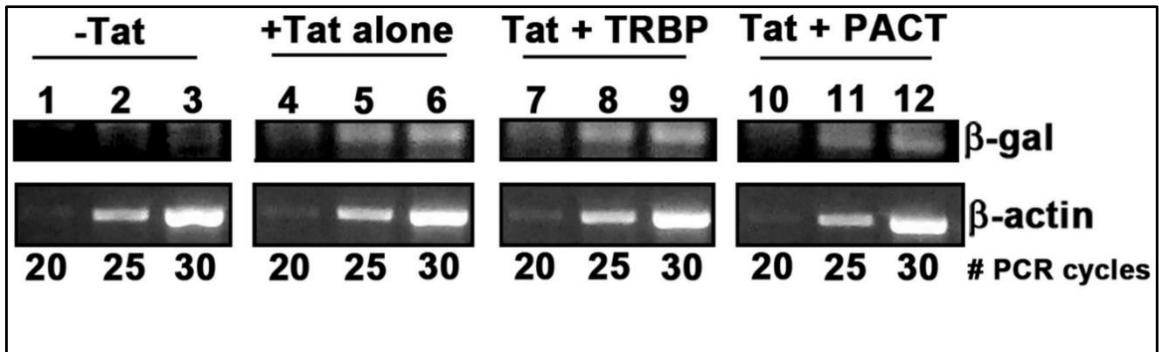


**Figure 2.2: PACT does not increase the steady –state mRNA levels of HIV-1 LTR-driven  $\beta$ -galactosidase.**

RNA was isolated from HeLa-MAGI-CCR5 cells transfected with pcDNA 3.1<sup>+</sup> only (-Tat, lanes 1-3), Tat/pcDNA 3 (+ Tat alone, lanes 4-6), Tat/pcDNA 3 and Flag TRBP/pcDNA 3.1<sup>+</sup> (Tat + TRBP, lanes 7-9), or Tat/pcDNA 3 and Flag PACT/pCMV2 (Tat + PACT, lanes 10-12). The RNA preparation was treated extensively with DNase to digest any DNA contamination.  $\beta$ -Galactosidase mRNA expression levels were analyzed by semi-quantitative RT-PCR at the indicated number of reaction cycles.  $\beta$ -actin mRNA levels were also analyzed as a normalization control for each cycle number. No PCR products were obtained in the absence of reverse transcriptase.

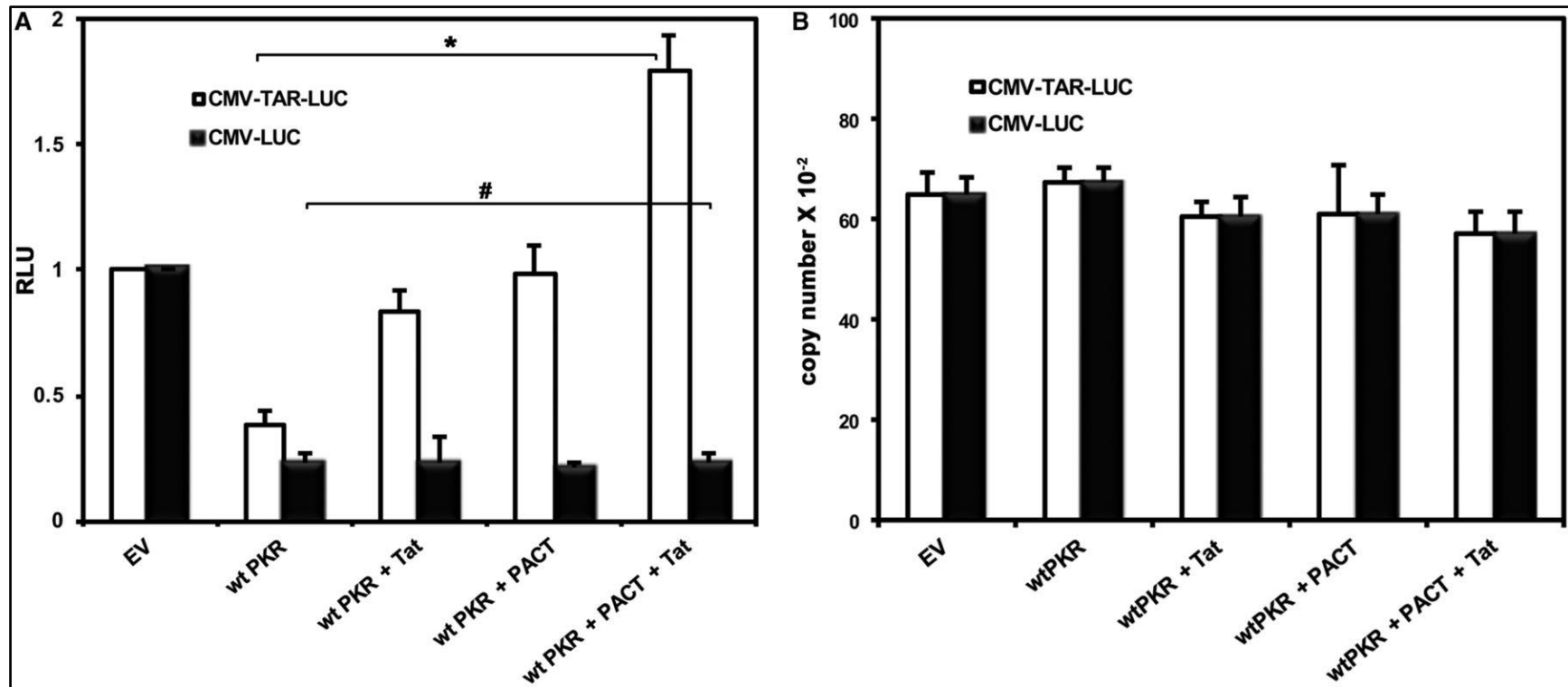


**Figure 2.3: PACT inhibits PKR activation induced by TAR-containing mRNAs.**

**A. Tat enhances PACT mediated PKR inhibition on TAR containing mRNAs.** PKR<sup>-/-</sup> MEFs were co-transfected with CMV-TAR-Luciferase or CMV-Luciferase (in pGL3 Basic plasmid backbone), and indicated combinations of Tat/pcDNA3, Flag PKR/pcDNA 3.1<sup>-</sup>, and Flag PACT/pCMV2. Firefly luciferase activity was assayed 24 h post-transfection and the error bars represent the standard deviation from three experiments. The *P*-values (0.0018 and 0.4601) calculated using statistical analyses indicated significant and non-significant differences between the RLU values indicated by the brackets marked as '\*' and '#' respectively.

**Figure 2.3 (continued) B. qRT-PCR analysis.** qRT-PCR analysis was performed to analyze luciferase mRNA expression levels in samples from PKR<sup>-/-</sup> MEFs transfected as described in **A**. Data represents the average from six replicate experiments from two different RNA isolations. All results are normalized to  $\beta$ -actin.



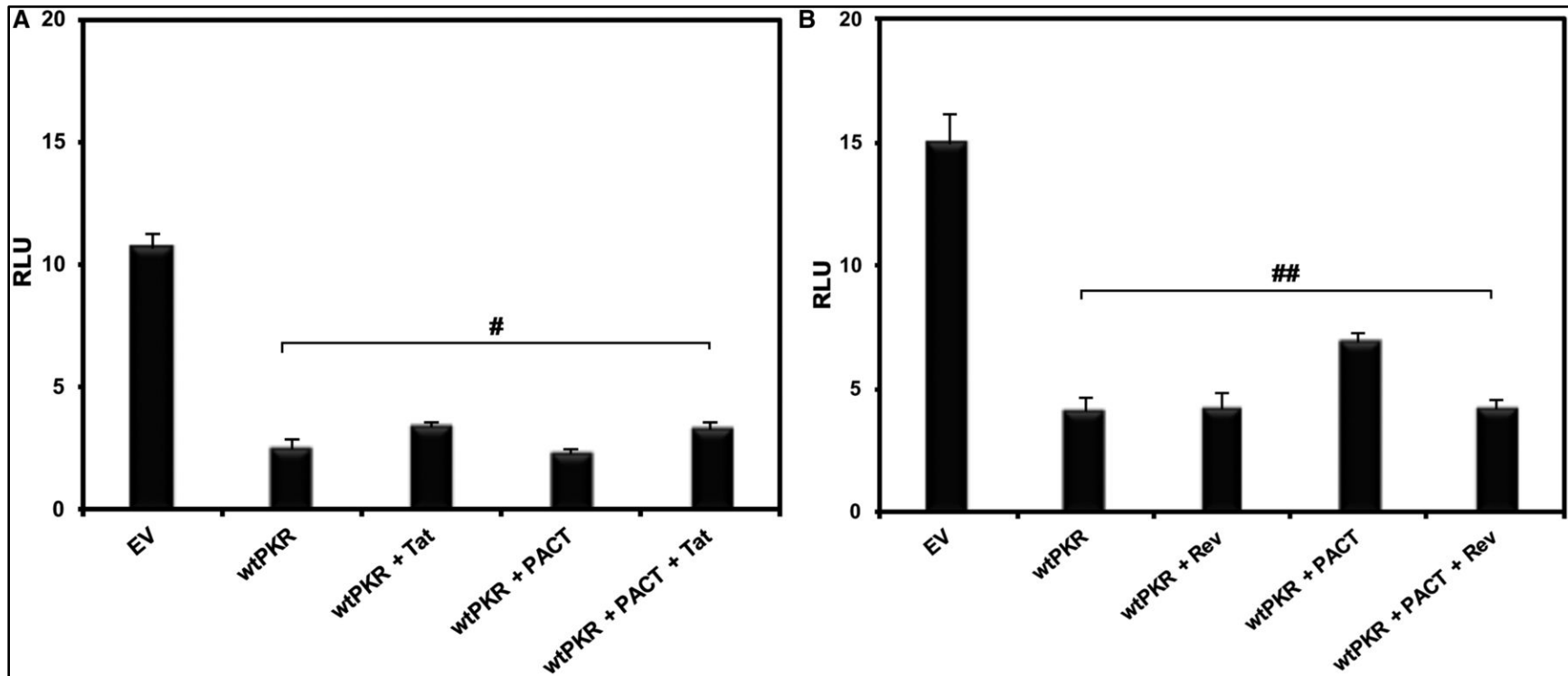


**Figure 2.4: Tat serves a specific function in mediating inhibition of PKR.**

**A. Tat's binding to the TAR is essential for PACT mediated PKR inhibition.** PKR<sup>-/-</sup> MEFs were co-transfected with CMV mutant-TAR Luciferase (in pGL3-Basic plasmid backbone:EV) in which the mutant TAR element does not bind to Tat and the indicated combinations of Tat/pcDNA 3, Flag PKR/pcDNA 3.1<sup>-</sup>, and Flag PACT/pcMV2. Firefly Luciferase activity was assayed 24 h post-transfection and the error bars represent the standard deviation from three experiments. The *P*-value (0.5852) calculated using statistical analyses indicated a non-significant difference between the RLU values indicated by the bracket marked as '#'.

**B. Rev, another HIV-1 encoded RNA-binding protein cannot substitute for Tat's function.** PKR<sup>-/-</sup> MEFs were co-transfected with the CMV TAR Luciferase expression construct and the indicated combinations of Rev/pcDNA 3, Flag PKR/pcDNA 3.1<sup>-</sup>, and Flag PACT/pcMV2. Luciferase activity was assayed 24 h after transfection and the error bars represent the standard deviation from three

**Figure 2.4 (continued)** experiments. The  $P$ -value (0.5852) calculated using statistical analyses indicates no significant difference between the RLU values indicated by the bracket marked as '##'.

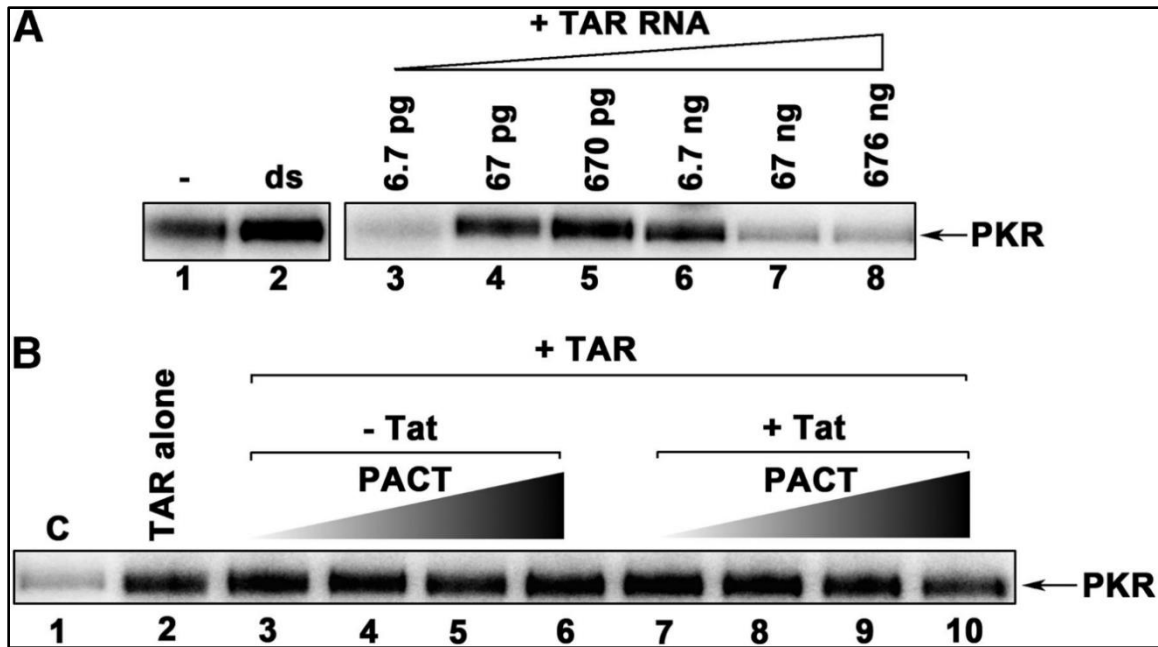


**Figure 2.5: PACT and Tat are insufficient to inhibit TAR RNA dependent PKR activation.**

**A. TAR RNA activates PKR:** PKR immunoprecipitated from HeLaM cell extracts was activated by the addition of increasing amounts of TAR RNA as indicated (Lanes 3-8) or poly I:poly C (Lane 2, ds). Lane 1 indicates activity in the absence of any activator. The phosphorylated proteins were analyzed by SDS-PAGE and phosphorimager analysis.

**B. Efficient inhibition of PKR requires components in addition to PACT and Tat.** PKR immunoprecipitated from HeLaM cell extracts was activated with 67 pg TAR RNA [Lanes 2-10]. Increasing amounts of pure recombinant PACT [Lanes 3-6 and Lanes 7-10] were added in absence of Tat [Lanes 3-6] or in combination with 4 ng of pure recombinant Tat [Lanes 7-10]. PACT amounts are as follows: 4 pg [Lanes 3 and 7], 40 pg [Lanes 4 and 8], 400 pg [Lanes 5 and 9], and 4 ng [Lanes 6 and 10]. Lane 1 (C) shows the PKR activity without any added activator. The phosphorylated proteins were analyzed by SDS-PAGE and phosphorimager analysis.

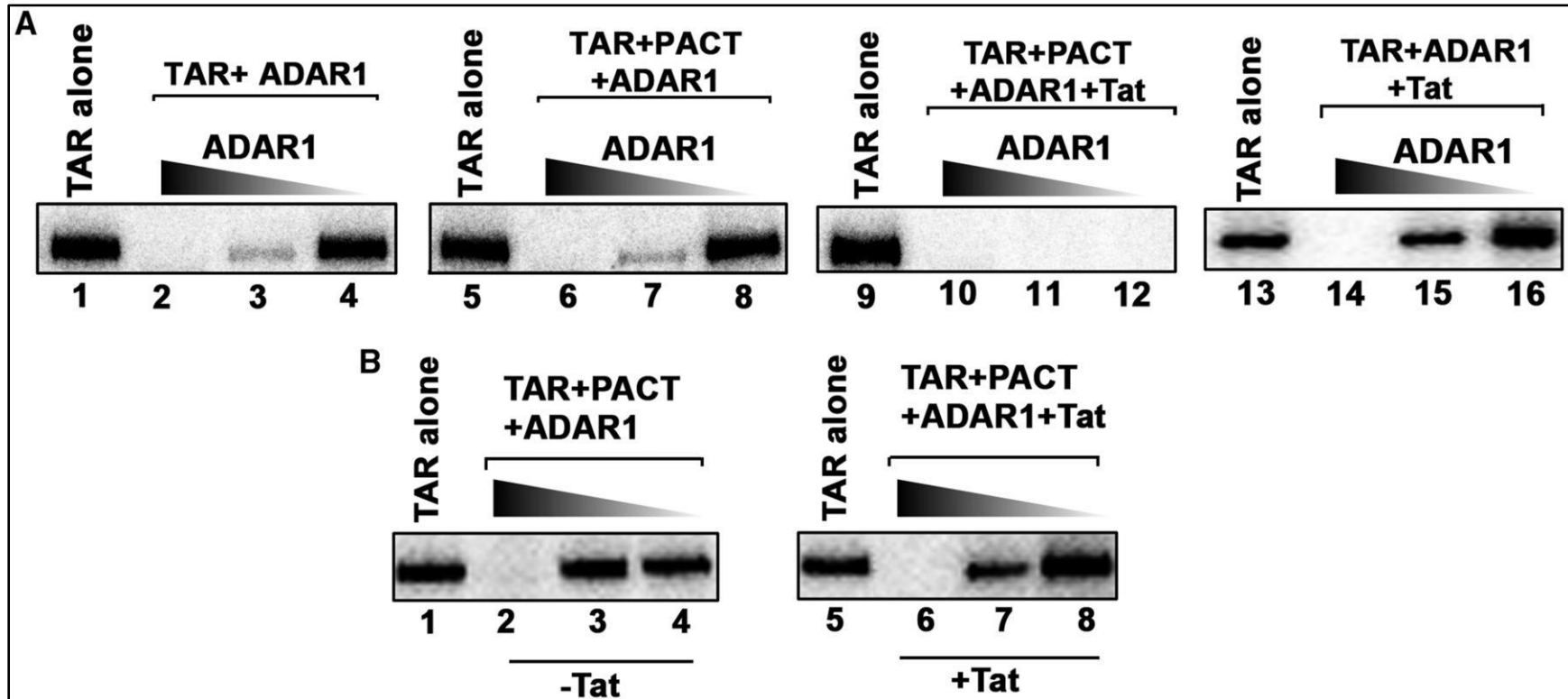


**Figure 2.6. ADAR1 is essential for an efficient inhibition of PKR.**

**(A) ADAR1, PACT, and Tat inhibit PKR efficiently.** PKR immunoprecipitated from HeLaM cell extracts was activated with 67 pg of TAR RNA and varying amounts (150, 15, and 1.5 ng) of ADAR1 (Lanes 2-4, lanes 6-8, 10-12, and 14-16) were added as indicated to assess the inhibition of PKR. Lanes 2-4: PKR activity in presence of varying amounts of ADAR1; Lanes 6-8: PKR activity in the presence of 4 ng of PACT and varying amounts of ADAR1, lanes 10-12: PKR activity in the presence of 4 ng of PACT, 4 ng of Tat, and varying amounts of ADAR1; lanes 14-16: PKR activity in the presence of 4 ng of Tat and varying amounts of ADAR1. The phosphorylated proteins were analyzed by SDS-PAGE and phosphorimager analysis.

**Figure 2.6 (continued) B. ADAR1 and PACT inhibit PKR more efficiently in the presence of Tat.** PKR immunoprecipitated from HeLaM cell extracts was activated with 67 pg of TAR RNA and varying amounts (1.5 ng, 150 pg, and 15 pg) of ADAR1 (Lanes 2-4 and lanes 6-8) were added as indicated to assess the inhibition of PKR. Lanes 2-4: PKR activity in presence of varying amounts of ADAR1 and 4 ng of PACT; Lanes 6-8: PKR activity in the presence of varying amounts of ADAR1, 4 ng of PACT, and 4 ng of Tat. The phosphorylated proteins were analyzed by SDS-PAGE and phosphorimager analysis.

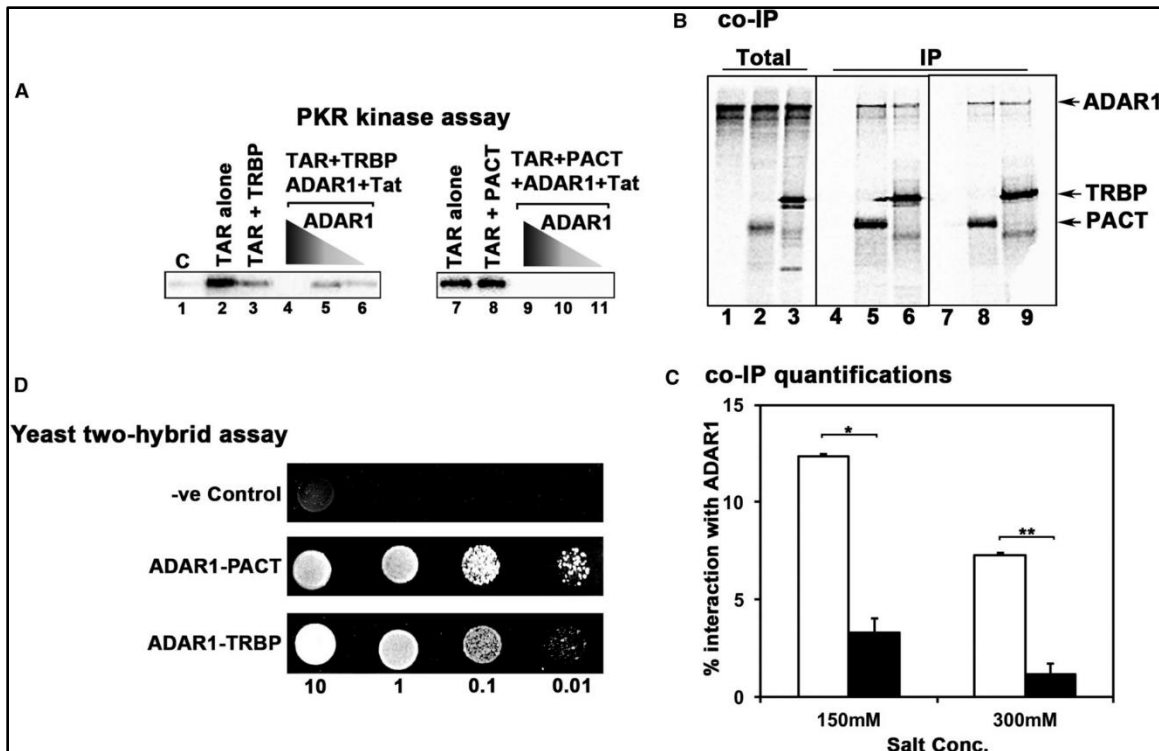


**Figure 2.7. Comparison of TRBP and PACT's PKR inhibitory activity on TAR RNA.**  
**(A) PACT is more efficient compared with TRBP in forming a PKR inhibitory complex.** PKR immunoprecipitated from HeLaM cell extracts was activated with 67 pg of TAR RNA. Either 4 ng of PACT (lane 2) or TRBP (lane 8) or 4 ng of TRBP (lanes 4-6) or PACT (lanes 9-11), 4 ng Tat, and varying amounts (150, 15, and 1.5 ng) of ADAR1 (Lanes 4-6 and 9-11) were added as indicated to assess the inhibition of PKR. Lanes 4-6 represent PKR activity in the presence of 4 ng of TRBP. Lanes 9-11 represent PKR activity in the presence of 4 ng of PACT. Lane 1 (C) shows the PKR activity without any added activator. The phosphorylated proteins were analyzed by SDS-PAGE and phosphorimager analysis.  
**(B) PACT interacts with ADAR1 with higher affinity when compared with TRBP.** A 5  $\mu$ l aliquot of *in vitro* translated,  $^{35}$ S-labeled Flag-tagged PACT and TRBP proteins was mixed with 5  $\mu$ l of *in vitro* translated,  $^{35}$ S-labeled ADAR1. Flag-PACT proteins were immunoprecipitated using anti-Flag mAb-agarose, and ADAR1 co-immunoprecipitation was analyzed by SDS-PAGE. Total: input (20% of the IP samples); IP: immunoprecipitates. The bands seen at lower positions than the TRBP band in lanes 3, 6, and 9 are truncated TRBP proteins produced by translation initiation at internal methionines in the reticulocyte lysate system.  
**(C) Quantification of data in B.** The radioactivity present in the bands was measured by phosphorimager analysis and the % co-IP was calculated as follows: (radioactivity present in the co-immunoprecipitated ADAR1 band/the radioactivity present in the ADAR1 band in the total lane) X 100. This value was normalized to the amount of radioactivity present in the PACT or TRBP bands in IP lanes to correct for differences in translation/immunoprecipitation. Error bars: standard deviation from three independent experiments. The *P*-values (0.000029 and 0.000051) calculated using

**Figure 2.7 (continued)** statistical analyses indicate significant difference between % co-IP of ADAR1 with PACT (white bars) and TRBP (black bars) at 150 mM (\*) and 300 mM (\*\*) salt concentrations respectively.

**(D) Yeast two-hybrid assay to compare TRBP-ADAR1 and PACT-ADAR1 interactions.**

TRBP or PACT in pGBKT7 and ADAR1 in PGADT7 or empty pGADT7 plasmids were co-transformed into AH109 yeast cells and selected on SD double dropout media lacking tryptophan, and leucine. Aliquots (10  $\mu$ l) of serial dilutions ( $OD_{600}$  = 10, 1.0, 0.1, 0.01) were spotted for each transformant on triple dropout SD medium plate that lacks tryptophan, leucine and histidine. Plates were incubated for three days at 30°C. Transformation of PACT or TRBP constructs in pGBKT7 and empty vector pGADT7 served as negative controls.

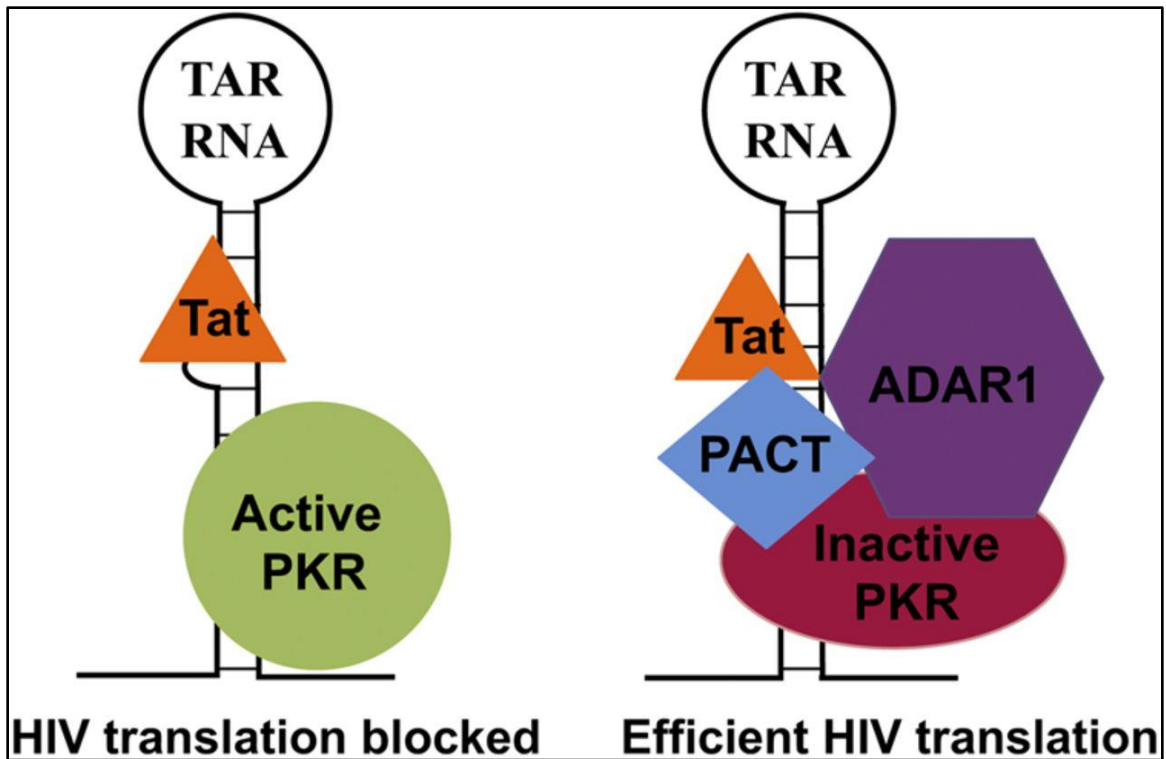


**Figure 2.8: Schematic model.** When TAR RNA present at the 5' end of HIV-1 encoded transcripts binds PKR, activated PKR blocks translation of TAR-containing HIV-1 mRNAs. Efficient translation of HIV-1 viral proteins occurs by recruiting viral protein Tat and host factors PACT and ADAR1, to efficiently block PKR activation, thereby allowing synthesis of viral proteins. In this complex, the PKR activating role of PACT is suppressed by the presence of ADAR1.



## CHAPTER 3

### STRESS-INDUCED TRBP PHOSPHORYLATION ENHANCES ITS INTERACTION WITH PKR TO REGULATE CELLULAR SURVIVAL<sup>3</sup>

---

<sup>3</sup> Chukwurah, E. and Patel R.C. Submitted to *Scientific Reports*, 2017

### 3.1 ABSTRACT

Transactivation response element RNA-binding protein (TRBP or TARBP2) initially identified to play an important role in human immunodeficiency virus (HIV) replication has also emerged as a regulator of microRNA biogenesis. In addition, TRBP functions in signaling pathways by negatively regulating the interferon-induced double-stranded RNA (dsRNA)-activated protein kinase (PKR) during viral infections and cell stress.

During cellular stress, PKR is activated and phosphorylates the  $\alpha$  subunit of the eukaryotic translation factor eIF2, leading to the cessation of general protein synthesis. TRBP inhibits PKR activity by direct interaction as well as by binding to PKR's two known activators, dsRNA and PACT, thus preventing their interaction with PKR.

In this study, we demonstrate for the first time that TRBP is phosphorylated in response to oxidative stress and upon phosphorylation, inhibits PKR more efficiently promoting cell survival. These results establish that PKR regulation through stress-induced TRBP phosphorylation is an important mechanism ensuring cellular recovery and preventing apoptosis due to sustained PKR activation.

### 3.2 INTRODUCTION

The double-stranded RNA (dsRNA)-activated protein kinase (PKR) is an interferon (IFN)-induced serine/threonine protein kinase expressed ubiquitously in mammalian cells<sup>108,121,168</sup>. Although IFNs induce expression of PKR at a transcriptional level, PKR's kinase activity stays latent until it binds to one of its activators leading to its autophosphorylation and catalytic activation<sup>169</sup>. The best-characterized cellular

substrate of PKR is the translation initiation factor, eIF2 $\alpha$ , the phosphorylation of which on serine 51 (S51) results in an inhibition of protein synthesis<sup>115,170</sup>. An immediate response of cells exposed to various forms of stress is a general inhibition of protein synthesis, which is mainly caused by the increased S51 phosphorylation of eIF2 $\alpha$ <sup>2</sup>. The eIF2 $\alpha$  phosphorylation thus serves an important function to block the general protein synthesis and allow cells to either recover from stress or undergo apoptosis when the damage is beyond repair<sup>1</sup>. PKR plays an important role in regulating apoptosis after exposure to several diverse stress signals that include viral pathogens, oxidative stress, endoplasmic reticulum (ER) stress, and growth factor or serum deprivation<sup>34,171</sup>.

During viral infections, the double-stranded dsRNA, which is a replication intermediate for several viruses<sup>172</sup>, activates PKR by a direct interaction. The dsRNA binds to PKR via the two dsRNA-binding motifs (dsRBMs) present at the N terminus<sup>45,173–175</sup>, changing the conformation of PKR to expose the ATP-binding site<sup>44,50</sup> and consequent autophosphorylation<sup>48</sup>. The two dsRBMs also mediate dsRNA-independent protein-protein interactions with other proteins that carry similar domains<sup>176,177</sup>. Among these are proteins inhibitory for PKR activity such as TAR RNA-binding protein (TRBP)<sup>95</sup>, and also a PKR activating protein (PACT)<sup>58,60</sup>. PKR activation in response to stress signals is tightly regulated by PACT and TRBP, both acting to regulate its catalytic activity by a direct interaction with PKR as well as with each other<sup>67,98</sup>. As the dsRBMs in PKR, PACT, and TRBP mediate protein-protein interactions<sup>178</sup>, these three proteins form both heterodimers as well as homodimers and the stress-dependent phosphorylation of PACT changes the relative strengths of PKR-PACT, PACT-TRBP, and PACT-PACT interactions to

bring about timely and transient PKR activation with precise control<sup>67,68</sup>. This regulates the general kinetics as well as level of eIF2 $\alpha$  phosphorylation thereby influencing the cellular response to stress either to recovery and survival or elimination by apoptosis<sup>179</sup>.

TRBP has three dsRBMs; the first two are true dsRBMs and interact with dsRNA, while the third carboxy-terminal dsRBM mediates TRBP's interactions with other proteins such as Dicer, and Merlin<sup>91,123,178</sup>. TRBP inhibits PKR by interacting with dsRNA and sequestering it away from PKR as well as by forming PKR-TRBP heterodimers<sup>95,120</sup>. In the absence of viral infections and stress signals, TRBP forms heterodimers with both PKR and PACT, preventing their association and PACT-mediated PKR activation<sup>97,180</sup>. Importantly, the stress-induced serine 287 phosphorylation of PACT decreases its interaction with the PKR inhibitory protein TRBP thereby further aiding in rapid PKR activation following exposure to stress signals<sup>67,180</sup>. In contrast, not much is known about how similar post-translational modifications may affect TRBP's interaction with PKR and consequently, its ability to inhibit PKR during cellular stress. Previous reports indicate that TRBP is phosphorylated by the two MAPKs; ERK 1/2 and JNK, with specific effects on RISC component stability and PKR activation by endogenous *Alu* transcripts during mitosis respectively<sup>92,181</sup>.

In this study, we used various biochemical assays to determine if TRBP undergoes stress-induced phosphorylation, and if this affects TRBP's ability to inhibit PKR during oxidative stress. Our findings implicate MAPKs (ERK1/2 and JNK) in oxidative stress-induced TRBP phosphorylation, and show that TRBP phosphorylation significantly

enhances TRBP's ability to interact with and inhibit PKR during oxidative stress to regulate apoptosis.

### 3.3 MATERIALS AND METHODS

#### 3.3.1 REAGENTS, CELL LINES AND ANTIBODIES.

HeLaM and HeLa Tet off cells were cultured in Dulbecco's Modified Eagle's Medium (DMEM) containing 10% fetal bovine serum and penicillin/streptomycin. Transfections were performed with Effectene Transfection Reagent (Qiagen) according to the manufacturer's protocol.

Tetracycline inducible cell lines stably expressing Flag TRBP were generated by transfection of HeLa Tet off cells with 500 ng of Flag TRBP/pTRE2pur expression plasmid. Selection of puromycin-resistant colonies was carried out 24 hours after transfection by the addition of 700 ng/ml puromycin. Another cell line was also established using the pTRE2 puro plasmid as a control. Doxycycline inducibility was quantified in Flag TRBP/pTRE2pur cell clones after removal of doxycycline by western blot analysis.

Sodium arsenite, phosphatase inhibitor cocktail (Phosphatase Inhibitor Cocktail 2 – P5726), and the JNK inhibitor (SP600125, Catalog number S5567) were purchased from Sigma Aldrich. MEK1/MEK2 inhibitor (PD0325901) was purchased from Calbiochem (444968).

Antibodies used are as follows: mouse monoclonal anti-FLAG M2 HRP (Sigma-Aldrich A8592), mouse monoclonal anti-c-Myc HRP 9E10 (Santa Cruz Biotechnology SC-40), mouse monoclonal anti-polyhistidine clone His-1 HRP (Sigma-Aldrich A7058), mouse

monoclonal anti-PKR (R&D systems MAB1980), rabbit polyclonal anti-phospho PKR Thr 451 (Cell Signaling Technology 3075), rabbit monoclonal anti-Phospho-p44/42 MAPK (Erk1/2) (Thr202/Tyr204) (D13.14.4E) XP<sup>®</sup> (Cell Signaling Technology 4370), rabbit monoclonal anti-p44/42 MAPK (Erk1/2) (137F5) (Cell Signaling Technology 4695), rabbit polyclonal anti-PARP (Cell Signaling Technology 9542), mouse monoclonal anti- $\beta$ -Actin HRP (Sigma-Aldrich A3854), mouse monoclonal anti-GAPDH HRP (Sigma-Aldrich G9295), goat anti-mouse IgG HRP (Sigma-Aldrich A3682), and goat anti-rabbit IgG HRP (BioRad 170-6515).

### 3.3.2 PLASMIDS

The Flag TRBP/BSIIS<sup>+</sup>, TRBP/pGBKT7, K296R PKR/pGAD424 and PKR /pYES2 expression plasmids were prepared as previously<sup>56,67,182</sup>. Full length TRBP1 ORF with an N-terminal Flag tag from Flag TRBP/BSIIS<sup>+</sup> was inserted into the *NotI* and *EcoRV* restriction sites of the tetracycline-responsive vector, pTRE2pur (Clontech) to generate Flag TRBP/pTRE2pur. The phospho-defective (TRBP AAAA) and phospho-mimic (TRBP DDDD) point mutants were generated at S121, S131, S262, and S265 by substituting each serine with alanine or aspartic acid using the following primers:

*TRBP sense:*

5'-GCTCTAGACATATGGAAATGCTGGCCGCAACC-3'

*S121D antisense:*

5'- GTTCCATGGCGGGGTCCCTGGTTAGGACTACAGATGGAACTGGGG-3'

*S121A antisense:*

5'- GTTCCATGGCGGGGGCCCTGGTTAGGACTACAGATGGAACTGGGG-3'

*S131D sense:*

5'-CGCCATGGAACTGCAGCCCCCTGTCGACCCTCAGC-3'

*S262D S265D antisense:*

5'CGGAGCTCACTGAGGACACGGCAGCAGGCAGGGCCCAGGGCACCCAGGTGCGCCAGGTTCGC  
AACTGC-3'

*S131A sense:*

5'- CGCCATGGAACTGCAGCCCCCTGTCGCCCTCAGC -3'

*S262A S265A antisense:*

5'CGGAGCTCACTGAGGACACGGCAGCAGGCAGGGCCCAGGGCACCCAGGGCGCCAGGGCG  
CAACTGC-3'

The PCR products were sub-cloned into the pGEMT-Easy vector (Promega) and each sequence was verified. Full length AAAA TRBP and DDDD TRBP point mutants were generated in the pGBKT7 yeast expression vector (Clontech) by three-piece ligation of *NdeI-NcoI* restriction fragment from S121A or S121D/pGEMT-Easy, *NcoI-SacI* restriction fragment from S131D S262D S265D or S131A S262A S265A/pGEMT Easy and *NdeI-SacI* cut TRBP/pGBKT7. Each point mutant was subsequently introduced into the pGADT7 yeast expression vector (Clontech) by insertion of the *NdeI-BamHI* restriction fragment from AAAA TRBP or DDDD TRBP/pGBKT7 into the *NdeI-BamHI* restriction sites in pGADT7.

Flag-tagged full length AAAA and DDDD TRBP point mutants in pcDNA 3.1<sup>+</sup> (Invitrogen) were generated by first introducing the *NdeI-BamHI* restriction piece from AAAA TRBP/pGBKT7 or DDDD TRBP/pGBKT7 into *NdeI-BamHI* cut Flag/TRBP BSIKS<sup>+</sup>, and then inserting the *XbaI-BamHI* restriction fragment from Flag/AAAA TRBP BSIKS<sup>+</sup> or Flag/DDDD TRBP BSIKS<sup>+</sup> into the *XbaI-BamHI* sites in pcDNA 3.1<sup>+</sup>. Myc-tagged full length AAAA and DDDD TRBP point mutants were generated by introducing *HincII-BamHI* restriction fragments from AAAA TRBP/pGBKT7 and DDDD TRBP/pGBKT7 into the *EcoRV-BamHI* restriction sites in pcDNA 3.1<sup>+</sup>.

### 3.3.3 DNA FRAGMENTATION ANALYSIS

5 X 10<sup>6</sup> Flag TRBP/pTRE2pur and pTRE2pur HeLa tet off cells described in “Reagents, Cell Lines and Antibodies” were treated with 10 μM sodium arsenite for the indicated time points. Cells were collected and washed with ice cold 1X PBS, and lysed in 100 μl of lysis buffer [10mM Tris-HCl pH 7.5, 10mM EDTA, and 0.5% Triton-X 100] for 5 minutes on ice. Lysates were centrifuged at 13200 rpm for 5 minutes, and were incubated with 100 μg Proteinase K at 37°C for 2 hours. 5 μl of 6M NaCl and 110 μl of isopropanol were subsequently added to the lysates which were then incubated at 20°C overnight. The precipitated DNA was then collected by centrifugation at 14,000 rpm for 5 minutes. After the isopropanol was removed from each sample, the DNA was dissolved in 20 μl TE Buffer [10 mM Tris-HCl pH 7.5, 10 mM EDTA]. The DNA was incubated with 20 μg/ml RNase A at 37°C for 1 hour before analysis on a 1.5% agarose gel.

### 3.3.4 WESTERN BLOT ANALYSIS

Cells were treated with sodium arsenite alone or in combination with 10 μM MEK1/MEK2 inhibitor PD0325901 (Calbiochem) or 10 μM JNK inhibitor SP600125 and harvested at indicated time points. Cells were washed twice with ice cold 1X PBS. Harvested cells were lysed in western lysis buffer [2% Triton X-100, 20 mM Tris-HCl pH 7.5, 100 mM KCl, 200 mM NaCl, 4 mM MgCl<sub>2</sub>, 40% Glycerol, and phosphatase inhibitor cocktail 2 (Sigma) at 1:100 dilution] for 5 minutes on ice. Lysates were centrifuged at 13,200 rpm for 2 minutes. Protein concentration in the supernatant was quantified



using Bradford reagent. Western blot was performed with the indicated antibodies and western blot images were analyzed using the Typhoon FLA 7000 and ImageQuant LAS 4000 (GE Health).

### 3.3.5 TRBP-PKR PULL-DOWN ASSAY

Flag TRBP/pTRE2pur HeLa Tet off cells grown to 50% confluency in 100-mm dishes were treated with 25  $\mu$ M sodium arsenite for the indicated time points. Cell extracts were prepared in 100  $\mu$ l co-immunoprecipitation buffer [20 mM Tris-HCl pH 7.5, 150 mM NaCl, 1 mM EDTA, 1 mM DTT, 1% Triton-X 100, 2% Glycerol, and phosphatase inhibitor cocktail 2 (Sigma) at 1:100 dilution]. 25  $\mu$ g of cell extract was bound to 500  $\mu$ g of recombinant, hexahistidine-tagged PKR (His-PKR) protein immobilized on Ni<sup>2+</sup>-agarose resin (Novagen) in 100  $\mu$ l co-immunoprecipitation buffer at 4°C for 1 hour.

The beads were washed in 500  $\mu$ l of co-immunoprecipitation buffer three times and bound Flag-TRBP was analyzed by western blot analysis using anti-Flag antibody. Blot was then stripped and re-probed with anti-His antibody to ascertain equal His-PKR pull down. 25  $\mu$ g aliquots of whole cell-lysate were analyzed by western blot analysis with anti-Flag and anti-GAPDH antibodies to ensure that equal amounts of cell lysate were used for immunoprecipitation.

### 3.3.6 TRBP-TRBP CO-IMMUNOPRECIPITATION ASSAY

HeLa cells were co-transfected in 6-well culture dishes with 250 ng each of (i) myc TRBP DDDD/ pcDNA 3.1<sup>+</sup> and Flag TRBP DDDD/ pcDNA 3.1<sup>+</sup> (ii) myc TRBP DDDD/

pcDNA 3.1<sup>+</sup> and pcDNA 3.1<sup>+</sup> (iii) myc TRBP AAAA/ pcDNA 3.1<sup>+</sup> and Flag TRBP AAAA/  
pcDNA 3.1<sup>+</sup>, (iv) myc TRBP AAAA/ pcDNA 3.1<sup>+</sup> and pcDNA 3.1<sup>+</sup> using the Effectene reagent  
(Qiagen). 24 hours after transfection, cell extracts were prepared in co-IP buffer (150  
mM NaCl, 30 mM Tris-HCl pH 7.5, 1 mM MgCl<sub>2</sub>, 10% Glycerol, 0.4% Igepal). Flag TRBP  
AAAA and Flag TRBP DDDD were immunoprecipitated with anti-Flag mab-agarose  
(Sigma) in co-IP buffer. The agarose beads were washed 5 times in co-IP buffer. The  
bound proteins were then analyzed by western blot analysis with the anti-c-myc (Santa  
Cruz Biotechnology) and anti-Flag (Sigma) antibodies.

### 3.3.7 YEAST GROWTH INHIBITION ASSAY

Wild-type and TRBP phospho-mimic and phospho-defective point mutants were  
subcloned into the pYES3CT yeast expression plasmid (Invitrogen). Wild-type PKR was  
subcloned into the pYES2 yeast expression vector (Invitrogen) as previously described  
for galactose inducible PKR expression. The constructs were introduced into InvSc1  
yeast cells (Invitrogen) using the Clontech Yeast Transformation Kit. Transformed yeast  
cells were grown to an OD<sub>600</sub> of 2 in YPD media (yeast extract, peptone, and dextrose).  
500 µl of each culture was pelleted and resuspended in an appropriate amount of  
distilled water to yield an OD<sub>600</sub> of 10. Serial dilutions were then made to yield OD<sub>600</sub>  
values of 1, 0.1, and 0.01. 10 µl of each dilution was then spotted onto synthetic  
medium lacking uracil and tryptophan and containing either glucose or galactose as a  
carbon source (Clontech).

### 3.3.8 YEAST TWO-HYBRID INTERACTION ASSAY

To test TRBP-PKR interaction, full length K296R PKR was expressed as a GAL4 DNA-activation domain fusion protein from the pGAD424 vector and the AAAA and DDDD TRBP point mutants were expressed as GAL4 DNA-binding domain fusion proteins from the pGBKT7 vector. Full length AAAA and DDDD TRBP point mutants were expressed as GAL4 DNA-activation domain fusion proteins from the pGADT7 vector and GAL4 DNA-binding domain fusion proteins from the pGBKT7 vector to test TRBP-TRBP interaction. The AAAA TRBP and DDDD TRBP pGBKT7 /pGADT7 construct pairs and PKR/pGAD424 and AAAA (DDDD) TRBP/pGBKT7 construct pairs were co-transformed into AH109 yeast cells (Clontech) and the transformed yeast cells were plated on double dropout SD minimal medium lacking tryptophan and leucine. In order to check for the transformants' ability to grow on triple dropout media, transformed yeast cells were grown to an OD<sub>600</sub> of 2 in YPD media (yeast extract, peptone, and dextrose). 500 µl of each culture was pelleted and resuspended in an appropriate amount of distilled water to yield an OD<sub>600</sub> of 10. Serial dilutions were then made to yield OD<sub>600</sub> values of 1, 0.1, and 0.01. 10 µl of each dilution was then spotted onto triple dropout SD minimal media lacking histidine, tryptophan, and leucine in the presence of 10 mM 3-amino-1,2,4-triazole (3-AT). Plates were incubated at 30°C for 5 days.

### 3.3.9 APOPTOSIS ASSAY

HeLa cells were grown to 50% confluency in six-well plates and co-transfected with 200 ng of Flag TRBP AAAA or TRBP DDDD/pcDNA 3.1<sup>+</sup> and 200 ng of pEGFPC1

(Clontech) using Effectene (Qiagen). Cells were also co-transfected with 200 ng BSIKS<sup>+</sup> (Agilent) and 200 ng pEGFPC1 as a control. The cells were observed for GFP fluorescence 24 hours after transfection using an inverted fluorescence microscope (EVOS<sup>®</sup> FL Imaging System). Cells were treated with 25  $\mu$ M sodium arsenite, and cellular morphology was monitored at 1 hour intervals. 12 hours after treatment, the cells were rinsed with ice-cold phosphate buffered saline (PBS) and fixed in 2% paraformaldehyde for 10 minutes. Cells were washed twice in ice-cold PBS and permeabilized with 0.1% Triton-X for 10 minutes, after which the cells were washed twice in ice-cold PBS. Cells were stained with the DAPI nuclear stain (4,6-diamidino-2-phenylindole) at 0.5  $\mu$ g/ml in for 10 minutes at room temperature in the dark. The cells were rinsed once with PBS and viewed under the fluorescent microscope.

At least 300 GFP-positive cells were counted as apoptotic or live based on their morphology. Cells showing normal flat morphology were scored as live, while cells showing cell shrinkage, membrane blebbing, rounded morphology and nuclear condensation with intense fluorescence as apoptotic. The percentage of cells undergoing apoptosis (*Percent apoptosis*) was calculated using the formula: (EGFP-expressing cells with intense DAPI nuclear staining/Total EGFP-expressing cells) x 100.

### 3.3.10 PKR-INHIBITION AND APOPTOSIS ASSAY

HeLa cells were grown on coverslips and transfected with 500 ng of wt PKR pEGFPC1 and 20 ng pcDNA 3.1<sup>+</sup>, Flag TRBP AAAA/ pcDNA 3.1<sup>+</sup>, or Flag TRBP DDDD/ pcDNA 3.1<sup>+</sup> using Effectene (Qiagen). 24 hours after transfection, the cells were rinsed

with ice-cold phosphate buffered saline (PBS) and fixed in 2% paraformaldehyde for 10 minutes. Cells were washed twice in ice-cold PBS and permeabilized with 0.1% Triton-X for 10 minutes, after which the cells were washed twice in ice-cold PBS. The cover slips were mounted in Vectashield mounting medium containing DAPI (Vector Laboratories). Cells were then viewed under the fluorescence microscope (EVOS® FL Imaging System). At least 500 EGFP-positive cells were scored as live or apoptotic as described in 'Apoptosis Assay'.

### 3.3.11 ESTIMATION OF MITOCHONDRIAL MEMBRANE POTENTIAL.

HeLa cells were grown to 50% confluency in six-well plates and transfected with 500 ng of wt PKR pEGFPC1 and 20 ng pcDNA 3.1<sup>+</sup>, Flag TRBP AAAA/ pcDNA 3.1<sup>+</sup>, or Flag TRBP DDDD/ pcDNA 3.1<sup>+</sup>. MitoPT® TMRM assay was performed using the manufacturer's instructions (ImmunoChemistry Technologies MitoPT® TMRM Assay Kit). Green fluorescence (EGFP-PKR) and changes in red fluorescence (changes in mitochondrial polarization) were observed under an inverted fluorescence microscope (EVOS® FL Imaging System). At least 500 PKR expressing cells (GFP positive cells) were scored as live or dead based on decreased or absent red fluorescence. The percentage of cells undergoing apoptosis (*Percent apoptosis*) was calculated using the formula: (EGFP- expressing cells with decreased or absent red fluorescence/Total EGFP- expressing cells) x 100.

### 3.3.12 STATISTICAL ANALYSIS

Statistical significance of western blot quantifications and percent apoptosis were determined by two-tailed Student's T-test assuming equal variance or one-way ANOVA followed by post-Hoc Tukey test respectively. Figure legends indicate the statistical test used, and *P*-values are denoted by brackets and special characters. Alpha level was  $p = 0.05$ .

## 3.4 RESULTS

### 3.4.1 TRBP OVEREXPRESSION INHIBITS OXIDATIVE STRESS-INDUCED APOPTOSIS.

To evaluate TRBP's effect on the cellular response to oxidative stress, we established a stable HeLa-Tet off cell line that would conditionally overexpress Flag-TRBP only when doxycycline was absent from the growth medium. A HeLa-Tet off cell line with stably transfected empty vector pTRE2pur was established as a control. We initially characterized 20 individual puromycin resistant clones and selected one clone that showed the least expression of Flag-TRBP in the presence of doxycycline and showed a good induction of Flag-TRBP expression in the absence of doxycycline. As seen in Figure 3.1A, the Flag-TRBP expression is induced to high levels in a time dependent manner after removal of doxycycline from the growth medium (lanes 2-5). We used these cells for assaying the effects of TRBP overexpression on apoptosis induced by oxidative stress. After the cells were grown in doxycycline-deficient growth medium for 24h, they were exposed to sodium arsenite to induce oxidative stress. The cells were thus expressing high levels of Flag-TRBP when exposed to oxidative stress and this

allowed us to assay the effect of TRBP overexpression on cellular apoptosis and PKR activation.

In order to compare the relative apoptosis in control and TRBP overexpressing cells we used DNA fragmentation analysis. DNA fragmentation is a late marker of apoptotic cells as the DNA is cleaved by caspase-activated DNases (CADs) into nucleosomal fragments of 180 bp<sup>183</sup>. As seen in Figure 3.1B, the control cells stably transfected with empty vector (EV-HeLa) showed high levels of DNA fragmentation in response to sodium arsenite (lanes 5-8). In comparison, the cells overexpressing Flag-TRBP (TRBP-HeLa) have significantly less DNA fragmentation after exposure to sodium arsenite (lanes 1-4). These results indicate that TRBP overexpressing cells are significantly protected from oxidative stress-induced apoptosis.

In order to further assess the protection from cellular apoptosis by TRBP overexpression, we compared the cleavage of Poly-ADP Ribose Polymerase (PARP1) in response to arsenite treatment. The 116 kDa protein PARP1 is cleaved into an 89kDa fragment by Caspase-3 in response to apoptosis-inducing stimuli<sup>184</sup>. We measured and quantified PARP1 cleavage in both sets of cells after treatment with arsenite (Figure 3.1C and 3.1D). As seen in Figure 3.1C, there is a steady increase in the levels of cleaved PARP1 in the control (EV-HeLa) and TRBP-overexpressing (TRBP-HeLa) cells in a time dependent manner. After 24 hours of arsenite exposure, there is significantly more cleaved PARP1 in the EV-HeLa cells (Lane 4) as compared to the TRBP-HeLa cells (Lane 8). The percentage of cleaved PARP1 is about 90% in the HeLa cells (Figure 3.1D, 24 hr.), and only about 45% in the TRBP-HeLa cells (Figure 3.1D, 24 hr.). These results indicate

that caspase-3 activation and subsequent PARP1 cleavage is significantly impaired in cells overexpressing TRBP, and demonstrate that TRBP overexpression protects the cells from apoptosis in response to oxidative stress.

#### 3.4.2 BOTH ERK AND JNK PHOSPHORYLATE TRBP IN RESPONSE TO OXIDATIVE STRESS

In order to determine if TRBP undergoes post-translational modifications in response to stress signals with any functional implications on TRBP's ability to inhibit PKR, we performed western blot analysis of extracts from TRBP-HeLa cells exposed for 24 hours to sodium arsenite. The analysis revealed the presence of an additional Flag-TRBP band with reduced electrophoretic mobility as indicated by an asterisk (Fig. 3.2A) that increased in intensity from 8 to 12 hours after arsenite treatment and declined at 24 hours after treatment (Figure 3.2A, Flag-TRBP panel, Lanes 5 - 8). These results suggested that the slow migrating Flag-TRBP band may be indicative of TRBP phosphorylation at late time points after arsenite exposure. Interestingly, we also noted that the strengthening of the TRBP doublet banding pattern from 8 to 12 hours after treatment coincides with the gradual decrease in phosphorylated eIF2 $\alpha$  levels at these time points after sodium arsenite treatment (Figure 3.2B: p-eIF2 $\alpha$  panel, Lanes 6-8) and a decrease in phosphorylated PKR levels (Figure 3.2B: p-PKR panel, Lanes 5 -8). These results suggest that TRBP phosphorylation may regulate PKR activation and consequent eIF2 $\alpha$  phosphorylation in response to arsenite.

To test this, we investigated if the slow migrating TRBP band resulted from phosphorylation by using phosphatase treatment in the presence and absence of



phosphatase inhibitors. Phosphatase treatment of cell extract prepared 8 and 12 hours after arsenite treatment completely removed the stress-induced slow-migrating band (Figure 3.2C, lanes 5 and 8), demonstrating that the slower mobility band (denoted 'p-TRBP') did result from TRBP phosphorylation in response to oxidative stress. The p-TRBP band persisted when the phosphatase treatment was performed in the presence of phosphatase inhibitors, thereby confirming that the disappearance of the band in lanes 5 and 8 was indeed due to phosphatase activity and not due to the presence of any contaminating proteolytic activity. These results indicate a possible link between the timing of PKR activation and its eventual inactivation during cell stress and the timing of TRBP phosphorylation in response to oxidative stress.

The Mitogen-activated protein kinase (MAPK) signaling pathways are activated in response to diverse stimuli<sup>185</sup>, and elicit either pro-apoptotic or pro-survival cellular responses. Previous studies have demonstrated that MAPKs such as the Extracellular-signal regulated Kinase (ERK 1/2) and c-Jun N-terminal kinase (JNK) play important roles in mediating the cellular response to oxidative stress<sup>186</sup>. To test if ERK 1/2 phosphorylates TRBP in response to oxidative stress, we pretreated the Flag TRBP overexpressing cells with the MEK inhibitor PD0325901, and exposed the cells to sodium arsenite. In the samples not pretreated with PD0325901, we observed the p-TRBP band at 8 and 12 hrs. after treatment (Figure 3.2D: TRBP panel, Lanes 1 -4).

Furthermore, we also observed that the increase in TRBP phosphorylation closely mirrored the increase in phospho-ERK levels at 8, and 12 hours of treatment (Figure 3.2D, p-ERK panel, Lanes 1-4). With the inhibition of ERK phosphorylation,

(Figure 3.2D, p-ERK panel, Lanes 5-8) the p-TRBP band is significantly diminished (Figure 3.2D, TRBP panel, Lanes 5-8). To test if JNK also phosphorylates TRBP in response to oxidative stress, we pretreated the Flag TRBP overexpressing cells with the JNK inhibitor SP600125, and exposed the cells to sodium arsenite. In the samples not pretreated with SP600125, we observed the p-TRBP band at 8 and 12 hrs after treatment (Figure 3.2E: TRBP panel, Lanes 1-4). Furthermore, we also observed that the increase in TRBP phosphorylation closely mirrored the increase in phospho-JNK levels at 8, and 12 hours of treatment (Figure 3.2E, p-ERK panel, Lanes 1-4). With the inhibition of JNK phosphorylation, (Figure 3.2E, p-JNK panel, Lanes 5-8) the p-TRBP band is completely absent (Figure 3.2E, TRBP panel, Lanes 5-8). The results in Figures 3.2D and 3.2E suggest that both ERK and JNK phosphorylate TRBP in response to oxidative stress.

#### 3.4.3 EFFECT OF TRBP PHOSPHORYLATION ON CELLULAR RESPONSE TO STRESS

Having demonstrated that TRBP is phosphorylated by JNK and ERK 1/2 in response to oxidative stress, we wanted to determine how TRBP phosphorylation affects oxidative stress and PKR-mediated cellular apoptosis. To evaluate the involvement of phosphorylation, we generated a phospho-defective TRBP point mutant (TRBP AAAA) which contains alanine for serine substitution at 4 sites (S142, S152, S283, S286) previously identified as MAPK/ERK 1/2 substrate sites<sup>181</sup>. Of these sites, S142 and S152 have also been previously shown to be phosphorylated by JNK<sup>92</sup>. A phospho-mimic TRBP point mutant (TRBP DDDD) was also generated by substituting aspartic acid for serine at the same four sites (Figure 3.3A).

To examine the effect of TRBP phosphorylation on oxidative stress-induced apoptosis, we transfected HeLa cells with each TRBP phospho-mutant and observed changes in the induction of apoptosis in response to oxidative stress. As seen in Figure 3.3B, the cells transfected with the empty vector (EV) alone showed 5.6% apoptosis (Untreated, black bar) in the absence of stress which increased to 46.9% at 24 h after sodium arsenite treatment (24 hrs, black bar). The DDDD TRBP phospho-mimic mutant showed significantly reduced apoptosis in response to oxidative stress with only 29.1% cells undergoing apoptosis at 24 h after treatment (24 hrs, red bar).

Statistical analysis also showed a significant difference between the % apoptosis in the cells expressing the empty vector as compared to the cells expressing the TRBP phospho-mimic mutant, indicating that TRBP phosphorylation does have a protective effect on cells during oxidative stress. Analysis of the % apoptosis in the cells expressing the AAAA TRBP phospho-defective mutant to that of cells expressing EV showed no statistical difference, highlighting the importance of phosphorylation for TRBP's anti-apoptotic activity.

We next examined the effect of TRBP phosphorylation on PKR-induced apoptosis. An overexpression of active PKR in mammalian cells is sufficient to trigger cellular apoptosis in the absence of any stress signals<sup>187,188</sup>. It has been previously observed by us and others that PKR-EGFP fusion construct encodes a constitutively active PKR, which induces apoptosis when transfected in mammalian cells<sup>189</sup>. Thus, cells were transfected with a constitutively active PKR expression plasmid (wt-PKR-EGFP+EV) or in combination with the TRBP AAAA phospho-defective or DDDD phospho-mimic mutant and assayed for changes in apoptosis induced by active PKR. We

used nuclear condensation as a hallmark sign of apoptosis as indicated by intense DAPI fluorescence<sup>190</sup>. There is a significant amount of apoptosis at 87.5% (Figure 3.3C, wt PKR, black bar) in transfected cells that express constitutively active PKR. The percentage cell death is significantly reduced with the co-expression of both AAAA phospho-defective (65.9 %) and DDDD phospho-mimic TRBP (49.5 %) mutants with PKR-EGFP (Figure 3.3C, wt PKR + AAAA and wt PKR + DDDD, blue and red bars). Consistent with our previous results in Figure 3.3A, we also observe greater reduction in apoptosis with expression of the TRBP phospho-mimic mutant, indicating that although AAAA phospho-defective mutant can still inhibit PKR, the DDDD phospho-mimic mutant inhibits PKR much more efficiently.

We further assayed apoptosis by using the mitochondrial membrane depolarization as an early marker for apoptotic cells<sup>191</sup>. The effect of TRBP phospho-mutants (TRBP AAAA or TRBP DDDD) on apoptosis induced by constitutively active PKR-EGFP was measured. Similar to our result in Figure 3.3C, we observed apoptosis (~75 %) in cells expressing constitutively active PKR. Cells co-expressing the AAAA TRBP phospho-defective mutant had a 16 % decrease in cell death compared to the cells expressing PKR-EGFP alone, while the cells co-expressing the DDDD TRBP phospho-mimic mutant had a 63% decrease in cell apoptosis compared to the cells expressing PKR-EGFP alone. Taken together, these results clearly demonstrate that TRBP phosphorylation is protective during oxidative stress, and this protection is mediated via inhibition of PKR.

#### 3.4.4 TRBP PHOSPHORYLATION INHIBITS PKR'S KINASE ACTIVITY MORE EFFICIENTLY

To determine if protection from apoptosis was a direct result of enhanced PKR inhibition by the phosphorylated TRBP isoform, we performed a yeast growth inhibition assay using the INVSc1 *S. cerevisiae* yeast strain (Figure 3.4). The expression of active PKR in *S. cerevisiae* suppresses yeast growth, and this growth inhibition can be reversed by co-expression of PKR inhibitors such as the dominant negative PKR mutant, K296R<sup>58,173,192</sup>. We introduced a galactose-inducible wt PKR yeast expression plasmid (wt PKR/pYES2) in combination with K296R, wt TRBP, AAAA TRBP, or DDDD TRBP expression plasmids (pYES3CT) into INVSc1 yeast cells. As expected, induction of PKR expression on galactose-containing media inhibited yeast cell growth (+ GAL panel, wt PKR alone). We also observed that co-expression of K296R or wt TRBP reversed the PKR-mediated growth phenotype (+ GAL panel, K296R, wt TRBP) in accordance with previous reports that have shown that K296R and TRBP inhibit PKR activity<sup>96,97</sup>. Interestingly, when we co-expressed the phospho-deficient TRBP mutant (AAAA TRBP), it was unable to reverse the growth phenotype (compare wt PKR alone to AAAA TRBP, + GAL panel) suggesting that TRBP phosphorylation is crucial for TRBP's ability to inhibit PKR.

On the other hand, co-expression of the phospho-mimic TRBP mutant (DDDD TRBP) reversed the PKR-mediated growth inhibition more efficiently as compared to wt TRBP. These results indicate that phosphorylated TRBP inhibits PKR's kinase activity in a more efficient manner.

### 3.4.5 STRESS-INDUCED TRBP PHOSPHORYLATION ENHANCES TRBP-PKR INTERACTIONS, WHILE WEAKENING TRBP-TRBP INTERACTIONS.

To understand how stress-induced phosphorylation of TRBP affects its interaction with PKR, we used the yeast-two hybrid system to test the strength of interaction between PKR and TRBP phospho-mimic and phospho-defective point mutants. The TRBP DDDD and TRBP AAAA point mutants were expressed in yeast as GAL4 DNA binding domain fusion proteins (pGBKT7) with PKR was expressed as a GAL4 activation domain fusion protein. In this system, a stronger interaction between TRBP and PKR is indicated by increased yeast growth in media lacking tryptophan, leucine, and histidine in the presence of the imidazole glycerol-phosphate dehydratase competitive inhibitor, 3-Amino-1,2,4-triazole (3-AT). As seen in Figure 3.5A, the TRBP DDDD point mutant shows significantly stronger interaction with PKR as compared to the TRBP AAAA point mutant, suggesting that the stronger PKR inhibition by DDDD TRBP we observed in Figures 3.3 and 3.4 results from an enhanced TRBP-PKR interaction.

Since we showed enhanced interaction with PKR resulting in more efficient PKR inhibition with the phospho-mimic DDDD TRBP mutant, we tested if we would also observe significantly increased TRBP-PKR interaction in response to arsenite at 8 and 12 hours post-treatment when we observe the strongest TRBP phosphorylation (Figure 3.2A). We tested this by assaying if TRBP from treated cells interacts better with PKR in a pull-down assay. As seen in Figure 3.5B, in the absence of stress signals there is weak interaction between PKR and TRBP (Bound panels, Lane 2) which substantially decreases at 2 and 4 hours (Bound panels, Lanes 3 and 4) due to PKR's disassociation from TRBP in

response to stress. We observed much stronger re-association between PKR and TRBP at 8 hours and 12 hours after treatment (Bound panels, Lanes 5 and 6). A quantification of the pull-down assay shown as a bar graph shows that both the reduction in TRBP-PKR interaction after stress and the reassociation of TRBP with PKR at later time points after stress is statistically significant. Thus, our results strongly support that TRBP's interaction with PKR and consequently its ability to inhibit PKR effectively during cell stress is closely linked to its phosphorylation status.

Since stress-induced phosphorylation is essential for efficient PACT-PACT interactions<sup>68</sup>, we investigated how phosphorylation affects TRBP-TRBP interactions. We expressed both TRBP phospho-mutants in yeast as GAL4 DNA-binding domain fusion proteins (pGBKT7) and GAL4 activation domain fusion proteins (pGADT7) and assayed for the strength of TRBP AAAA and TRBP DDDD homomeric interactions by the amount of yeast growth on nutrient deficient media in the presence of 3-AT. As seen in Figure 3.5C, yeast cells expressing both AAAA TRBP expression vectors show growth at all dilutions, indicating strong homodimer interaction between unphosphorylated TRBP proteins. In contrast to this, there was a complete absence of growth even at the most concentrated dilution of yeast cells (10 OD) expressing both DDDD TRBP yeast expression vectors, which indicates that TRBP phosphorylation is highly unfavorable to the formation of TRBP homodimers.

We also examined TRBP AAAA and TRBP DDDD homomeric interactions in mammalian cells using a co-immunoprecipitation assay. As seen in Figure 3.5D, we observed that significantly less myc-DDDD TRBP was co-immunoprecipitated with Flag-

DDDD TRBP (IP Myc panel, Lane 1) compared to the myc-AAAA TRBP co-immunoprecipitated with Flag-AAAA TRBP (IP Myc panel, Lane 3). The Flag panels demonstrate that comparable amounts of Flag-DDDD TRBP (IP panel, Lane 1) and Flag-AAAA TRBP (IP panel, Lane 3) were immunoprecipitated, thereby confirming that the significant difference seen in co-immunoprecipitated bands reflects difference in TRBP homomeric interactions. The absence of co-immunoprecipitated myc-DDDD or myc-AAAA TRBP without co-expression of Flag-DDDD TRBP (IP, Lane 2) or Flag-AAAA TRBP (IP, Lane 4) rules out any nonspecific immunoprecipitation.

Taken together, these results strongly demonstrate that stress-induced TRBP phosphorylation significantly weakens homomeric interactions between TRBP molecules while simultaneously enhancing TRBP-PKR interactions, which plays an important role in attenuating sustained PKR activation during cell stress and inhibits excessive apoptosis. The results presented here contribute to our understanding of how PKR activity is regulated negatively at later time points after oxidative stress to prevent excessive apoptosis.

### 3.5 DISCUSSION

Activation of PKR during cellular stress is regulated by PACT and TRBP, PACT acting positively to activate PKR and TRBP acting negatively to suppress excessive PKR activity<sup>60,67,180</sup>. Initially at early time points after stress, PACT activates PKR to aid inhibition of protein synthesis via phosphorylation of eIF2 $\alpha$ <sup>60,62,67</sup>. Our results presented here, for the first time demonstrate that TRBP is phosphorylated by ERK 1/2 and JNK in



response to oxidative stress at late time points and the phosphorylated TRBP inhibits PKR's kinase activity more efficiently to protect cells from apoptosis. In addition, the enhanced PKR inhibition and protection from apoptosis by phospho-TRBP is brought about by an increased interaction between phospho-TRBP and PKR as well as decreased phospho-TRBP homomeric interactions. The timely downregulation of PKR activity and eIF2 $\alpha$  phosphorylation is achieved in part by induction of GADD34, a regulatory subunit of protein phosphatase 1 (PP1)<sup>193,194</sup>.

Our data indicates that TRBP also plays an important role in the downregulation of PKR activity. Thus, PKR activity during cell stress is dictated not only by stress-induced changes in interactions between PACT and PKR, but also by interactions between PKR and TRBP. TRBP interacts with both PACT and PKR and although TRBP phosphorylation enhances its affinity for PKR while reducing the TRBP-TRBP interactions, we observed no effect of TRBP phosphorylation on TRBP-PACT interactions (data not shown). On the contrary, stress-induced PACT phosphorylation reduces the PACT-TRBP interactions while increasing PACT-PACT interactions and PACT-PKR interactions, thereby leading to PKR activation<sup>62,195</sup>. Strikingly, although TRBP and PACT are very homologous, the stress-induced phosphorylation affects the protein-protein interaction properties of PACT and TRBP quite differently.

Based on our data, we present a schematic model for TRBP-mediated downregulation of PKR activity at late time points after cellular stress. As depicted in Figure 3.6, PKR and unphosphorylated TRBP interact under unstressed conditions in the cell, preventing PKR activation, and eIF2 $\alpha$  phosphorylation. Unphosphorylated TRBP also

forms homodimers efficiently. In response to oxidative stress, PKR is activated by phosphorylated PACT homodimers (not depicted) and eIF2 $\alpha$  is phosphorylated to bring about a transient protein synthesis inhibition. TRBP at this point remains unphosphorylated, and efficiently forms TRBP-TRBP homodimers. Late after the onset of the stressful event, ERK1/2 and JNK phosphorylate TRBP, leading to significantly decreased TRBP-TRBP interactions, and increased TRBP-PKR interactions. Phospho-TRBP interacts with PKR at significantly higher affinity to bring about efficient PKR inactivation, and eIF2 $\alpha$  is dephosphorylated. Phospho-TRBP does not form homodimers efficiently and this could partly explain efficient PKR inhibition as it is established that PKR is activated mainly by trans-autophosphorylation and PKR-PKR interactions. Thus, monomeric phospho-TRBP could potentially function to inhibit PKR by preventing PKR-PKR interactions.

The dsRBM motifs present in PKR, TRBP, and PACT possess the characteristic alpha-beta-beta-beta-alpha fold that has two well-characterized functions to bind structured RNA molecules and to mediate protein-protein interactions<sup>176,196</sup>. This motif is widely distributed in eukaryotic proteins, as well as in proteins from bacteria and viruses and the dsRBM-containing proteins are involved in a variety of cellular processes ranging from RNA editing, nucleocytoplasmic transport, RNA localization, protein phosphorylation in translational control, and contain a variable number of dsRBM domains<sup>197</sup>. In addition, dsRBMs can also recognize non-RNA targets (proteins and DNA), and act in combination with other dsRBMs and non-dsRBM motifs to play a regulatory role in catalytic processes<sup>198</sup>. Our work presented here adds one more layer

of complexity to the versatility of the dsRBM as it demonstrates that phosphorylation sites residing outside the dsRBM influence the strength of protein-protein interactions mediated via the dsRBMs. This also underscores the importance of optimal juxtaposition of the multiple dsRBM motifs relative to each other in regulating protein interactions as the phosphorylation of specific serines outside the motif can possibly bring about significant changes in overall protein conformations. In other members of the diverse family of dsRBM-containing proteins, the role of phosphorylation and post-translational modifications in regulating interactions with RNA or proteins remains to be investigated in future.

Our results on the effect of TRBP phosphorylation on PKR activity are in agreement with Kim et al. who reported that phospho-TRBP efficiently inhibits PKR during M-G1 transition to regulate cell cycle<sup>99</sup>. In this study, the phosphorylation of TRBP during M-G1 transition was shown to be mediated by JNK. Of the four sites we studied, S142 and S152 were also identified by Kim et al. to be phosphorylated by JNK during M phase. ERK mediated phosphorylation of TRBP on S142, S152, S283, and S286 was reported in response to mitogenic signaling and was accompanied by a coordinated increase in the levels of growth-promoting miRNAs and a reduction in the levels of tumor suppressor let-7 miRNA<sup>181</sup>. TRBP phosphorylation has been reported to occur in response to metabolic stress and inhibition of TRBP phosphorylation during metabolic stress reduced inflammation and improved systemic insulin resistance and glucose metabolism<sup>100,199</sup>. However, the exact functions of TRBP and PKR in high-fat diet-induced obesity and associated metabolic and inflammatory complications remains

unclear and controversial<sup>101</sup>. TRBP plays an important pro-viral function in HIV infected cells by regulating PKR activity and promoting HIV replication<sup>109,118</sup>. Any effect of TRBP phosphorylation in HIV-infected cells also remains unexplored at present. Our work on the impact of TRBP phosphorylation on the stress signaling pathway and cellular survival thus presents an additional paradigm for exploring the existence and importance of such TRBP-mediated regulatory mechanisms in virus infected cells as well as miRNA expression and function in response to cellular stress.

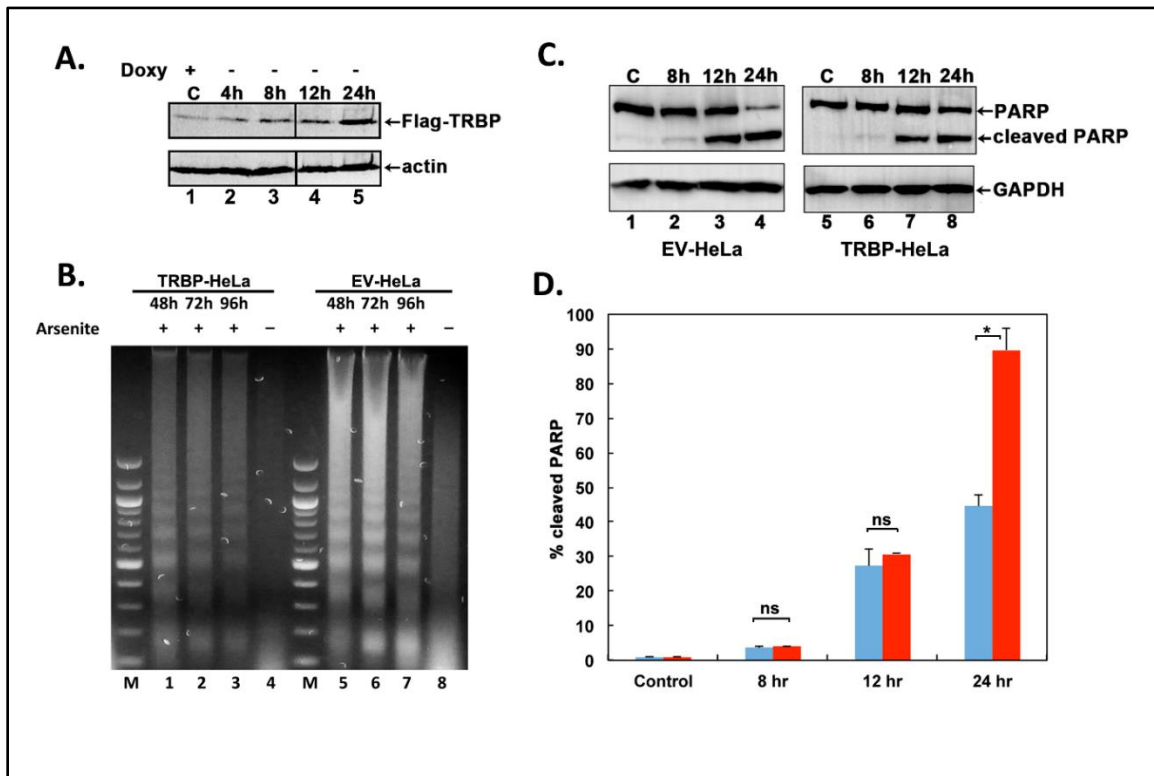


**Figure 3.1: TRBP overexpression protects cells from arsenite-induced apoptosis.**

**(A) Establishment of a stable doxycycline-inducible HeLa cell line overexpressing Flag-TRBP.** HeLa-Tet off (Clontech) cells were transfected with either FlagTRBP/pTRE2pur expression construct or pTRE2pur (Clontech) empty vector (EV). Puromycin resistant clones were isolated, characterized, and one clone (TRBP-HeLa) that showed inducible expression of FlagTRBP was selected for further studies. Induction of FlagTRBP expression after removal of doxycycline from the growth medium at indicated time points is shown. Western blot analysis of cell lysates using 50  $\mu$ g of total protein was performed using anti-Flag and anti- $\beta$ -actin antibodies. The black line between lanes 3 and 4 represents where different lanes from the same western blot were joined.

**(B) DNA Fragmentation Analysis.** TRBP-HeLa cells overexpressing FlagTRBP (Lanes 1 -4) or EV-HeLa control cells (Lanes 5 -8) were treated with 10  $\mu$ M sodium arsenite for 48, 72, and 96 hours, fragmented DNA was isolated and analyzed. M: 100-bp ladder, Lanes 1 & 5: 48 hr treatment. Lanes 2 & 6: 72 hr treatment, Lanes 3 & 7: 96 hr treatment, and Lanes 4 & 8: untreated cells.

**(C) Analysis of PARP cleavage in response to arsenite treatment.** TRBP-HeLa and EV-HeLa cells were treated with 25  $\mu$ M sodium arsenite for the indicated time points, and western blot analysis using anti-PARP antibody was performed on cell lysates containing 50  $\mu$ g of total protein to assess increases in poly ADP-ribose polymerase (PARP1) cleavage. Western blot was also performed with anti-GAPDH antibody to ensure equal protein in all samples.

**(D) Quantification of PARP cleavage.** PARP1 and cleaved PARP1 bands were quantified using ImageQuant TL Software. The percentage of cleaved PARP1 was calculated as

**Figure 3.1 (continued)** (cleaved PARP1 band intensity/cleaved + uncleaved bands intensities) X 100. Bars represent percentages of cleaved PARP1 from 3 independent experiments. Error bars represent standard deviation (S.D.) from three experiments. Student's t tests were performed to determine statistical significance – ns: not significant, asterisk: *P* value of 0.000352

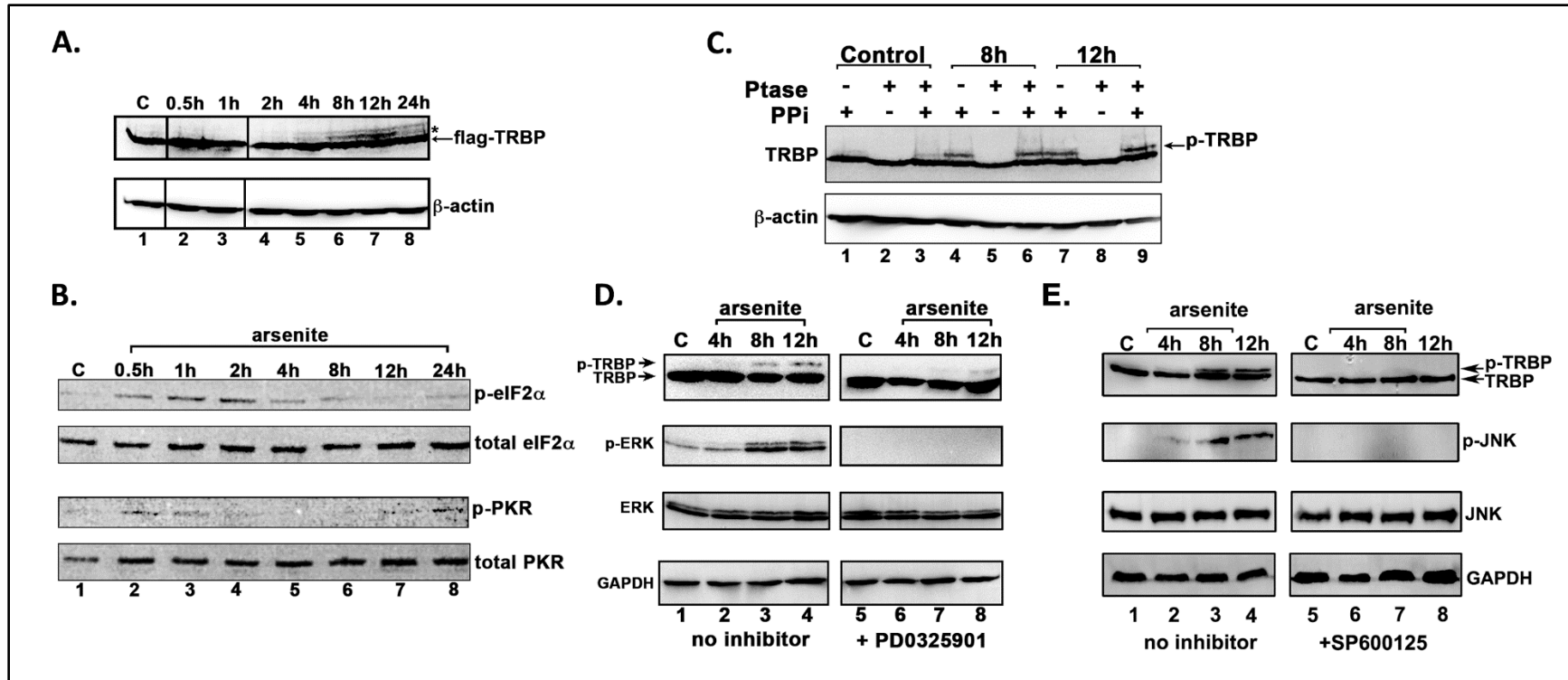


**Figure 3.2: TRBP is phosphorylated by ERK and JNK in response to arsenite-induced oxidative stress.**

**(A) TRBP's electrophoretic mobility shifts in response to sodium arsenite treatment.** Western blot analysis of 50  $\mu$ g protein per lane from HeLa-TRBP cells treated with 10  $\mu$ M sodium arsenite at the indicated time points is shown. Western blot analysis was performed with anti-Flag and anti- $\beta$  actin antibodies. The slower migrating TRBP band at 8h, and 12h is indicated by an asterisk. The line between lanes 1 and 2 as well as between lanes 3 and 4 represents where lanes from the same western blot were joined.

**(B) PKR phosphorylation and eIF2 $\alpha$  phosphorylation kinetics in response to sodium arsenite treatment.** HeLa cells were treated with 10  $\mu$ M sodium arsenite and cell extracts were prepared at the indicated time points. PKR and eIF2 $\alpha$  phosphorylation status at each time point was determined by a western blot analysis using anti-phospho-PKR and anti-phospho-eIF2 $\alpha$  specific antibodies using

**Figure 3.2 (continued)** 100  $\mu$ g and 10 $\mu$ g of total protein respectively. Each blot was subsequently stripped and re-probed with anti-eIF2 $\alpha$  or anti-PKR antibody to ensure equal loading in all lanes.

**(C) TRBP is phosphorylated in response to oxidative stress.** Extracts from untreated, and 8h, or 12h arsenite-treated TRBP-HeLa cells were prepared in the presence or absence of phosphatase inhibitor (PPI) as indicated above the lanes and subsequently treated with phosphatase (Ptase) or left untreated as indicated. Western blot was performed with anti-Flag antibody followed by anti- $\beta$ -actin antibody.

**(D) ERK is phosphorylated in response to oxidative stress and phosphorylates TRBP.** TRBP overexpressing TRBP-HeLa cells were treated with 10  $\mu$ M arsenite alone or in combination with the MEK inhibitor PD0325901 for 24 hours. Cell extracts were made at the indicated time points, and western blot analysis was performed using anti-Flag, anti-phospho-ERK, anti-total ERK, and anti-GAPDH antibodies.

**(E) JNK is phosphorylated in response to oxidative stress and phosphorylates TRBP.** TRBP overexpressing TRBP-HeLa cells were treated with 10  $\mu$ M arsenite alone or in combination with the MEK inhibitor SP600125 for 24 hours. Cell extracts were made at the indicated time points, and western blot analysis was performed using anti-Flag, anti-phospho-JNK, anti-total JNK, and anti-GAPDH antibodies.



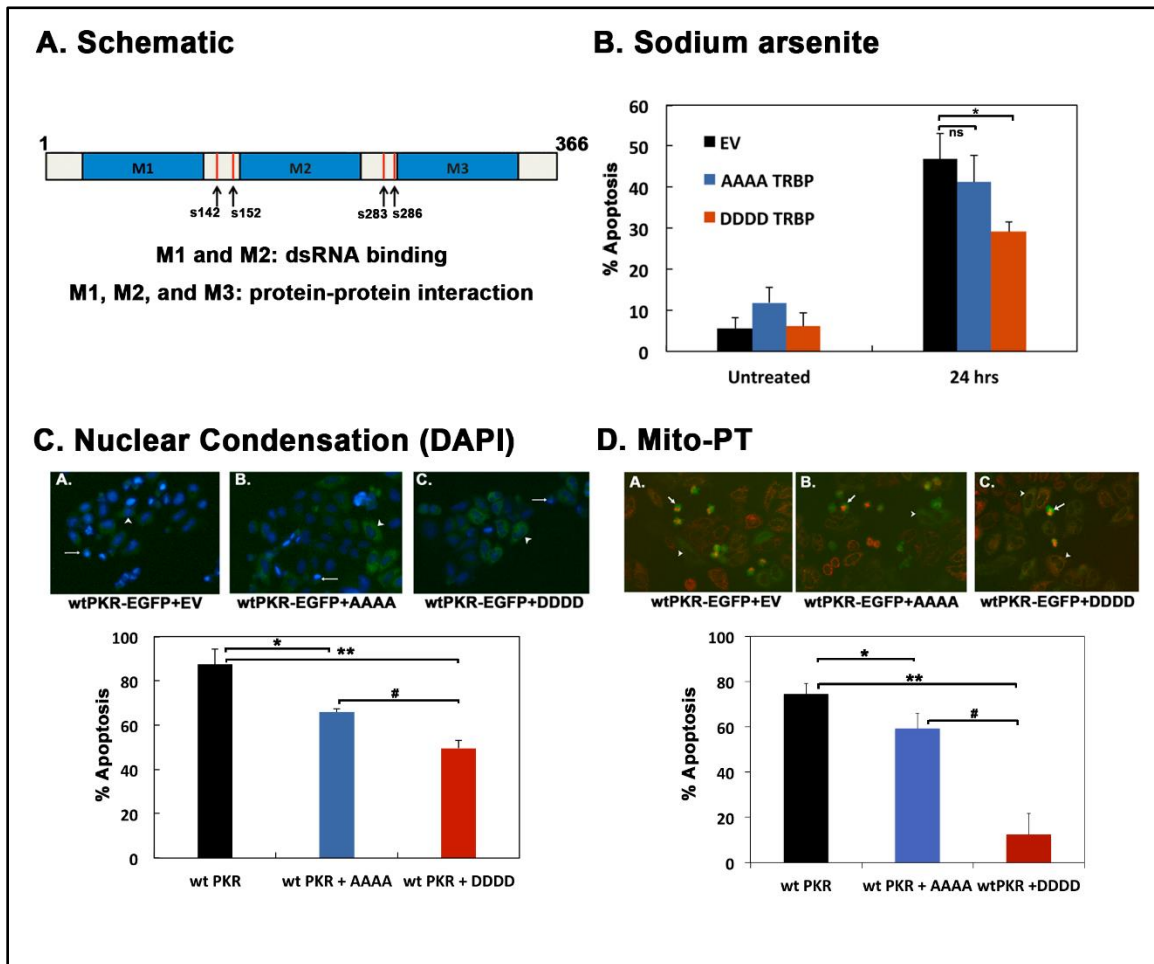


**Figure 3.3: TRBP phosphorylation inhibits PKR-mediated apoptosis during cell stress.**

**(A) Schematic representation of TRBP phosphorylation sites.** Blue boxes represent the three double-stranded RNA binding motifs (dsRBMs), M1, M2, and M3. Red vertical lines represent previously identified ERK 1/2 phosphorylation sites at S142, S152, S283, and S286.

**(B) Expression of phospho-mimic TRBP protects cells during oxidative stress.** HeLa cells were transfected with 200ng pEGFP-C1 (EV) alone (black bars) or with 200ng each of pEGFP-C1 and FlagTRBP AAAA/pcDNA 3.1<sup>-</sup> (blue bars) or with 200ng each of pEGFP-C1 and FlagTRBP DDDD/pcDNA 3.1<sup>-</sup> (red bars). 24 hours after transfection, the cells were treated with 25  $\mu$ M sodium arsenite, fixed and stained with DAPI nuclear stain. At least 300 EGFP-positive cells were scored apoptotic or live based on nuclear condensation indicated by intense DAPI nuclear staining and cell morphology. The percentage of cells undergoing apoptosis (% apoptosis) was calculated using the formula: (EGFP- expressing cells with intense DAPI nuclear staining/Total EGFP-expressing cells) x 100. Bars represent averages  $\pm$  S.D. from three independent experiments. One-way ANOVA followed by post-hoc Tukey test was performed, *ns*: not significant, asterisk: *P*-value of 0.016.

**Figure 3.3 (continued) (C) and (D) Phospho-mimic TRBP inhibits PKR mediated apoptosis more efficiently than phospho-defective TRBP (C)** HeLa cells were plated on coverslips and transfected with 500ng of wt PKR/pEGFPC1 and 20ng of empty vector pCDNA3.1<sup>-</sup> (wt PKR; black bar) or with 500ng of wt PKR/pEGFPC1 + 20 ng of Flag TRBP AAAA/ pcDNA 3.1<sup>-</sup> (blue bar) or 500ng of wt PKR/pEGFPC1 + 20ng of Flag TRBP DDDD/ pcDNA 3.1<sup>-</sup> (red bar). 24 hours after transfection, the cells were fixed and mounted in Vectashield mounting media with DAPI nuclear stain. Representative fluorescent micrographs of HeLa cells transfected with wt PKR pEGFPC1 alone (Panel A), or in combination with Flag TRBP AAAA/ pcDNA 3.1<sup>-</sup> (Panel B) or Flag TRBP DDDD/ pcDNA 3.1<sup>-</sup> (Panel C) are shown. At least 500 EGFP-PKR expressing cells were scored as apoptotic **Figure 3.3 (continued)** (white arrows) or live (white arrowheads) based on nuclear condensation indicated by intense DAPI staining and cellular morphology. The percentage of cells undergoing apoptosis was determined as described in (A). Bars represent averages  $\pm$  S.D. from three independent experiments. One-way ANOVA followed by post-hoc Tukey test was performed, asterisk \*: *P*-value 0.0034, double asterisk \*\*: *P*-value 0.0002, #: *P*-value 0.0134. **(D) Phospho-mimic TRBP expression abrogates mitochondrial depolarization during PKR-mediated apoptosis.** HeLa cells were plated on coverslips and transfected with 500ng of wt PKR/pEGFPC1 and 20ng of empty vector pCDNA3.1<sup>-</sup> (wt PKR; black bar) or with 500ng of wt PKR/pEGFPC1 + 20 ng of Flag TRBP AAAA/ pcDNA 3.1<sup>-</sup> (blue bar) or 500ng of wt PKR/pEGFPC1 + 20ng of Flag TRBP DDDD/ pcDNA 3.1<sup>-</sup> (red bar). 24 hours after transfection, changes in the mitochondrial potential of transfected cells were assessed using the MitoPT TMRM Assay kit and observed by fluorescence microscopy. Representative fluorescent micrographs of the cells transfected with wt-PKR pEGFPC1 alone (wt-PKR-EGFP + EV, Panel A), and AAAA TRBP (wt-PKR-EGFP + AAAA, Panel B) or DDDD TRBP (wt-PKR-EGFP + DDDD, Panel C) are represented. At least 500 PKR expressing cells (GFP positive cells) were scored as live (white arrowheads) or dead (white arrows) based on decreased or absent red fluorescence. The percentage of cells undergoing apoptosis (% apoptosis) was calculated using the formula: (EGFP- expressing cells with decreased or absent red fluorescence/Total EGFP-expressing cells) x 100. Bars represent averages  $\pm$  S.D. from three independent experiments. One-way ANOVA followed by post-hoc Tukey test was performed, asterisk \*: *P*-value 0.0108, double asterisk \*\*: *P*-value 0.0003, #: *P*-value 0.0002.

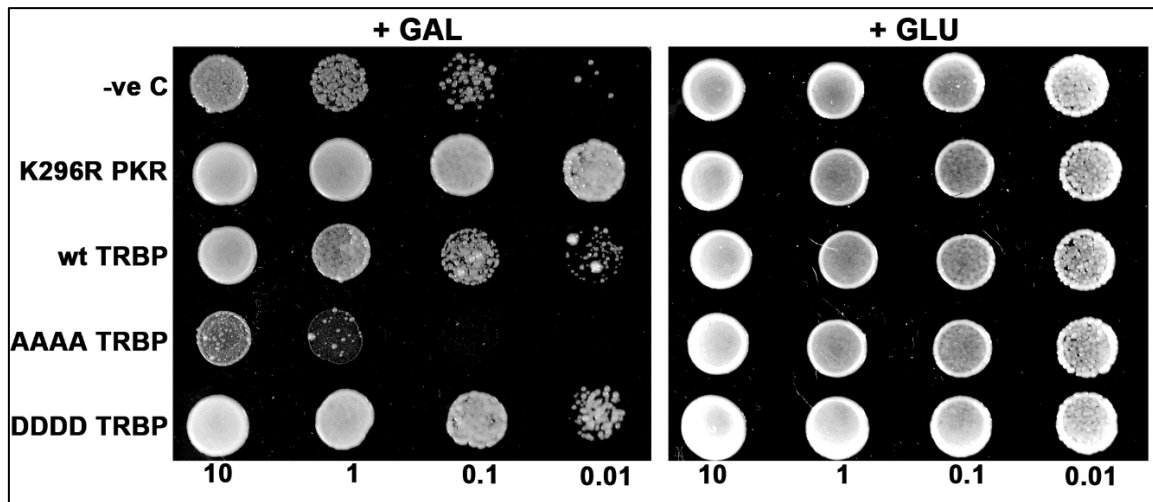


**Figure 3.4: The phosphorylated TRBP isoform efficiently reverses PKR's growth inhibition phenotype in yeast. (A) Yeast growth inhibition assay.** Yeast INVSc1 cells were co-transformed with wt PKR/pYES2 and empty vector pYES3CT (PKR alone), wt PKR/pYES2 and K296R PKR/pYES3CT (PKR+K296R), wt PKR/pYES2 and wt TRBP/pYES3CT (PKR+wtTRBP), wt PKR/pYES2 and AAAA TRBP/pYES3CT (PKR+AAAA), or wt PKR/pYES2 and DDDD TRBP/pYES3CT (PKR+DDDD). Ten microliters of transformed yeast cells ( $OD_{600} = 10, 1, 0.1, 0.01$ ) were spotted on double dropout media (-uracil, -tryptophan) with either glucose (+GLU) or galactose (+GAL) as sole carbon source. Plates were incubated for three days at 30°C. Transformation of INVSc1 with wt PKR/pYES2 and empty vector pYES3CT served as a control showing growth inhibition on galactose plates, while transformation with wtPKR/pYES2 and K296R PKR/pYES3CT served as a positive control for inhibition of PKR and a reversal of growth inhibition phenotype.

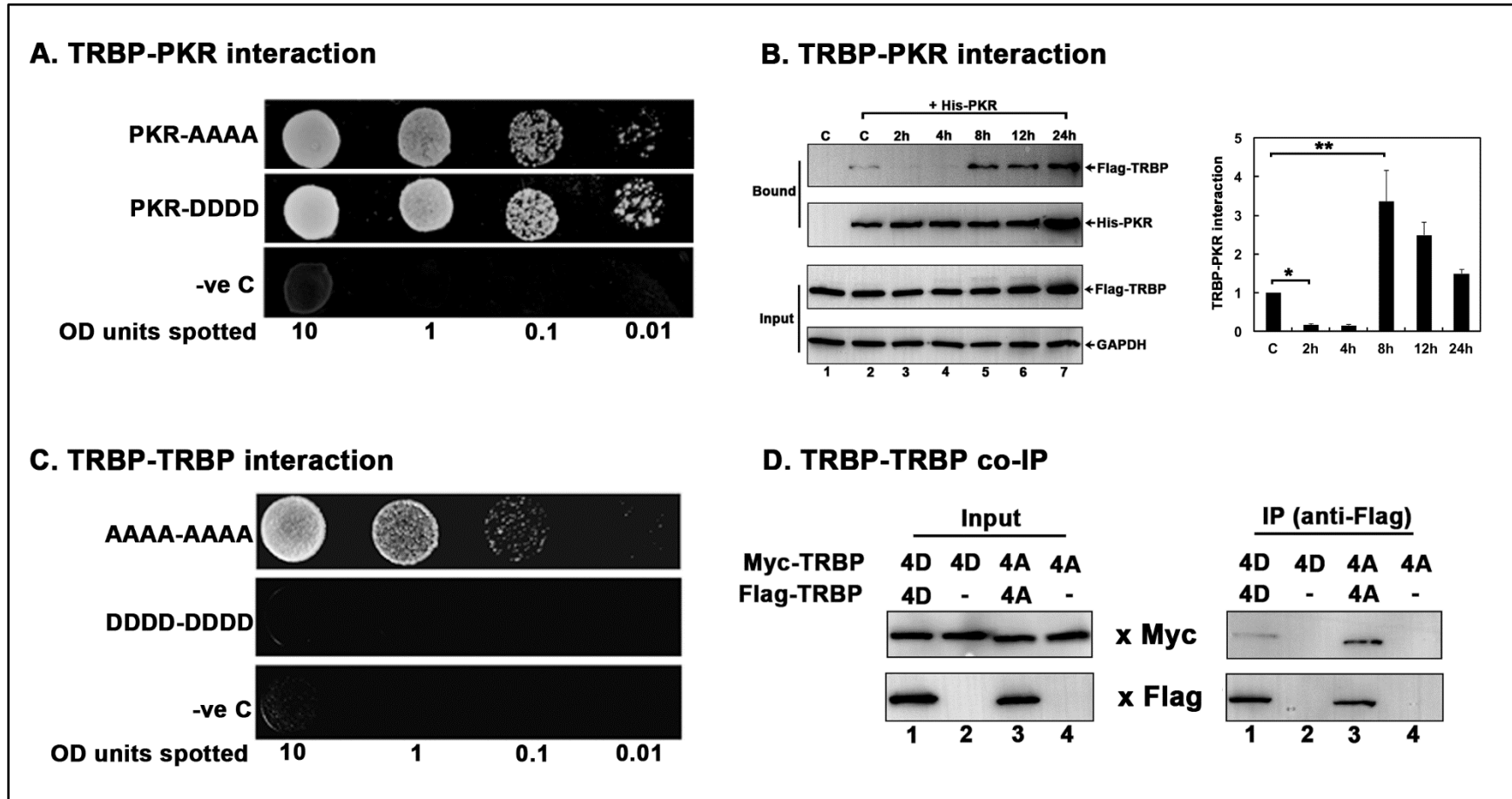


**Figure 3.5: TRBP phosphorylation strengthens PKR-TRBP interaction and weakens TRBP-TRBP interaction.**

**(A) Phosphomimic TRBP mutant interacts stronger with PKR compared to the phosphodeficient TRBP mutant in yeast two-hybrid assay.** PKR/ pGAD424 and either AAAA TRBP/pGBKT7, or DDDD TRBP/pGBKT7 were co-transformed into AH109 yeast cells and selected on SD double dropout media (-tryptophan, - leucine). Ten microliters of transformed yeast cells ( $OD_{600} = 10, 1, 0.1, 0.01$ ) were spotted on SD triple dropout media (-tryptophan, - leucine, - histidine) containing 10 mM 3-amino-1,2,4-triazole (3-AT).

**Figure 3.5 (continued)** Plates were incubated for 5 days at 30°C. Transformation of PKR in pGAD424 and pGBKT7 empty vector served as a negative control.

**(B) Changes in TRBP association with PKR.** Flag TRBP overexpressing cells were treated with 25  $\mu$ M sodium arsenite for the indicated time points. Cell extracts were prepared in the presence of a phosphatase inhibitor and 25  $\mu$ g of cell extract was incubated with 500 ng of pure recombinant hexahistidine (His)-tagged PKR immobilized on Ni<sup>2+</sup>-agarose beads. After washing the beads, PKR-associated Flag TRBP was analyzed by SDS polyacrylamide gel electrophoresis followed by western blot analysis with anti-Flag antibody. Western blot analysis was also performed with anti-His antibody to ensure equal His- PKR in each sample. 25  $\mu$ g of cell extract was also analyzed by western blot analysis with anti-Flag and anti-GAPDH antibodies to ensure equal addition of cell lysate for each pull down (Input). **Quantification of TRBP-PKR pull down:** Band intensities were quantified using ImageQuant TL Software, and the ratios of bound TRBP to bound PKR across all samples were calculated and normalized to the band intensities of Flag-TRBP input for each sample. Bound TRBP/his-PKR ratios for all samples were all expressed relative to the control sample (Lane 2). Averages from three independent experiments are plotted as bar graphs  $\pm$  S.D. One-way ANOVA followed by post-hoc Tukey test was performed, asterisk \*: p value 0.0000012 and double asterisk \*\*: p value 0.0066374.

**(C) Phosphomimic TRBP mutant shows stronger homomeric interaction compared to the phosphodeficient TRBP mutant in yeast two-hybrid assay.** AAAA TRBP or DDDD TRBP point mutants in pGADT7 and pGBKT7 were co-transformed into AH109 yeast cells and selected on SD double dropout media (-tryptophan, -leucine). Ten microliters of transformed yeast cells ( $OD_{600}$  = 10, 1, 0.1, 0.01) were spotted on SD triple dropout media plate (tryptophan, -leucine, -histidine) containing 10 mM 3-amino-1,2,4-triazole (3-AT). Plates were incubated for 5 days at 30°C. Transformation of pGADT7 and pGBKT7 empty vectors served as a negative control.

**(D) Phosphomimic TRBP mutant shows stronger homomeric interaction compared to the phosphodeficient TRBP mutant in mammalian cells.** HeLa cells were transfected with either myc TRBP DDDD/ pcDNA 3.1<sup>-</sup> and Flag TRBP DDDD/ pcDNA 3.1<sup>-</sup> or Flag TRBP AAAA/ pcDNA 3.1<sup>-</sup> and myc TRBP AAAA/ pcDNA 3.1<sup>-</sup>. The cells were harvested 24 hours after transfection, and Flag TRBP AAAA or DDDD was immunoprecipitated using anti-Flag monoclonal antibody conjugated agarose beads. The co-immunoprecipitation of myc-TRBP was analyzed by western blot analysis with an anti-myc antibody (IP: x Myc panel). Blot was subsequently stripped and re-probed with anti-Flag antibody to ensure equal Flag-TRBP immunoprecipitation from each sample (IP: x Flag panel). Equal AAAA TRBP and DDDD TRBP expression in all samples was tested by western blot analysis of equal amounts of total cell lysate with anti-myc, and anti-Flag antibodies (Input: x Myc and x Flag panels).

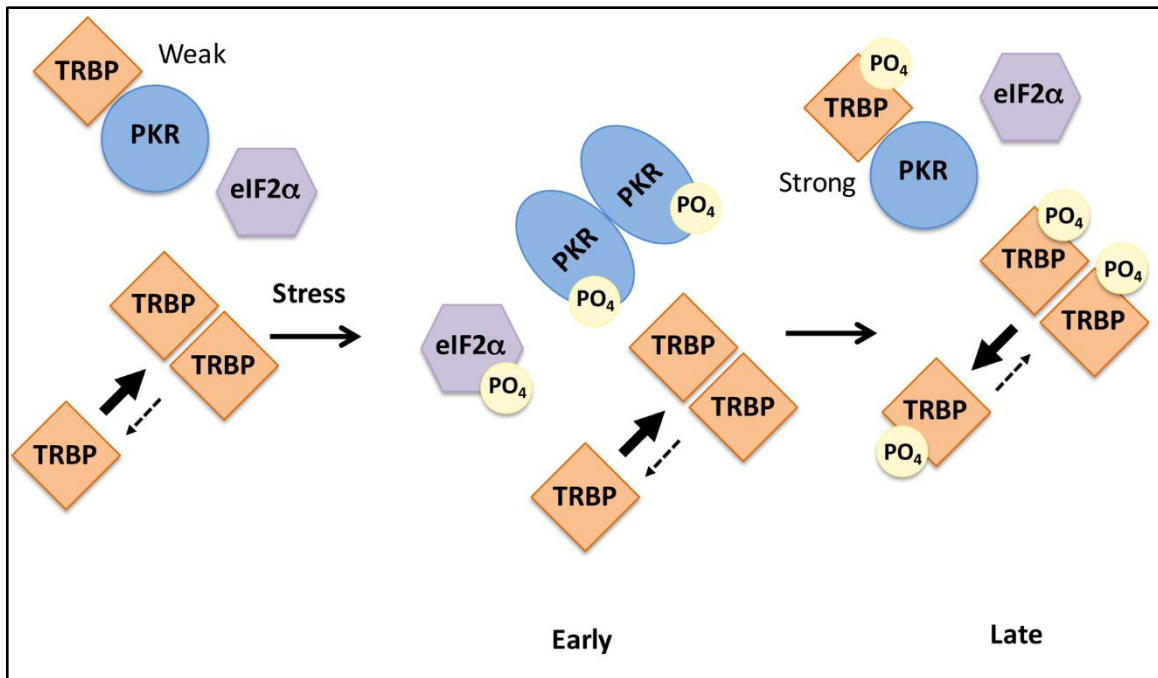


**Figure 3.6: A schematic model of PKR-TRBP interaction in response to oxidative stress.** As previously established<sup>60,95,176</sup>, in the absence of stress, TRBP heterodimerizes with PKR, PKR is catalytically inactive and eIF2 $\alpha$  is not phosphorylated. At early time points after ER stress, TRBP dissociates from PKR and PKR is activated leading to its autophosphorylation and eIF2 $\alpha$  phosphorylation. At late time points after stress, TRBP is phosphorylated by ERK and JNK and interacts with PKR with higher affinity. The cells recover by forming TRBP-PKR heterodimers and turning off PKR and eIF2 $\alpha$  phosphorylation. Phosphorylated TRBP largely remains monomeric as TRBP-TRBP interactions are weakened by phosphorylation of TRBP.

## CHAPTER 4

### CONTRIBUTION OF THE TWO DSRBM MOTIFS TO THE DOUBLE-STRANDED RNA BINDING AND PROTEIN INTERACTIONS OF PACT<sup>4</sup>

---

<sup>4</sup> Chukwurah E., Willingham V., Singh M., Castillo D., and Patel RC Submitted to *Journal of Cellular Biochemistry* 2017.

#### 4.1. ABSTRACT

PACT is a stress-modulated activator of protein kinase PKR (protein kinase, RNA activated), which is involved in antiviral innate immune responses and stress-induced apoptosis. Stress-induced phosphorylation of PACT is essential for PACT's increased association with PKR leading to PKR activation, phosphorylation of translation initiation factor eIF2 $\alpha$ , inhibition of protein synthesis, and apoptosis. PACT-induced PKR activation is negatively regulated by TRBP (Transactivation response element RNA-binding protein), which dissociates from PACT after PACT phosphorylation in response to stress signals. The conserved double-stranded RNA binding motifs (dsRBMs) in PKR, PACT, and TRBP mediate protein-protein interactions, and the stress-dependent phosphorylation of PACT changes the relative strengths of PKR-PACT, PACT-TRBP, and PACT-PACT interactions to bring about a timely and transient PKR activation. This regulates the general kinetics as well as level of eIF2 $\alpha$  phosphorylation, thereby influencing the cellular response to stress either as recovery and survival or elimination by apoptosis. In the present study, we evaluated the effect of specific mutations within PACT's two evolutionarily conserved dsRBMs on dsRNA-binding, and protein-protein interactions between PKR, PACT, and TRBP. Our data shows that the two motifs contribute to varying extents in dsRNA binding, and protein interactions. These findings indicate that although the dsRBM motifs have high sequence conservation, their functional contribution in the context of the whole protein needs to be determined by mutational analysis. Furthermore, using a PACT mutant that is deficient in PACT-PACT interaction but competent for



PACT-PKR interaction, we demonstrate that PACT-PACT interaction is essential for efficient PKR activation.

## 4.2 INTRODUCTION

PACT is a double-stranded RNA binding protein that was identified originally as a Protein Activator of PKR (protein kinase, RNA activated: encoded by the *Eif2ak2* gene) in human cells and later as PKR associated protein (RAX) in mouse. The gene that encodes PACT is designated as *Prkra* and recently several mutations that lead to the movement disorder dystonia have been described in the *Prkra* gene. PACT and RAX proteins are mostly identical with only 6 out of 313 residues being different with 4 of these substitutions being conservative. Initial studies on PACT focused on its ability to induce the autophosphorylation and activation of the interferon (IFN)-inducible, double-stranded (ds) RNA dependent serine/threonine protein kinase (PKR) in response to various stress signals. Activation of PKR results in phosphorylation of eukaryotic protein synthesis initiation factor 2 $\alpha$  (eIF2 $\alpha$ ) leading to an inhibition of protein synthesis.

PKR is expressed ubiquitously and mediates IFN's antiviral actions in virally infected cells as well as regulates cellular survival and apoptosis in response to stress in uninfected cells. PKR's kinase activity remains latent until one of its activators bring about a conformational change by direct binding to cause its enzymatic activation<sup>108</sup>. During the replication of several viruses dsRNA is produced, which binds to PKR's two dsRNA-binding motifs (dsRBMs)<sup>45,175,200</sup> to activate PKR and unmask the ATP-binding site<sup>50</sup> to promote autophosphorylation<sup>48</sup>. The two dsRBMs also mediate dsRNA-

independent protein-protein interactions with other proteins that carry similar domains<sup>176,177</sup>. Among these proteins, PACT functions to activate PKR in response to stress signals and in the absence of dsRNA<sup>58,60</sup> and TAR RNA-binding protein (TRBP) serves as an inhibitor.

PACT contains three copies of dsRBM (Figure 1.3), of which the two amino-terminal motifs (M1 and M2) bind to dsRNA and also to dsRBMs of PKR. The third carboxy-terminal motif 3 (M3) lacks the conserved lysines required for dsRNA-binding and thus does not bind dsRNA. M3 is also dispensable for interaction with PKR's dsRBM motifs but is essential for PKR activation and interacts with a specific region in its kinase domain<sup>63,64</sup>. Although purified, recombinant PACT can activate PKR by direct interaction *in vitro*<sup>58</sup>, PACT-dependent PKR activation in cells occurs in response to stress signals<sup>59-62</sup> such as arsenite, peroxide, growth factor withdrawal, thapsigargin, and tunicamycin, and leads to phosphorylation of the translation initiation factor eIF2 $\alpha$  and cellular apoptosis<sup>59-61</sup>. PACT (and its murine homolog RAX) are phosphorylated in response to stress leading to its increased association with PKR<sup>59-61</sup>. The stress-induced phosphorylation site in PACT is at serine 287 (S287) and a constitutive phosphorylation at serine 246 (S246) is required for S287 phosphorylation in response to oxidative stress. The phosphorylation of S287 in response to oxidative stress increases the PACT-PKR and PACT-PACT interactions but decreases PACT-TRBP interactions promoting PKR activation. TRBP also has three dsRBMs; the first two are true dsRBMs and interact with dsRNA, while the third carboxy-terminal dsRBM does not bind dsRNA but mediates TRBP's interactions with other proteins such as Dicer, and Merlin<sup>91,123,178</sup>. TRBP inhibits

PKR by interacting with dsRNA and sequestering it away from PKR as well as by forming PKR-TRBP heterodimers<sup>95,120</sup>. In the absence of viral infections and stress signals, TRBP forms heterodimers with both PKR and PACT, preventing their association and PACT-mediated PKR activation<sup>97,180</sup>. PKR activation in response to stress signals is thus tightly regulated by PACT and TRBP, both regulating its catalytic activity by a direct interaction<sup>180,195</sup>. As the dsRBMs in PKR, PACT, and TRBP mediate protein-protein interactions<sup>201</sup>, these three proteins form both heterodimers as well as homodimers and the stress-dependent phosphorylation of PACT changes the relative strengths of PKR-PACT, PACT-TRBP, and PACT-PACT interactions to bring about a timely and transient PKR activation with precise control<sup>68,195</sup>. This regulates the general kinetics as well as level of eIF2 $\alpha$  phosphorylation thereby influencing the cellular response to stress either as recovery and survival or elimination by apoptosis<sup>179</sup>.

In this report, we examined the contribution of specific conserved amino acids within the two amino-terminal dsRBM domains in PACT to its dsRNA-binding and protein-protein interaction activities. Our results identify the conserved lysines and specific hydrophobic amino acids within the two dsRBMs that are important for dsRNA-binding and protein-protein interactions respectively. In addition, the work underscores the importance of PACT-PACT interactions in PKR activation following oxidative stress as a phosphomimetic PACT mutant that is incapable of facilitating PACT-PACT interactions fails to activate PKR and induce apoptosis. The results shed light on the mechanism of PKR activation by PACT.

## 4.3 MATERIALS AND METHODS

### 4.3.1 REAGENTS AND CELL LINES

HeLaM and COS-1 cells were cultured in Dulbecco's Modified Eagle's Medium (DMEM) containing 10% Fetal Bovine Serum and penicillin/streptomycin. Transfections were performed with the Effectene Transfection Reagent (Qiagen) per the manufacturer's instructions.

### 4.3.2 PLASMIDS

The TRBP/pGBKT7, K296R PKR/pGBT9, Flag PACT S246D S287D (DD PACT)/pcDNA 3.1<sup>-</sup>, wt PACT/BSIIKS<sup>+</sup>, Flag PACT/pCMV2, wt PACT/VP16 and wt PACT/GAL4 expression plasmids were prepared as previously described. The M1 (K84E, K88E, A91E, A92D, L99E), and M2 (K177A, K181E, A184E, A185E, and F192E) point mutations were introduced into wt PACT using the Gene Editor Site Directed Mutagenesis Kit (Promega). After the sequence of each point mutant was verified, the point mutants in BSIIKS<sup>+</sup> were subcloned into the pGBKT7 and pGADT7 (Takara Bio USA, Inc) yeast expression vectors at the *NdeI* and *BamHI* restriction sites. The Flag-tagged L99E S246D S287D (DD-L99E) PACT triple point mutant in BSIIKS<sup>+</sup> (Agilent Technologies) was generated by a three-piece ligation of the *NdeI* – *EcoRI* restriction fragment from L99E BSIIKS<sup>+</sup>, *EcoRI* – *EcoRI* restriction fragment from DD PACT pcDNA 3.1<sup>-</sup>, and the *NdeI* – *EcoRI* cut Flag BSIIKS<sup>+</sup> fragment. The Flag tagged triple mutant from BSIIKS<sup>+</sup> was then introduced into the *XbaI* – *EcoRI* sites of the pcDNA 3.1<sup>-</sup> expression vector (Invitrogen).

#### 4.3.3 DSRNA BINDING ASSAY

*In vitro* translated, <sup>35</sup>S-labeled PACT proteins (wt, PACT M1 and M2 mutants) were synthesized using the TNT® T7 Coupled Reticulocyte Lysate System (Promega). The dsRNA-binding activity of each mutant was measured by the previously described poly(I)·poly(C)–agarose binding assay [Patel and Sen, 1992]. 4 µl of the translation products were diluted with 25 µl of binding buffer [20 mM Tris–HCl, pH 7.5, 0.3 M NaCl, 5 mM MgCl<sub>2</sub>, 1 mM DTT, 0.1 mM PMSF, 0.5% Igepal, 10% glycerol], mixed with 25 µl of poly(I)·poly(C) – agarose beads and incubated at 30°C for 30 minutes. The beads were subsequently washed four times with 500 µl of binding buffer and the proteins bound to the beads after the washes were analyzed by SDS–PAGE and autoradiography. The T (Total) lanes represent the total synthesized <sup>35</sup>S-labeled proteins from the rabbit reticulocyte lysate, and the B (Bound) lanes represent the proteins that remained bound to the poly(I).poly(C) – agarose beads after washes. The interaction of each PACT protein with dsRNA was quantified using ImageQuant (GE Healthcare) by analyzing the band intensities of the total and bound PACT proteins. The percentage of the PACT protein bound to poly(I)·poly(C) – agarose beads was calculated from the band intensity values using this formula:

$$\% \text{ Binding} = (100 * \text{band intensity of protein in the Bound lane}) / (\text{band intensity of protein in the Total Lane}).$$

The calculated percentages were then plotted on bar graphs. The poly(I)·poly(C)–agarose binding assay was also performed with *in vitro* translated <sup>35</sup>S-labelled firefly luciferase protein to demonstrate specific interaction between the PACT proteins and the poly(I).poly(C) synthetic dsRNA.

#### 4.3.4 YEAST TWO-HYBRID INTERACTION ASSAYS

To test the interaction between the various indicated PACT point mutants and PKR, full length K296R PKR was expressed as a GAL4 DNA binding domain fusion protein from the pGBT9 vector while the PACT M1 and M2 mutants were expressed as GAL4 DNA activation domain fusion proteins from the pGADT7 vector.

The PKR/PACT mutant construct pairs were co-transformed into AH109 yeast cells (Takara Bio USA) using the lithium acetate method<sup>192</sup>, which were plated on double dropout synthetic defined (SD) minimal media plates lacking tryptophan and leucine. The transformants were grown to an OD<sub>600</sub> of 2 in YPD (yeast extract, peptone and dextrose) media, and 500 µl of each culture was pelleted and resuspended in an appropriate amount of distilled water to yield an OD<sub>600</sub> of 10. Serial dilutions were then made to yield OD<sub>600</sub> values of 1, 0.1, 0.01. 10 µl of each serial dilution was spotted on triple dropout SD media plates lacking histidine, tryptophan and leucine and incubated at 30°C for 4 days. AH109 cells were also co-transformed with wt PACT/pGADT7 and K296R/pGBT9 as a positive control, and with either A91E PACT/pGADT7, A92D PACT/pGADT7, A184E PACT/pGADT7, A185E PACT/pGADT7, or F192E PACT/pGADT7 and pGBKT7 as negative controls.

The relative strengths of the homomeric interactions of the PACT M1 and M2 point mutants were assayed by co-transforming AH109 yeast cells with the PACT mutants expressed as both GAL4 DNA binding and activation domain fusion proteins from the pGBKT7 and pGADT7 vectors. Similarly, the strengths of the PACT mutants' heteromeric interaction with TRBP were tested by co-transforming the yeast cells with

the PACT mutants expressed as GAL4 activation domain fusion proteins from the pGADT7 vector and TRBP expressed as a GAL4 DNA binding domain fusion protein from the pGBKT7 vector.

Selection of double transformant yeast cells and preparation of serial dilutions was carried out as previously described, and the serial dilutions were spotted on triple dropout media lacking histidine, tryptophan, and leucine in the presence of 10 mM 3-amino-1,2,4-triazole (3-AT), a competitive inhibitor of histidine synthesis. The plates were incubated at 30°C for 4 days. As positive controls, AH109 cells were transformed with wt PACT/pGADT7 and wt PACT/pGBKT7 and wt PACT/pGADT7 and TRBP/pGBKT7 for the PACT homodimer interaction and PACT-TRBP heterodimer interaction respectively.

For negative controls for the PACT-PACT homodimer yeast two-hybrid experiments, AH109 cells were co-transformed with either A91E PACT/pGBKT7, A92D PACT/pGBKT7, A184E PACT/pGBKT7, A185E PACT/pGBKT7, or F192E PACT/pGBKT7 and pGADT7 vectors. Negative controls for the PACT-TRBP heterodimer yeast two-hybrid experiments were AH109 yeast cells co-transformed with either the A91E PACT/pGADT7, A92D PACT/pGADT7, A184E PACT/pGADT7, A185E PACT/pGADT7, or F192E PACT/pGADT7 and pGBKT7 expression vectors.

#### 4.3.5 MAMMALIAN TWO HYBRID INTERACTION ASSAY

Sequences encoding the L99E, S246D S287D (*DD*), or L99E S246D S287D (*DD-L99E*) PACT point mutants were introduced into the pSG424 expression construct to

generate an in-frame fusion of each protein to the GAL4 transcription DNA binding domain (GAL4 DBD). In frame fusions of each protein to the activation domain of the herpes simplex virus protein VP16 were also generated by introducing the sequences into the pVP16AASV19N vector (VP16 AD).

COS-1 cells were transfected with 200 ng of each GAL4 DBD and VP16 AD construct pair and 200 ng of the pG5Luc (Firefly luciferase) reporter construct using the Effectene transfection reagent (Qiagen). The cells were also transfected with 1 ng of the pRL Null vector (*Renilla* luciferase) (Promega) to normalize for transfection efficiency. The cells were harvested 24 hours after transfection and assayed for firefly and *Renilla* luciferase activity using the Dual-Luciferase® Reporter Assay System (Promega).

#### 4.3.6 APOPTOSIS ASSAY

HeLaM cells were grown to 30% confluency in six-well plates and transfected with 300 ng of Flag wt PACT/pCMV2, Flag DD PACT/pcDNA 3.1<sup>-</sup>, or Flag L99E DD PACT/pcDNA 3.1<sup>-</sup> and 200 ng of pEGFPC1 (Takara Bio USA) using the Effectene Transfection reagent (Qiagen). As a control, cells were transfected with 300 ng BSIKS<sup>+</sup> (Agilent Technologies) and 200 ng pEGFPC1.

The cells were observed for EGFP fluorescence 24 hours after transfection using an inverted fluorescent microscope (EVOS®FL Imaging System, Thermo Fisher Scientific), at which time they were washed twice with PBS and fixed in 4% paraformaldehyde for 5 minutes. The cells were subsequently washed with PBS and incubated with DAPI at 0.5 µg/ml in PBS for 10 minutes at room temperature. The cells were washed again in PBS



and viewed under the fluorescent microscope. At least 300 GFP positive cells were scored as apoptotic or non-apoptotic based on their morphology. Cells showing normal flat morphology were scored as non-apoptotic, while cells showing cell shrinkage, membrane blebbing, round morphology and nuclear condensation with intense DAPI fluorescence were scored as apoptotic. The percentage of cells that underwent apoptosis (% Apoptosis) was calculated using the formula: (EGFP-positive cells with intense DAPI nuclear fluorescence/Total EGFP-positive cells) \* 100.

#### 4.3.7 STATISTICAL ANALYSES

Statistical significance of the dsRNA-binding quantifications, percent apoptosis, and results from the mammalian two-hybrid interaction assay were determined by Student's T test or one-way ANOVA followed by post-hoc Tukey test as indicated in the figure legends. *P*-values are denoted by brackets and special characters. Alpha level was  $p = 0.05$ .

## 4.4 RESULTS

The high-affinity interaction between PKR and PACT is mainly mediated by PACT's M1 and M2 motifs and M3 motif is dispensable for PKR-PACT interaction but is essential for PKR activation<sup>63,64</sup>. The M1 and M2 motifs are also involved in dsRNA binding via the conserved dsRBMs, which possess the characteristic amphipathic helix also present in PKR<sup>49,202</sup>. Specific lysines on the charged side of this amphipathic helix are important for dsRNA-binding, whereas hydrophobic amino acids on the opposite

side are important for the protein-protein interactions. In order to characterize the contribution of specific amino acids within the M1 and M2 motifs to dsRNA-binding and PKR-PACT, TRBP-PACT, and PACT-PACT interactions, we created point mutations using site-directed mutagenesis. As shown in Fig. 4.1 A, five residues were mutated individually in M1 and M2. The selected residues are conserved in the M1 and M2 motifs of both PACT and TRBP (Fig. 4.1 B). We tested the effect of these mutations on PACT's dsRNA-binding (Fig. 4.1 C and D). Mutations in both M1 and M2 affected dsRNA binding, but the M1 mutations showed a more drastic reduction in dsRNA binding where all five mutations reduced the dsRNA binding to less than 20% of the wild type PACT. The mutations in M2 showed a moderate effect with reduced dsRNA binding that ranged from 15% to 65% of the wild type PACT. These results indicate that the M1 motif contributes most to the dsRNA binding activity and M2 motif serves a supplementary role.

The dsRBMs are also involved in mediating protein-protein interactions in a dsRNA independent manner<sup>176</sup>. To understand the role of the hydrophobic residues within the M1 and M2 motifs in mediating protein-protein interactions, we tested the direct interactions of the point mutants with PKR, PACT, and TRBP using a yeast two hybrid assay. Specifically, the three hydrophobic residues have been previously shown to contribute towards PKR homodimer formation<sup>49,202</sup>. We have used the yeast two-hybrid assay to understand the interactions between PKR, PACT, and TRBP successfully and the system is sensitive enough to allow for detecting moderate to subtle changes in protein interaction affinities<sup>68,179,195</sup>. As seen in Figure 4.2, the A91E and A92D mutants

showed a drastic reduction in interaction with PKR, but the L99E mutant showed strong interaction with PKR. Contrary to M1 mutants, none of the M2 mutations showed any effect on the PACT-PKR interaction. These results strongly suggest the important role of alanine 91 and alanine 92 in M1 motif for mediating the interaction between PACT and PKR.

PACT-PACT interactions are important for PACT mediated PKR activation in response to stress<sup>68,179</sup> and we next examined the effect of the point mutations on PACT-PACT interactions. The effect of M1 mutations on PACT-PACT interaction was quite drastic with A91E, A92D, and L99E mutants showing a complete lack of interaction (Figure 4.3). However, the M2 mutations showed no effect on PACT-PACT interaction indicating that the PACT-PACT interaction is mainly mediated by the M1 motif. TRBP interacts with both PACT and PKR to act as an inhibitor of PKR and the TRBP-PACT interaction regulates PACT's ability to activate PKR in a negative manner during stress signaling. Our results shown in Figure 4.4 indicate that the TRBP-PACT interaction is mainly mediated by PACT's M1 motif as the A91E, A92D, and L99E mutations resulted in a complete lack of TRBP-PACT interaction. The M2 motif mutations A184E, A185E, and F192E had no effect on the TRBP-PACT interaction. These results indicate that similar to PACT-PACT interaction shown in Figure 4.4, the TRBP-PACT interaction is also mediated mainly by the M1 motif in PACT.

Our previous results had indicated that the stress-induced PKR activation by PACT is dependent on efficient PACT-PACT interactions and the stress-induced phosphorylation at serine 287 of PACT enhances PACT-PACT and PACT-PKR interactions

while decreasing TRBP-PACT interactions<sup>195</sup>. Since the L99E mutant retains its ability to interact efficiently with PKR but loses its ability for PACT-PACT interactions, we wanted to create a triple mutant by combining the L99E mutation with phosphomimetic S246D and S287D mutations. The phosphomimetic S246D and S287D double mutant (DD mutant) activates PKR in the absence of stress signals, induces apoptosis, and shows enhanced PACT-PACT and PACT-PKR interactions<sup>60,62,91,195</sup>. Thus, we wanted to test if the DD mutation, when combined with the L99E mutation will promote PACT-PACT interactions. We used the mammalian two-hybrid assay to test this and the results are shown in Fig. 4.5 A. The wild type PACT shows good PACT-PACT interaction and the L99E mutant shows no PACT-PACT interaction above the EV control. The DD mutant shows enhanced PACT-PACT interaction as compared to wild type PACT and in contrast to this, the combined triple mutant DD-L99E shows a lack of PACT-PACT interaction. This allowed us to examine if the phosphomimetic DD mutant would promote apoptosis if it lacked the PACT-PACT interactions.

In order to understand the contribution of PACT-PACT interactions towards PACT mediated PKR activation, we performed the apoptosis assay using nuclear condensation as a marker of apoptotic cells. We overexpressed the wild type PACT, DD mutant, and DD-L99E mutant in HeLa cells and assayed for apoptosis induction. The overexpression of both wild type and DD mutant PACT proteins is known to induce apoptosis in the absence of any stress signals. As seen in Fig. 4.5 B, an overexpression of wtPACT induced apoptosis in about 25% of the cells as compared to the 5% apoptosis in empty vector transfected cell. The overexpression of the DD

mutant caused apoptosis in about 36% cells and in contrast to this, the overexpression of DD-L99E mutant showed apoptosis in only 8% of the transfected cells. These results indicate that the PACT-PACT interaction is crucial for induction of apoptosis and the lack of PACT-PACT interactions inactivate PACT's ability to activate PKR. These results underscore the importance of enhanced PACT-PACT interactions in response to stress signals.

#### 4.5 DISCUSSION

In this report, we investigated the role of conserved residues within the M1 and M2 motifs in PACT towards dsRNA-binding, and interaction with PKR, TRBP and PACT. Overall, M1 motif plays a more significant role in dsRNA-binding activity of PACT. Similar to the two lysines at positions 60 and 150 in PKR, the corresponding lysines at positions 84 and 177 showed an essential role in dsRNA-binding. The lysine 88 mutation also showed a significant reduction in dsRNA-binding similar to the corresponding lysine 64 mutation in PKR. However, the lysine 181 mutation in M2 motif of PACT showed a much smaller reduction in dsRNA-binding as compared to a drastic effect of corresponding lysine 154 mutation in PKR.

These results indicate that although the dsRBMs are well conserved in various members of this diverse family of proteins, the effect of individual analogous point mutations in various motifs in the context of whole proteins needs to be examined in a case by case manner. Certain hydrophobic residues in M1 motif (alanine 91, alanine 92, and leucine 99) as well as in motif 2 (alanine 184) play an important role in dsRNA-

binding, similar to alanine 68 in M1 and alanine 158 in M2 of PKR<sup>202</sup>. When we tested the dsRNA-binding of individual M1 or M2 motifs previously, both M1 and M2 showed strong dsRNA-binding activity<sup>63</sup>. The data presented here underscores the importance of testing the effect of point mutations in the whole protein context instead of individual domains. The M2 motif, although fully capable of binding dsRNA on its own when existing as a separate domain, plays an auxiliary role towards dsRNA-binding in the PACT protein as a whole. Many members of the family of proteins have multiple dsRBMs present in tandem similar to PACT, TRBP, and PKR<sup>196</sup>. The dsRBM is known to be a versatile motif and the individual dsRBMs present in the same protein are known to have properties that differ in terms of dsRNA-binding and dimerization/multimerization contributing to their unique contribution to the functionality of the whole protein<sup>203</sup>.

An investigation of the relative contribution of the hydrophobic residues in M1 and M2 motifs to the protein-protein interactions demonstrated that M1 motif contributes maximally for the PKR-PACT, PACT-PACT, and PACT-TRBP interactions. All three residues (alanine 91, alanine 92, and leucine 99) were indispensable for PACT-PACT and PACT-TRBP interactions. In contrast to this, for the PKR-PACT interactions, the mutation of leucine 99 showed no effect and the alanine 91 and alanine 92 mutations showed a slight reduction in interaction. The M2 mutations showed no effect on any of the interactions. These results indicate that either of the M1 or M2 motifs can effectively mediate the interaction between PKR and PACT. In future, it may be interesting to test the effects of double mutants in M1 and M2 motifs on PKR-PACT interactions. The observation that M1 mutations had similar effect on PACT-PACT and

PACT-TRBP interactions indicates that the individual PACT molecules in cells would either be present as heteromeric complexes with TRBP or as homomeric PACT-PACT complexes. However, if the two proteins are capable of forming multimers, it remains to be determined if the stoichiometry of such complexes may change in response to stress signals to change the biological consequence and alter survival versus apoptosis equilibria.

Our previous results demonstrated that a phosphomimetic mutant of PACT with an aspartic acid substitution at both serines 246 and 287 (DD mutant) shows enhanced PACT-PACT interactions as compared to wild type PACT indicating that PACT-PACT interaction promotes PACT-PKR interaction and consequently PKR activation<sup>68</sup>. Thus, we further investigated if PACT-PACT interaction may be essential for PACT's ability to activate PKR and induce apoptosis by generating a triple mutant where we combined the DD mutation with L99E mutation. L99E mutation disables PACT-PACT interactions but keeps the PKR-PACT interaction intact and we previously have demonstrated that the L99E mutant was unable to activate PKR<sup>68</sup>. Thus, the triple mutant (S246D, S287D, L99E) allowed us to test if the phosphomimetic mutant could activate PKR if it cannot form PACT-PACT interactions.

The inability of the triple mutant to show interaction in mammalian cells as well as its inability to induce apoptosis, underscores the importance of PACT-PACT interactions in PKR activation. These results are very significant for understanding the stress-induced signaling pathways leading to apoptosis since they add an additional layer of complexity brought about by phosphorylation-mediated changes in the

relative affinity of various binding partners within the dsRBM family. This is an aspect that has not been explored to date and can have a significant influence on the various biological processes regulated by the dsRBM containing proteins<sup>176,196</sup>.

The essential role of PKR dimerization in activating its kinase function has been established in many studies when dsRNA is the activating agent<sup>177,204,205</sup>. PKR activation is brought about mainly when two PKR molecules bind to a single dsRNA molecule<sup>140,206</sup>. PKR's second dsRBM motif interacts with the catalytic domain to keep PKR in a closed conformation that prevents ATP binding<sup>50,207</sup>. Binding to dsRNA induces a conformational change that releases the dsRBM from the catalytic domain, thus allowing for ATP-binding. Structural and biophysical data also indicates that dsRNA principally functions to induce dimerization of PKR via the kinase domain<sup>208</sup>. Although PKR exists in an equilibrium between monomeric and dimeric states in the absence of its interaction with dsRNA, binding to dsRNA shifts this equilibrium towards the dimeric form and also induces a conformational change necessary to relieve the autoinhibition<sup>209</sup>.

In contrast to this, activated PKR phosphorylated on several serines and threonines exists in monomeric as well as dimeric forms and both forms are competent in kinase function and active in phosphorylating eIF2 $\alpha$ <sup>210</sup>. Similar to dsRNA mechanisms, it is likely that two or more molecules of PKR are brought in close proximity by virtue of their interaction with PACT dimer or multimer. Thus, PACT may serve the same function that a dsRNA molecule of sufficient length serves, which is to allow for binding of two PKR molecules to promote trans-autophosphorylation. It is interesting to note that



PACT-PKR interaction is strongest when PKR is not catalytically active and PACT interacts much weakly with catalytically active PKR. PKR activation thus seems to dissociate PACT from PKR. In future, it will be interesting to study if protein-protein interactions play similar regulatory roles in RNAi<sup>69,70,72</sup>, and innate immunity<sup>73</sup> pathways that are regulated by PACT.

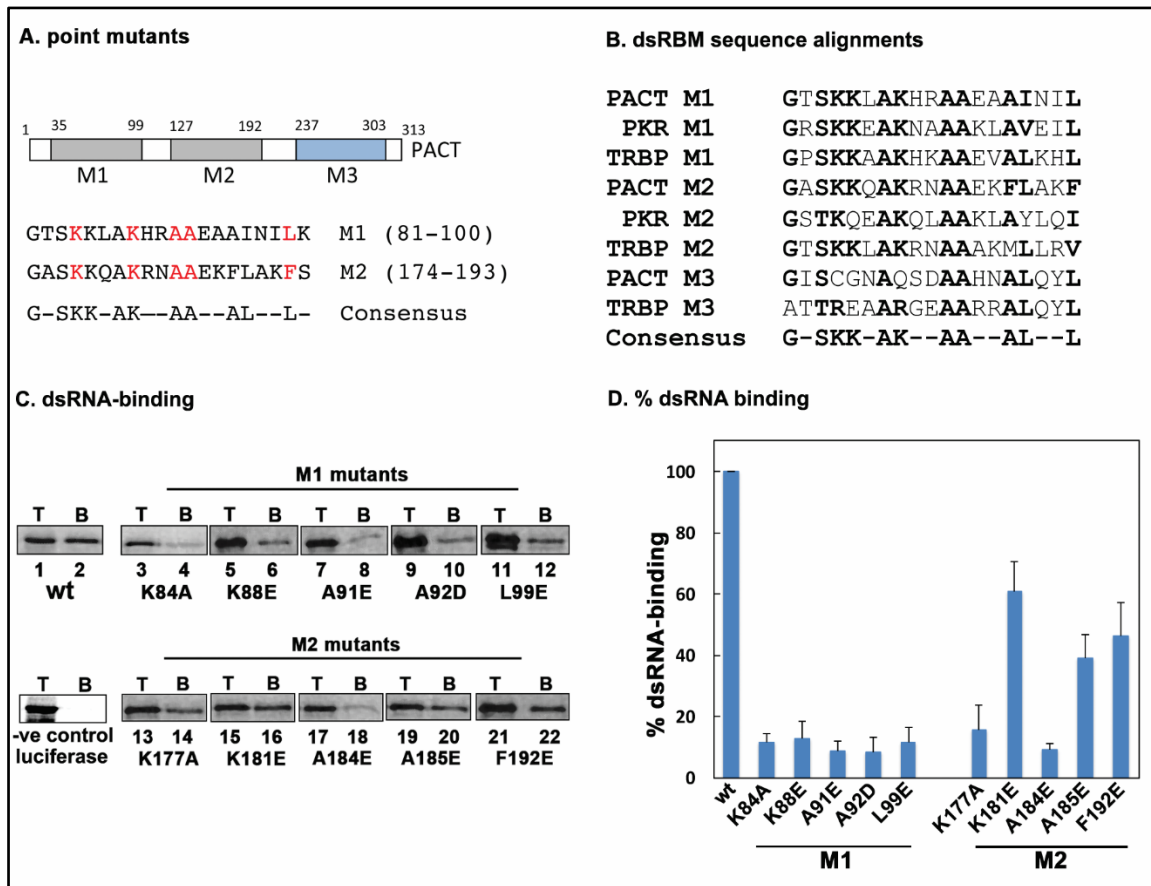


**Figure 4.1: Mutations in conserved amino acids in PACT's M1 and M2 dsRNA binding motifs (dsRBMs) disrupt PACT's interaction with dsRNA.**

**(A) Schematic representation of PACT's domain structure and conserved amino residues in PACT's M1 and M2 dsRBMs.** Gray boxes represent PACT's dsRNA binding M1 and M2 motifs, while the blue box represents PACT's M3 motif which does not interact with dsRNA, but is essential for PKR activation by PACT. Conserved residues in PACT's M1 and M2 motifs are displayed; residues in red were mutated for this study.

**(B) Sequence alignment of PACT, TRBP, and PKR's dsRNA binding motifs.** The three conserved dsRBMs of PACT (PACT M1, PACT M2, PACT M3) are aligned to those of TRBP (TRBP M1, TRBP M2, TRBP M3) and PKR (PKR M1, PKR M2). Amino acid residues in bold are conserved residues present in all 8 dsRBMs or conservative changes from the consensus sequence below. Note the presence of several hydrophobic amino acid residues (**AA---AL---L**) in all 8 dsRBMs which are known to be important in mediating each protein's homodimer and heterodimer interactions and with dsRNA.

**(C) dsRNA binding assay.** The dsRNA binding activity of each M1 and M2 PACT point mutant was compared to that of wt PACT using a poly(I).poly(C)-agarose binding assay with *in vitro* translated <sup>35</sup>S-labeled proteins. <sup>35</sup>S-labeled *in vitro* translated firefly luciferase protein was used as a control to demonstrate specific PACT

interaction with poly(I).poly(C). T represents the total input, while B represents the proteins still bound to poly(I).poly(C)-agarose beads after washes.

**(D) Quantification of the dsRNA binding assay.** Band intensities of the total and bound proteins were quantified by phosphorimager analysis, and % dsRNA binding was calculated for each PACT protein. % dsRNA-binding averages from four independent experiments are plotted as bar graphs  $\pm$  S.D.

One-way ANOVA followed by post-hoc Tukey test showed a statistically significant difference between wt PACT dsRNA binding and that of each of the PACT mutants. *P* value wt PACT vs. K84A, K88E, A91E, A92D, L99E, K177E, and K184E PACT mutants = 0.000013, *P*-value wt PACT vs. K181E PACT mutant = 0.000198, *P*-value wt PACT vs. A185E PACT mutant = 0.000014, and *P*-value wt PACT vs. F192E PACT = 0.000078

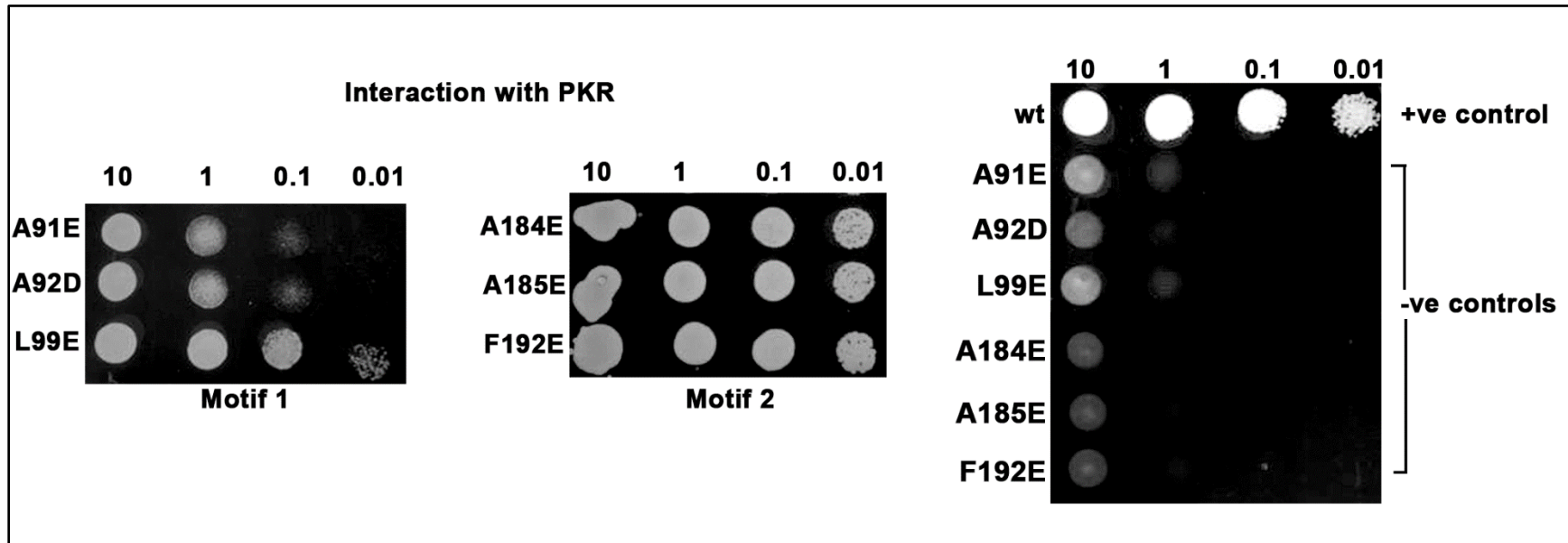
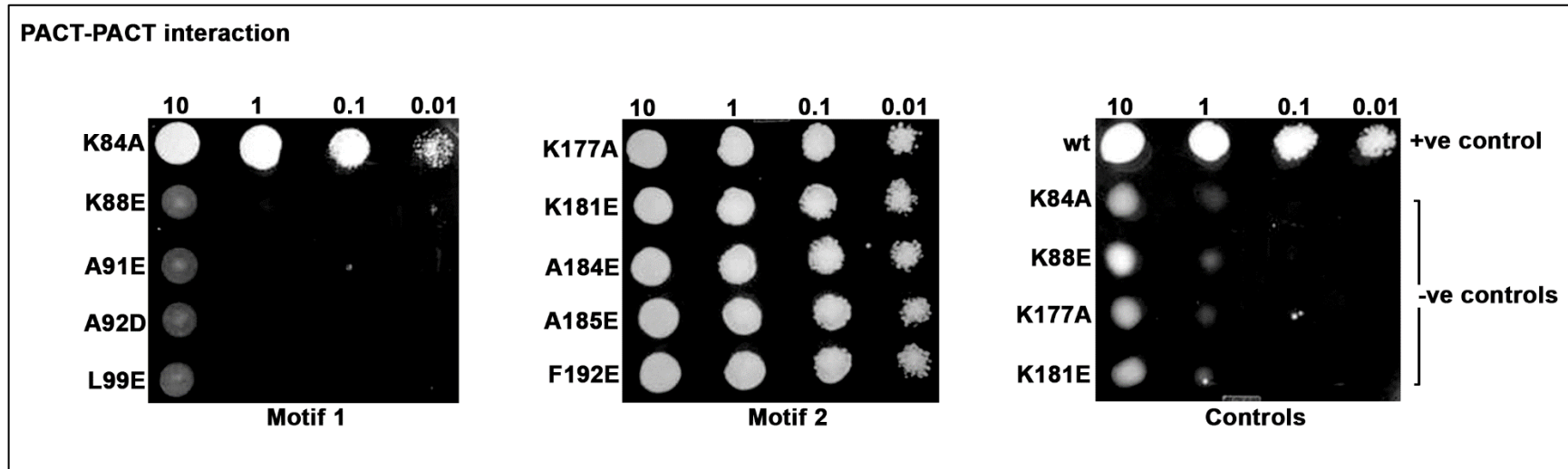


**Figure 4.2: Mutations of specific hydrophobic residues in PACT's M1 dsRBM disrupt PACT's interaction with PKR.** The K296R PKR/pGBT9 yeast expression vector and PACT M1 and M2 mutants in the pGADT7 yeast expression vector were co-transformed into AH109 yeast cells. Co-transformants were selected on SD double dropout media (-Tryptophan, -Leucine). 10 microliters of the transformed yeast cells ( $OD_{600} = 10, 1, 0.1, 0.01$ ) were spotted on SD triple dropout media agar plates (-Tryptophan, -Leucine, -Histidine). Plates were incubated at 30°C for 4 days. AH109 cells were co-transformed with wt PACT/pGADT7 and K296R PKR/pGBT9 expression vectors as a positive control, and with either the A91E PACT/pGADT7, A92D PACT/pGADT7, L99E PACT/pGADT7, A184E PACT/pGADT7, A185E PACT/pGADT7, or F192E PACT/pGADT7 and pGBT7 expression vector as negative controls.



133

**Figure 4.3: Mutations of hydrophobic residues in PACT's M1 dsRBM disrupt PACT-PACT homodimer interaction.** Each M1 and M2 PACT point mutant in the pGBKT7 and pGADT7 yeast expression vectors were co-transformed into AH109 yeast cells, and successfully co-transformed yeast cells were selected on SD double dropout media (-Tryptophan, - Leucine). 10 microliters of the transformed yeast cells ( $OD_{600} = 10, 1, 0.1, 0.01$ ) were spotted on SD triple dropout media agar plates (-Tryptophan, -Leucine, -Histidine) containing 10mM 3-amino-1,2,4-triazole (3-AT). Plates were incubated at 30°C for 4 days. AH109 cells were also co-transformed with wt PACT/pGBKT7 and wt PACT/pGADT7 as a positive control, and with either A91E PACT/pGADT7, A92D PACT/pGADT7, L99E PACT/pGADT7, A184E PACT/pGADT7, A185E PACT/pGADT7, or F192E PACT/pGADT7 and pGBKT7 as negative controls.

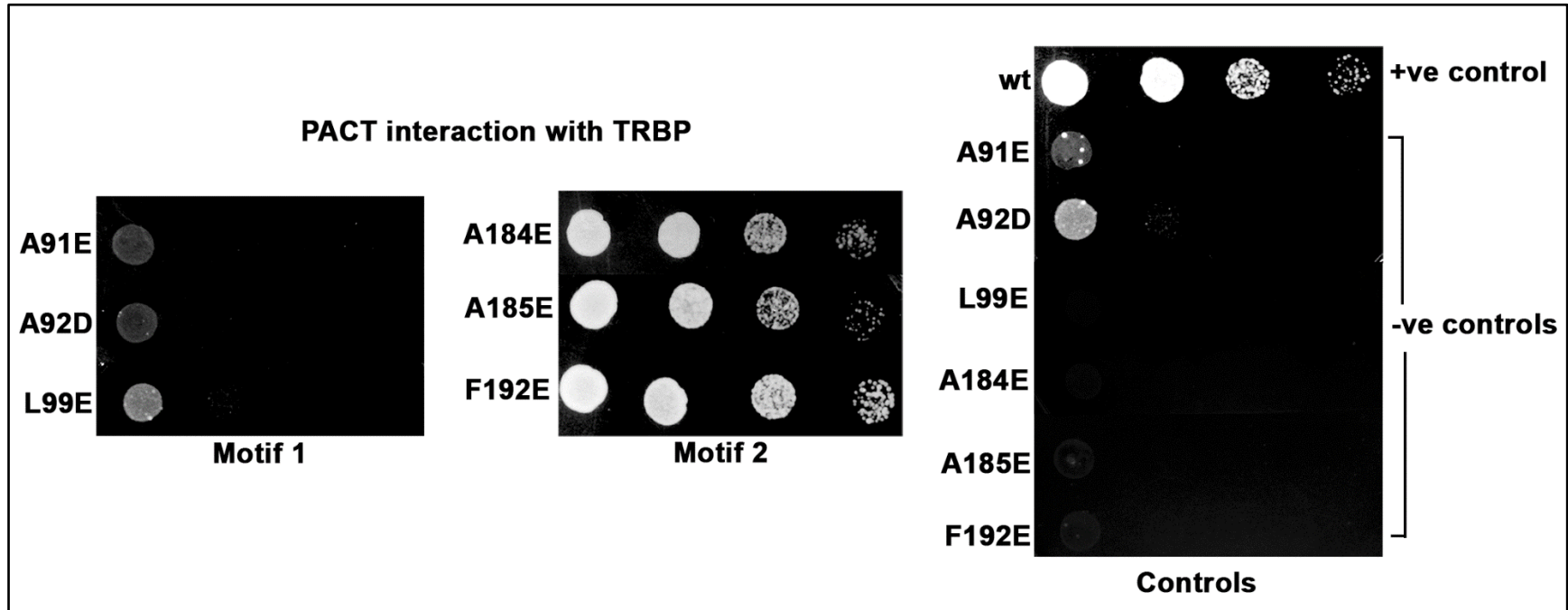


**Figure 4.4: Hydrophobic residue mutations in PACT's M1 dsRBM disrupt PACT-TRBP heterodimer interaction.** AH109 cells were co-transformed with the TRBP/pGBKT7 yeast expression vectors and each of the previously described PACT M1 and M2 point mutants in the pGADT7 yeast expression vector. Co-transformed yeast cells were selected on SD double dropout media (-Tryptophan, -Leucine). 10 microliters of serial dilutions ( $OD_{600} = 10, 1, 0.1, 0.01$ ) of the yeast cells were spotted on SD triple dropout media agar plates (-Tryptophan, -Leucine, -Histidine) containing 10mM 3-amino-1,2,4-triazole (3-AT). Plates were incubated at 30°C for 4 days. AH109 yeast cells co-transformed with TRBP/pGBKT7 and wt PACT/pGADT7 served as the positive control, while AH109 cells co-transformed with either A91E PACT/pGADT7, A92D PACT/pGADT7, L99E PACT/pGADT7, A184E PACT/pGADT7, A185E PACT/pGADT7, or F192E PACT/pGADT7 and pGBKT7 were negative controls.

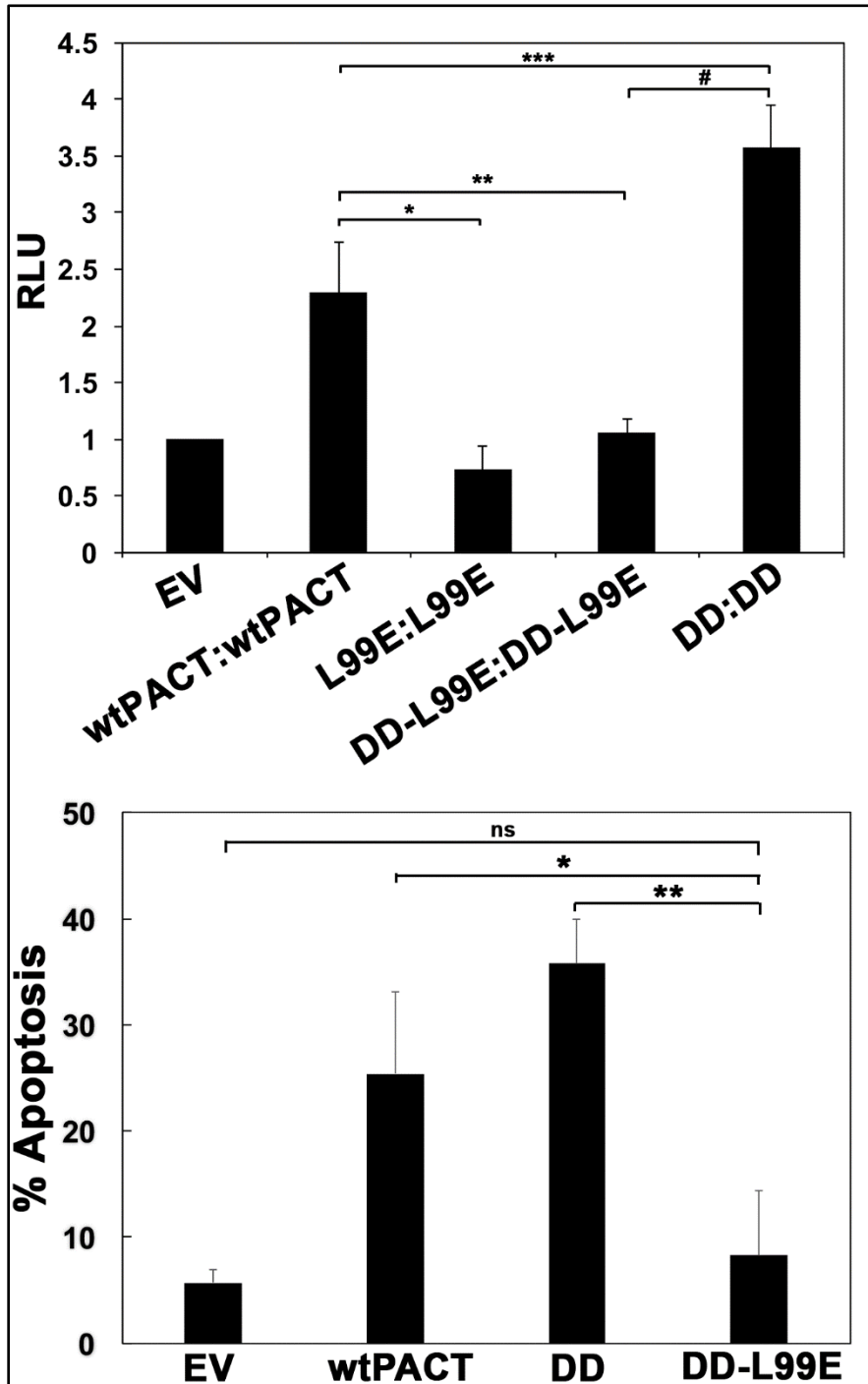


Figure 4.5: PACT homodimer interaction is required for stress-induced PACT-PACT interaction and PACT-mediated apoptotic induction.

(A) The phosphomimetic point mutation is unable to rescue L99E PACT's homodimerization defect. COS-1 cells were transfected with 200 ng each of the indicated GAL4 DBD and VP16 AD construct pairs, 200 ng of the pG5 Luc reporter construct, as well

**Figure 4.5 (continued)** as 1ng of the pRL-Null construct to normalize for different transfection efficiencies. Cells were harvested 24 hours after transfection, and lysates were assayed for Firefly and Renilla luciferase activity. Experiments were performed thrice in triplicate, and the bars represent the averages of the experiments  $\pm$  S.D. Student's t tests were performed to determine statistical significance – asterisk \*  $P$ -value = 0.0027, double asterisk \*\* $P$ -value = 0.000764, triple asterisk \*\*\*  $P$ -value = 0.015, #  $P$ -value = 0.001158.

**(B) Loss of PACT homodimer interaction significantly weakens the induction of apoptosis due to PACT phosphorylation.** HeLaM cells were transfected with 200ng of pEFPC1 and 300ng of Flag wt PACT/pCMV2 (wtPACT), 300ng of the phosphomimetic PACT expression construct (Flag DD PACT/pcDNA 3.1<sup>-</sup> (DD)) or 300 ng of the PACT triple mutant construct (Flag L99E DD PACT/ pcDNA 3.1<sup>-</sup> (DD-L99E)). Cells were also transfected with 300 ng of BSIIKS+ and 200 ng of pEGFPC1 (EV) as a control. The cells were observed for GFP expression 24 hours after transfection, and at least 300 GFP positive cells were scored as non-apoptotic or apoptotic based on nuclear condensation indicated by intense DAPI staining. The percentage of apoptotic cells (% Apoptosis) was calculated using the formula: (EGFP- expressing cells with intense DAPI nuclear staining/Total EGFP-expressing cells) x 100. Bars represent averages  $\pm$  S.D. from three independent experiments. Student's t tests were performed to determine statistical significance – *ns*: not significant, \* asterisk:  $P$ -value of 0.0391, \*\* double asterisk:  $P$ -value of 0.00294.



## CHAPTER 5

### GENERAL DISCUSSION

This dissertation focused on the various mechanisms through which the interferon-induced eIF2 $\alpha$  kinase, PKR, is regulated during viral infection and oxidative stress via its interactions with the dsRNA binding proteins, PACT and TRBP. This dissertation also underscored the importance of both of PACT's M1 and M2 dsRBMs in mediating efficient PACT homodimerization, PACT-TRBP and PACT-PKR heterodimerization, and consequently PKR activation during cellular stress.

In **Chapter 2**, we demonstrated that PACT, which normally acts as a cellular activator of PKR during non-viral cellular stress, is co-opted by the HIV-1 virus to subvert PKR's antiviral activity through the formation of a PKR-inhibitory complex that includes ADAR1, Tat, and dsRNA-containing HIV-1 transcripts. While we have established that ADAR1 suppresses PACT's PKR activating function during HIV-1 infection, the effects of the observed increased ADAR - PACT interaction on potential viral infection-induced PACT phosphorylation have yet to be elucidated. *In vivo* <sup>32</sup>P orthophosphate labelling of PACT over the course of infection in cells could establish if PACT is phosphorylated in virally infected cells, and if ADAR1 precludes this phosphorylation and consequent PACT-mediated-PKR activation. As both ADAR1 and PACT contain dsRBMs which are known to mediate both dsRNA and protein-protein interactions, determination of the essential dsRBMs and residues in each protein responsible for their interaction can facilitate peptide-mediated disruption of PACT-ADAR1 interaction during HIV-infection and enhance PKR-mediated inhibition of viral replication in infected cells. This would be an exciting novel therapeutic approach in the combinatorial therapy options used currently for HIV patients.

In **Chapter 3**, we examined the functional importance of TRBP phosphorylation on TRBP's homomeric interactions as well as its heteromeric interactions with PKR, and consequently, on PKR inhibition and cell fate during oxidative stress. Our work established for the first time that TRBP is phosphorylated in response to oxidative stress and consequently exhibits increased interaction with PKR to limit the negative effects of sustained PKR activation and ensure cellular recovery. Since TRBP phosphorylation by ERK has been shown to stimulate the expression of pro-growth miRNAs and enhance the stability of the RNA induced silencing complex<sup>181</sup>, an investigation into any TRBP phosphorylation dependent alterations of miRNA profiles in response to stress signals may reveal an additional layer of TRBP mediated modulation of the cellular stress response independent of PKR and translational inhibition.

In **Chapter 4**, we determined the relative contributions of each of PACT's dsRNA binding motifs to the entire protein's interactions with dsRNA, with itself, as well as with PKR and TRBP. Our experiments established that while both dsRBMs mediate dsRNA interaction, PACT's M1 motif is important for heterodimeric interactions with TRBP and PKR and PACT-PACT homodimer formation and highlight the critical role that stress-induced PACT phosphorylation and PACT-PACT homodimerization plays in ensuring a timely PKR activation in response to various stress. Future experiments can be performed to determine the importance of PACT homodimerization in various cellular processes in which PACT has been shown or suggested to play an important role such as the innate immune response through ADAR1 and the cytoplasmic RNA sensor RIG-I and RNA interference through interactions with Dicer and TRBP.

This work emphasizes the importance of stress-induced alterations in the interactions between these three dsRNA binding proteins in restoring cellular homeostasis after cellular stress, particularly in light of the fact that all three proteins are at the intersection of the cellular response to viral and non-viral stress, innate immunity and small RNA biogenesis.

## REFERENCES

1. Pakos-Zebrucka, K. *et al.* The integrated stress response. *EMBO Rep.* **17**, 1374–1395 (2016).
2. Holcik, M. & Sonenberg, N. Translational control in stress and apoptosis. *Nat. Rev. Mol. Cell Biol.* **6**, 318–327 (2005).
3. Wek, R. C., Jiang, H.-Y. & Anthony, T. G. Coping with stress: eIF2 kinases and translational control. *Biochem. Soc. Trans.* **34**, 7–11 (2006).
4. Harding, H. P. *et al.* An Integrated Stress Response Regulates Amino Acid Metabolism and Resistance to Oxidative Stress. *Mol. Cell* **11**, 619–633 (2003).
5. Mohr, I. & Sonenberg, N. Host Translation at the Nexus of Infection and Immunity. *Cell Host Microbe* **12**, 470–483 (2012).
6. Chen, J. J. & London, I. M. Regulation of protein synthesis by heme-regulated eIF-2 alpha kinase. *Trends Biochem. Sci.* **20**, 105–108 (1995).
7. Wek, S. A., Zhu, S. & Wek, R. C. The histidyl-tRNA synthetase-related sequence in the eIF-2 alpha protein kinase GCN2 interacts with tRNA and is required for activation in response to starvation for different amino acids. *Mol. Cell. Biol.* **15**, 4497–4506 (1995).

8. Prostko, C. R., Dholakia, J. N., Brostrom, M. A. & Brostrom, C. O. Activation of the Double-stranded RNA-regulated Protein Kinase by Depletion of Endoplasmic Reticular Calcium Stores. *J. Biol. Chem.* **270**, 6211–6215 (1995).
9. Krishnamoorthy, T., Pavitt, G. D., Zhang, F., Dever, T. E. & Hinnebusch, A. G. Tight Binding of the Phosphorylated Subunit of Initiation Factor 2 (eIF2 ) to the Regulatory Subunits of Guanine Nucleotide Exchange Factor eIF2B Is Required for Inhibition of Translation Initiation. *Mol. Cell. Biol.* **21**, 5018–5030 (2001).
10. Vattem, K. M. & Wek, R. C. Reinitiation involving upstream ORFs regulates ATF4 mRNA translation in mammalian cells. *Proc. Natl. Acad. Sci. U. S. A.* **101**, 11269–11274 (2004).
11. Ma, Y., Brewer, J. W., Diehl, J. A. & Hendershot, L. M. Two distinct stress signaling pathways converge upon the CHOP promoter during the mammalian unfolded protein response. *J. Mol. Biol.* **318**, 1351–1365 (2002).
12. Palam, L. R., Baird, T. D. & Wek, R. C. Phosphorylation of eIF2 Facilitates Ribosomal Bypass of an Inhibitory Upstream ORF to Enhance CHOP Translation. *J. Biol. Chem.* **286**, 10939–10949 (2011).
13. Novoa, I., Zeng, H., Harding, H. P. & Ron, D. Feedback inhibition of the unfolded protein response by GADD34-mediated dephosphorylation of eIF2alpha. *J. Cell Biol.* **153**, 1011–1022 (2001).
14. Luo, S., Baumeister, P., Yang, S., Abcouwer, S. F. & Lee, A. S. Induction of Grp78/BiP by Translational Block ACTIVATION OF THE Grp78 PROMOTER BY ATF4 THROUGH

AN UPSTREAM ATF/CRE SITE INDEPENDENT OF THE ENDOPLASMIC RETICULUM STRESS ELEMENTS. *J. Biol. Chem.* **278**, 37375–37385 (2003).

15. Dey, S. *et al.* Both Transcriptional Regulation and Translational Control of ATF4 Are Central to the Integrated Stress Response. *J. Biol. Chem.* **285**, 33165–33174 (2010).
16. He, C. H. *et al.* Identification of Activating Transcription Factor 4 (ATF4) as an Nrf2-interacting Protein IMPLICATION FOR HEME OXYGENASE-1 GENE REGULATION. *J. Biol. Chem.* **276**, 20858–20865 (2001).
17. Marciniak, S. J. *et al.* CHOP induces death by promoting protein synthesis and oxidation in the stressed endoplasmic reticulum. *Genes Dev.* **18**, 3066–3077 (2004).
18. Su, N. & Kilberg, M. S. C/EBP homology protein (CHOP) interacts with activating transcription factor 4 (ATF4) and negatively regulates the stress-dependent induction of the asparagine synthetase gene. *J. Biol. Chem.* **283**, 35106–35117 (2008).
19. Dever, T. E. *et al.* Mammalian eukaryotic initiation factor 2 alpha kinases functionally substitute for GCN2 protein kinase in the GCN4 translational control mechanism of yeast. *Proc. Natl. Acad. Sci.* **90**, 4616–4620 (1993).
20. Zhu, S., Sobolev, A. Y. & Wek, R. C. Histidyl-tRNA Synthetase-related Sequences in GCN2 Protein Kinase Regulate in Vitro Phosphorylation of eIF-2. *J. Biol. Chem.* **271**, 24989–24994 (1996).
21. Zhang, P. *et al.* The GCN2 eIF2 $\alpha$  Kinase Is Required for Adaptation to Amino Acid Deprivation in Mice. *Mol. Cell. Biol.* **22**, 6681–6688 (2002).

22. Harding, H. P., Zhang, Y., Bertolotti, A., Zeng, H. & Ron, D. Perk Is Essential for Translational Regulation and Cell Survival during the Unfolded Protein Response. *Mol. Cell* **5**, 897–904 (2000).
23. Hetz, C. The unfolded protein response: controlling cell fate decisions under ER stress and beyond. *Nat. Rev. Mol. Cell Biol.* **13**, 89–102 (2012).
24. Bertolotti, A., Zhang, Y., Hendershot, L. M., Harding, H. P. & Ron, D. Dynamic interaction of BiP and ER stress transducers in the unfolded-protein response. *Nat. Cell Biol.* **2**, 326–332 (2000).
25. Rafie-Kolpin, M. *et al.* Two Heme-binding Domains of Heme-regulated Eukaryotic Initiation Factor-2 $\alpha$  Kinase N TERMINUS AND KINASE INSERTION. *J. Biol. Chem.* **275**, 5171–5178 (2000).
26. Igarashi, J. *et al.* Elucidation of the Heme Binding Site of Heme-regulated Eukaryotic Initiation Factor 2 $\alpha$  Kinase and the Role of the Regulatory Motif in Heme Sensing by Spectroscopic and Catalytic Studies of Mutant Proteins. *J. Biol. Chem.* **283**, 18782–18791 (2008).
27. Guerra, S., López-Fernández, L. A., García, M. A., Zaballos, A. & Esteban, M. Human Gene Profiling in Response to the Active Protein Kinase, Interferon-induced Serine/threonine Protein Kinase (PKR), in Infected Cells INVOLVEMENT OF THE TRANSCRIPTION FACTOR ATF-3 IN PKR-INDUCED APOPTOSIS. *J. Biol. Chem.* **281**, 18734–18745 (2006).
28. Pflugheber, J. *et al.* Regulation of PKR and IRF-1 during hepatitis C virus RNA replication. *Proc. Natl. Acad. Sci. U. S. A.* **99**, 4650–4655 (2002).



29. D'Acquisto, F. & Ghosh, S. PACT and PKR: Turning on NF- $\kappa$ B in the Absence of Virus. *Sci. Signal.* **2001**, re1-re1 (2001).
30. Gil, J., Rullas, J., Garcia, M., Alcamí, J. & Esteban, M. *The catalytic activity of dsRNA-dependent protein kinase, PKR, is required for NF- $\kappa$ B activation.* **20**, (2001).
31. Cuddihy, A. R. *et al.* Double-Stranded-RNA-Activated Protein Kinase PKR Enhances Transcriptional Activation by Tumor Suppressor p53. *Mol. Cell. Biol.* **19**, 2475–2484 (1999).
32. Takada, Y., Ichikawa, H., Pataer, A., Swisher, S. & Aggarwal, B. B. Genetic deletion of PKR abrogates TNF-induced activation of I $\kappa$ B $\alpha$  kinase, JNK, Akt and cell proliferation but potentiates p44/p42 MAPK and p38 MAPK activation. *Oncogene* **26**, 1201–1212 (2006).
33. Camargos, S. *et al.* DYT16, a novel young-onset dystonia-parkinsonism disorder: identification of a segregating mutation in the stress-response protein PRKRA. *Lancet Neurol.* **7**, 207–215 (2008).
34. Marchal, J. A. *et al.* The impact of PKR activation: from neurodegeneration to cancer. *FASEB J.* **28**, 1965–1974 (2014).
35. Vance, R. E., Isberg, R. R. & Portnoy, D. A. Patterns of Pathogenesis: Discrimination of Pathogenic and Nonpathogenic Microbes by the Innate Immune System. *Cell Host Microbe* **6**, 10–21 (2009).
36. O'Neill, L. A. J. & Bowie, A. G. Sensing and Signaling in Antiviral Innate Immunity. *Curr. Biol.* **20**, R328–R333 (2010).

37. Gordon, J. & Minks, M. A. The interferon renaissance: molecular aspects of induction and action. *Microbiol. Rev.* **45**, 244–266 (1981).
38. Platanias, L. C. Mechanisms of type-I- and type-II-interferon-mediated signalling. *Nat. Rev. Immunol.* **5**, nri1604 (2005).
39. González-Navajas, J. M., Lee, J., David, M. & Raz, E. Immunomodulatory functions of type I interferons. *Nat. Rev. Immunol.* **12**, nri3133 (2012).
40. Interferon-Stimulated Genes: A Complex Web of Host Defenses | Annual Review of Immunology. Available at:  
<http://www.annualreviews.org/doi/abs/10.1146/annurev-immunol-032713-120231>. (Accessed: 28th October 2017)
41. Wiebe, M. E. & Joklik, W. K. The mechanism of inhibition of reovirus replication by interferon. *Virology* **66**, 229–240 (1975).
42. Friedman, R. M. *et al.* Mechanism of Interferon Action: Inhibition of Viral Messenger Ribonucleic Acid Translation in L-Cell Extracts. *J. Virol.* **10**, 1184–1198 (1972).
43. Krust, B., Galabru, J. & Hovanessian, A. G. Further characterization of the protein kinase activity mediated by interferon in mouse and human cells. *J. Biol. Chem.* **259**, 8494–8498 (1984).
44. Nanduri, S., Carpick, B. W., Yang, Y., Williams, B. R. G. & Qin, J. Structure of the double-stranded RNA-binding domain of the protein kinase PKR reveals the molecular basis of its dsRNA-mediated activation. *EMBO J.* **17**, 5458–5465 (1998).
45. Green, S. R. & Mathews, M. B. Two RNA-binding motifs in the double-stranded RNA-activated protein kinase, DAI. *Genes Dev.* **6**, 2478–2490 (1992).

46. Patel, R. C., Stanton, P. & Sen, G. C. Role of the amino-terminal residues of the interferon-induced protein kinase in its activation by double-stranded RNA and heparin. *J. Biol. Chem.* **269**, 18593–18598 (1994).
47. Romano, P. R., Green, S. R., Barber, G. N., Mathews, M. B. & Hinnebusch, A. G. Structural requirements for double-stranded RNA binding, dimerization, and activation of the human eIF-2 alpha kinase DAI in *Saccharomyces cerevisiae*. *Mol. Cell. Biol.* **15**, 365–378 (1995).
48. Cole, J. L. Activation of PKR: an open and shut case? *Trends Biochem. Sci.* **32**, 57–62 (2007).
49. Patel, R. C. & Sen, G. C. Requirement of PKR dimerization mediated by specific hydrophobic residues for its activation by double-stranded RNA and its antigrowth effects in yeast., Requirement of PKR Dimerization Mediated by Specific Hydrophobic Residues for Its Activation by Double-Stranded RNA and Its Antigrowth Effects in Yeast. *Mol. Cell. Biol. Mol. Cell. Biol.* **18**, **18**, 7009, 7009–7019 (1998).
50. Nanduri, S., Rahman, F., Williams, B. R. G. & Qin, J. A dynamically tuned double-stranded RNA binding mechanism for the activation of antiviral kinase PKR. *EMBO J.* **19**, 5567–5574 (2000).
51. Dar, A. C., Dever, T. E. & Sicheri, F. Higher-Order Substrate Recognition of eIF2 $\alpha$  by the RNA-Dependent Protein Kinase PKR. *Cell* **122**, 887–900 (2005).
52. Hovanessian, A. G. & Galabru, J. The double-stranded RNA-dependent protein kinase is also activated by heparin. *Eur. J. Biochem.* **167**, 467–473 (1987).

53. George, C. X., Thomis, D. C., McCormack, S. J., Svahn, C. M. & Samuel, C. E. Characterization of the heparin-mediated activation of PKR, the interferon-inducible RNA-dependent protein kinase. *Virology* **221**, 180–188 (1996).
54. Patel, R. C., Handy, I. & Patel, C. V. Contribution of Double-Stranded RNA-Activated Protein Kinase Toward Antiproliferative Actions of Heparin on Vascular Smooth Muscle Cells. *Arterioscler. Thromb. Vasc. Biol.* **22**, 1439–1444 (2002).
55. Fasciano, S., Patel, R. C., Handy, I. & Patel, C. V. Regulation of Vascular Smooth Muscle Proliferation by Heparin INHIBITION OF CYCLIN-DEPENDENT KINASE 2 ACTIVITY BY p27kip1. *J. Biol. Chem.* **280**, 15682–15689 (2005).
56. Fasciano, S., Hutchins, B., Handy, I. & Patel, R. C. Identification of the heparin-binding domains of the interferon-induced protein kinase, PKR. *FEBS J.* **272**, 1425–1439 (2005).
57. Anderson, E., Pierre-Louis, W. S., Wong, C. J., Lary, J. W. & Cole, J. L. Heparin Activates PKR by Inducing Dimerization. *J. Mol. Biol.* **413**, 973–984 (2011).
58. Patel, R. C. & Sen, G. C. PACT, a protein activator of the interferon-induced protein kinase, PKR. *EMBO J.* **17**, 4379–4390 (1998).
59. Ito, T., Yang, M. & May, W. S. RAX, a Cellular Activator for Double-stranded RNA-dependent Protein Kinase during Stress Signaling. *J. Biol. Chem.* **274**, 15427–15432 (1999).
60. Patel, C. V., Handy, I., Goldsmith, T. & Patel, R. C. PACT, a Stress-modulated Cellular Activator of Interferon-induced Double-stranded RNA-activated Protein Kinase, PKR. *J. Biol. Chem.* **275**, 37993–37998 (2000).

61. Bennett, R. L. *et al.* RAX, the PKR activator, sensitizes cells to inflammatory cytokines, serum withdrawal, chemotherapy, and viral infection. *Blood* **108**, 821–829 (2006).
62. Singh, M., Fowlkes, V., Handy, I., Patel, C. V. & Patel, R. C. Essential Role of PACT-Mediated PKR Activation in Tunicamycin-Induced Apoptosis. *J. Mol. Biol.* **385**, 457–468 (2009).
63. Huang, X., Hutchins, B. & Patel, R. C. The C-terminal, third conserved motif of the protein activator PACT plays an essential role in the activation of double-stranded-RNA-dependent protein kinase (PKR). *Biochem. J.* **366**, 175–186 (2002).
64. Peters, G., Hartmann, R., Qin, J. & Sen, G. *Modular Structure of PACT: Distinct Domains for Binding and Activating PKR.* **21**, (2001).
65. Gupta, V., Huang, X. & Patel, R. C. The carboxy-terminal, M3 motifs of PACT and TRBP have opposite effects on PKR activity. *Virology* **315**, 283–291 (2003).
66. Peters, G. A., Li, S. & Sen, G. C. Phosphorylation of Specific Serine Residues in the PKR Activation Domain of PACT Is Essential for Its Ability to Mediate Apoptosis. *J. Biol. Chem.* **281**, 35129–35136 (2006).
67. Singh, M., Castillo, D., Patel, C. & Patel, R. Stress-induced phosphorylation of PACT reduces its interaction with TRBP and leads to PKR activation. *Biochemistry (Mosc.)* **50**, 4550–60 (2011).
68. Singh, M. & Patel, R. C. Increased interaction between PACT molecules in response to stress signals is required for PKR activation. *J. Cell. Biochem.* **113**, 2754–2764 (2012).

69. Lee, Y. *et al.* The role of PACT in the RNA silencing pathway. *EMBO J.* **25**, 522–532 (2006).
70. Kok, K. H., Ng, M.-H. J., Ching, Y.-P. & Jin, D.-Y. Human TRBP and PACT Directly Interact with Each Other and Associate with Dicer to Facilitate the Production of Small Interfering RNA. *J. Biol. Chem.* **282**, 17649–17657 (2007).
71. Noland, C. L., Ma, E. & Doudna, J. A. siRNA Repositioning for Guide Strand Selection by Human Dicer Complexes. *Mol. Cell* **43**, 110–121 (2011).
72. Lee, H. Y., Zhou, K., Smith, A. M., Noland, C. L. & Doudna, J. A. Differential roles of human Dicer-binding proteins TRBP and PACT in small RNA processing. *Nucleic Acids Res.* **41**, 6568–6576 (2013).
73. Kok, K.-H. *et al.* The Double-Stranded RNA-Binding Protein PACT Functions as a Cellular Activator of RIG-I to Facilitate Innate Antiviral Response. *Cell Host Microbe* **9**, 299–309 (2011).
74. Lui, P.-Y. *et al.* PACT Facilitates RNA-Induced Activation of MDA5 by Promoting MDA5 Oligomerization. *J. Immunol.* **199**, 1846–1855 (2017).
75. Iwamura, T. *et al.* PACT, a Double-Stranded RNA Binding Protein Acts as a Positive Regulator for Type I Interferon Gene Induced by Newcastle Disease Virus. *Biochem. Biophys. Res. Commun.* **282**, 515–523 (2001).
76. Clerzius, G. *et al.* The PKR activator, PACT, becomes a PKR inhibitor during HIV-1 replication. *Retrovirology* **10**, 96 (2013).
77. Schneider, W. M., Chevillotte, M. D. & Rice, C. M. Interferon-Stimulated Genes: A Complex Web of Host Defenses. *Annu. Rev. Immunol.* **32**, 513–545 (2014).

78. Pfaller, C. K., Li, Z., George, C. X. & Samuel, C. E. Protein kinase PKR and RNA adenosine deaminase ADAR1: new roles for old players as modulators of the interferon response. *Curr. Opin. Immunol.* **23**, 573–582 (2011).
79. Chukwurah, E., Handy, I. & Patel, R. C. ADAR1 and PACT contribute to efficient translation of transcripts containing HIV-1 trans-activating response (TAR) element. *Biochem. J.* **474**, 1241–1257 (2017).
80. Cai, R., Carpick, B., Chun, R. F., Jeang, K.-T. & Williams, B. R. G. HIV-1 TAT Inhibits PKR Activity by Both RNA-Dependent and RNA-Independent Mechanisms. *Arch. Biochem. Biophys.* **373**, 361–367 (2000).
81. Endo-Munoz, L., Warby, T., Harrich, D. & McMillan, N. A. J. Phosphorylation of HIV Tat by PKR increases interaction with TAR RNA and enhances transcription. *Viol. J.* **2**, 17 (2005).
82. Brand, S. R., Kobayashi, R. & Mathews, M. B. The Tat Protein of Human Immunodeficiency Virus Type 1 Is a Substrate and Inhibitor of the Interferon-induced, Virally Activated Protein Kinase, PKR. *J. Biol. Chem.* **272**, 8388–8395 (1997).
83. Dabo, S. & Meurs, E. F. dsRNA-dependent protein kinase PKR and its role in stress, signaling and HCV infection. *Viruses* **4**, 2598–2635 (2012).
84. Lee, T., Tang, N., Thompson, S., Miller, J. & Katze, M. G. *The 58,000-dalton cellular inhibitor of the interferon-induced double-stranded RNA-activated protein kinase (PKR) is a member of the tetratricopeptide repeat family of proteins.* **14**, (1994).
85. Katze, M. G. *et al.* Influenza virus regulates protein synthesis during infection by repressing autophosphorylation and activity of the cellular 68,000-Mr protein

- kinase., Influenza virus regulates protein synthesis during infection by repressing autophosphorylation and activity of the cellular 68,000-Mr protein kinase. *J. Virol. J. Virol.* **62**, 3710, 3710–3717 (1988).
86. Clerzius, G. *et al.* ADAR1 interacts with PKR during human immunodeficiency virus infection of lymphocytes and contributes to viral replication. *J. Virol.* **83**, 10119–10128 (2009).
87. Gatignol, A., Buckler-White, A., Berkhout, B. & Jeang, K. T. Characterization of a human TAR RNA-binding protein that activates the HIV-1 LTR. *Science* **251**, 1597–1600 (1991).
88. Christensen, H. S. *et al.* Small interfering RNAs against the TAR RNA binding protein, TRBP, a Dicer cofactor, inhibit human immunodeficiency virus type 1 long terminal repeat expression and viral production. *J Virol* **81**, (2007).
89. Ong, C. L. *et al.* Low TRBP Levels Support an Innate Human Immunodeficiency Virus Type 1 Resistance in Astrocytes by Enhancing the PKR Antiviral Response. *J. Virol.* **79**, 12763–12772 (2005).
90. Haase, A. D. *et al.* TRBP, a regulator of cellular PKR and HIV-1 virus expression, interacts with Dicer and functions in RNA silencing. *EMBO Rep* **6**, (2005).
91. Daniels, S. M. *et al.* Characterization of the TRBP domain required for Dicer interaction and function in RNA interference. *BMC Mol. Biol.* **10**, 38 (2009).
92. Kim, Y. *et al.* Deletion of Human tarbp2 Reveals Cellular MicroRNA Targets and Cell-Cycle Function of TRBP. *Cell Rep.* **9**, 1061–1074 (2014).



93. Lee, Y. *et al.* The role of PACT in the RNA silencing pathway. *EMBO J.* **25**, 522–532 (2006).
94. Carpick, B. W. *et al.* Characterization of the Solution Complex between the Interferon-induced, Double-stranded RNA-activated Protein Kinase and HIV-I Trans-activating Region RNA. *J. Biol. Chem.* **272**, 9510–9516 (1997).
95. Benkirane, M. *et al.* Oncogenic potential of TAR RNA binding protein TRBP and its regulatory interaction with RNA-dependent protein kinase PKR. *EMBO J.* **16**, 611–624 (1997).
96. Cosentino, G. P. *et al.* Double-stranded-RNA-dependent protein kinase and TAR RNA-binding protein form homo- and heterodimers in vivo. *Proc. Natl. Acad. Sci.* **92**, 9445–9449 (1995).
97. Daher, A. *et al.* Two Dimerization Domains in the Trans-activation Response RNA-binding Protein (TRBP) Individually Reverse the Protein Kinase R Inhibition of HIV-1 Long Terminal Repeat Expression. *J. Biol. Chem.* **276**, 33899–33905 (2001).
98. Daher, A. *et al.* TRBP control of PACT-induced phosphorylation of PKR is reversed by stress. *Mol. Cell. Biol.* **29**, 254–65 (2008).
99. Kim, Y. *et al.* PKR is activated by cellular dsRNAs during mitosis and acts as a mitotic regulator. *Genes Dev.* **28**, 1310–1322 (2014).
100. Nakamura, T. *et al.* A Critical Role for PKR Complexes with TRBP in Immunometabolic Regulation and eIF2 $\alpha$  Phosphorylation in Obesity. *Cell Rep.* **11**, 295–307 (2015).

101. Lancaster, G. I. *et al.* PKR is not obligatory for high-fat diet-induced obesity and its associated metabolic and inflammatory complications. *Nat. Commun.* **7**, (2016).
102. Zuniga, E. I., Macal, M., Lewis, G. M. & Harker, J. A. Innate and Adaptive Immune Regulation During Chronic Viral Infections. *Annu. Rev. Virol.* **2**, 573–597 (2015).
103. Chow, J., Franz, K. M. & Kagan, J. C. PRRs are watching you: Localization of innate sensing and signaling regulators. *Virology* **479–480**, 104–109 (2015).
104. Samuel, C. E. Adenosine deaminases acting on RNA (ADARs) are both antiviral and proviral. *Virology* **411**, 180–193 (2011).
105. Gélinas, J.-F., Clerzius, G., Shaw, E. & Gatignol, A. Enhancement of Replication of RNA Viruses by ADAR1 via RNA Editing and Inhibition of RNA-Activated Protein Kinase. *J. Virol.* **85**, 8460–8466 (2011).
106. Bannwarth, S. & Gatignol, A. *Bannwarth, S. & Gatignol, A. HIV-1 TAR RNA: the target of molecular interactions between the virus and its host. Curr. HIV Res.* **3**, 61-71. **3**, (2005).
107. Rustagi, A. & Gale, M. Innate Antiviral Immune Signaling, Viral Evasion and Modulation by HIV-1. *J. Mol. Biol.* **426**, 1161–1177 (2014).
108. Meurs, E. *et al.* Molecular cloning and characterization of the human double-stranded RNA-activated protein kinase induced by interferon. *Cell* **62**, 379–390 (1990).
109. Burugu, S., Daher, A., Meurs, E. F. & Gatignol, A. HIV-1 translation and its regulation by cellular factors PKR and PACT. *Virus Res.* **193**, 65–77 (2014).

110. Yim, H. & R.G. Williams, B. Protein Kinase R and the Inflammasome. *J. Interferon Cytokine Res.* **34**, 447–454 (2014).
111. Galabru, J. & Hovanessian, A. Autophosphorylation of the protein kinase dependent on double-stranded RNA. *J. Biol. Chem.* **262**, 15538–15544 (1987).
112. Clemens, M. J. PKR—A protein kinase regulated by double-stranded RNA. *Int. J. Biochem. Cell Biol.* **29**, 945–949 (1997).
113. Gale, M. & Katze, M. G. Molecular Mechanisms of Interferon Resistance Mediated by Viral-Directed Inhibition of PKR, the Interferon-Induced Protein Kinase. *Pharmacol. Ther.* **78**, 29–46 (1998).
114. Dauber, B. & Wolff, T. Activation of the Antiviral Kinase PKR and Viral Countermeasures. *Viruses* **1**, 523–544 (2009).
115. Katze, M. G. Regulation of the interferon-induced PKR: can viruses cope? *Trends Microbiol.* **3**, 75–78 (1995).
116. Rosen, C. A., Sodroski, J. G. & Haseltine, W. A. The location of cis-acting regulatory sequences in the human T cell lymphotropic virus type III (HTLV-III/LAV) long terminal repeat. *Cell* **41**, 813–823 (1985).
117. Hinnebusch, A. G., Ivanov, I. P. & Sonenberg, N. Translational control by 5'-untranslated regions of eukaryotic mRNAs. *Science* **352**, 1413–1416 (2016).
118. Clerzius, G., Gélinas, J.-F. & Gatignol, A. Multiple levels of PKR inhibition during HIV-1 replication. *Rev. Med. Virol.* **21**, 42–53 (2011).

119. Edery, I., Petryshyn, R. & Sonenberg, N. Activation of double-stranded RNA-dependent kinase (dsl) by the TAR region of HIV-1 mRNA: A novel translational control mechanism. *Cell* **56**, 303–312 (1989).
120. Park, H. *et al.* TAR RNA-binding protein is an inhibitor of the interferon-induced protein kinase PKR. *Proc. Natl. Acad. Sci.* **91**, 4713–4717 (1994).
121. RG Williams, B. *PKR; A sentinel kinase for cellular stress.* **18**, (1999).
122. Williams, B. R. G. Signal Integration via PKR. *Sci STKE* **2001**, re2-re2 (2001).
123. Daniels, S. M. & Gatignol, A. The Multiple Functions of TRBP, at the Hub of Cell Responses to Viruses, Stress, and Cancer. *Microbiol. Mol. Biol. Rev.* **76**, 652–666 (2012).
124. X George, C., John, L. & E Samuel, C. An RNA editor, adenosine deaminase acting on double-stranded RNA (ADAR1). *J Interferon Cytokine Res* **34**, 437–446 (2014).
125. Nishikura, K. A-to-I editing of coding and non-coding RNAs by ADARs. *Nat. Rev. Mol. Cell Biol.* **17**, nrm.2015.4 (2015).
126. Heraud-Farlow, J. E. & Walkley, C. R. The role of RNA editing by ADAR1 in prevention of innate immune sensing of self-RNA. *J. Mol. Med.* **94**, 1095–1102 (2016).
127. Gatignol, A. Transcription of HIV: Tat and Cellular Chromatin. in *Advances in Pharmacology* **55**, 137–159 (Academic Press, 2007).
128. Chauhan, A. *et al.* Intracellular Human Immunodeficiency Virus Tat Expression in Astrocytes Promotes Astrocyte Survival but Induces Potent Neurotoxicity at Distant Sites via Axonal Transport. *J. Biol. Chem.* **278**, 13512–13519 (2003).

129. Yang, Y. L. *et al.* Deficient signaling in mice devoid of double-stranded RNA-dependent protein kinase. *EMBO J.* **14**, 6095–6106 (1995).
130. Daniels, S. *et al.* HIV-1 RRE RNA acts as an RNA silencing suppressor by competing with TRBP-bound siRNAs. *RNA Biol.* **12**, (2015).
131. Kimpton, J. & Emerman, M. Detection of replication-competent and pseudotyped human immunodeficiency virus with a sensitive cell line on the basis of activation of an integrated beta-galactosidase gene., Detection of replication-competent and pseudotyped human immunodeficiency virus with a sensitive cell line on the basis of activation of an integrated beta-galactosidase gene. *J. Virol. J. Virol.* **66**, **66**, 2232, 2232–2239 (1992).
132. Vodicka, M. A. *et al.* Indicator cell lines for detection of primary strains of human and simian immunodeficiency viruses. *Virology* **233**, 193–198 (1997).
133. Ammosova, T. *et al.* Nuclear Protein Phosphatase-1 Regulates HIV-1 Transcription. *J. Biol. Chem.* **278**, 32189–32194 (2003).
134. Paruch, S. *et al.* CCR5 signaling through phospholipase D involves p44/42 MAP-kinases and promotes HIV-1 LTR-directed gene expression. *FASEB J. Off. Publ. Fed. Am. Soc. Exp. Biol.* **21**, 4038–46 (2008).
135. Tempaku, A. Inhibition of Human Immunodeficiency Virus Type-1 (HIV-1) Replication at a Reverse Transcription Step by Human Cell Factor(s). *Biol. Pharm. Bull.* **28**, 893–7 (2005).
136. Roy, S., Agy, M., Hovanessian, A. G., Sonenberg, N. & Katze, M. G. The integrity of the stem structure of human immunodeficiency virus type 1 Tat-responsive

- sequence of RNA is required for interaction with the interferon-induced 68,000-Mr protein kinase. *J. Virol.* **65**, 632–640 (1991).
137. Dorin, D. *et al.* The TAR RNA-binding Protein, TRBP, Stimulates the Expression of TAR-containing RNAs in Vitro and in Vivo Independently of Its Ability to Inhibit the dsRNA-dependent Kinase PKR. *J. Biol. Chem.* **278**, 4440–4448 (2003).
138. Sanghvi, V. R. & Steel, L. F. The Cellular TAR RNA Binding Protein, TRBP, Promotes HIV-1 Replication Primarily by Inhibiting the Activation of Double-Stranded RNA-Dependent Kinase PKR. *J. Virol.* **85**, 12614–12621 (2011).
139. Bennett, R. L., Blalock, W. L. & May, W. S. Serine 18 Phosphorylation of RAX, the PKR Activator, Is Required for PKR Activation and Consequent Translation Inhibition. *J. Biol. Chem.* **279**, 42687–42693 (2004).
140. Zhang, F. *et al.* Binding of Double-stranded RNA to Protein Kinase PKR Is Required for Dimerization and Promotes Critical Autophosphorylation Events in the Activation Loop. *J. Biol. Chem.* **276**, 24946–24958 (2001).
141. Hosmalin, A. & Lebon, P. Type I interferon production in HIV-infected patients. *J. Leukoc. Biol.* **80**, 984–993 (2006).
142. Herbeuval, J.-P. & Shearer, G. M. HIV-1 immunopathogenesis: How good interferon turns bad. *Clin. Immunol.* **123**, 121–128 (2007).
143. Lavender, K. J. *et al.* Interferon Alpha Subtype-Specific Suppression of HIV-1 Infection In Vivo. *J. Virol.* **90**, 6001–6013 (2016).
144. Adelson, M. E., Martinand-Mari, C., Iacono, K. T., Muto, N. F. & Suhadolnik, R. J. Inhibition of human immunodeficiency virus (HIV-1) replication in SupT1 cells

- transduced with an HIV-1 LTR-driven PKR cDNA construct. *Eur. J. Biochem.* **264**, 806–815 (1999).
145. Dimitrova, D. I. *et al.* Lentivirus-mediated transduction of PKR into CD34(+) hematopoietic stem cells inhibits HIV-1 replication in differentiated T cell progeny. *J. Interferon Cytokine Res. Off. J. Int. Soc. Interferon Cytokine Res.* **25**, 345–360 (2005).
146. Muto, N. F., Martinand-Mari, C., Adelson, M. E. & Suhadolnik, R. J. Inhibition of Replication of Reactivated Human Immunodeficiency Virus Type 1 (HIV-1) in Latently Infected U1 Cells Transduced with an HIV-1 Long Terminal Repeat-Driven PKR cDNA Construct. *J. Virol.* **73**, 9021–9028 (1999).
147. George, C. X., Gan, Z., Liu, Y. & Samuel, C. E. Adenosine deaminases acting on RNA, RNA editing, and interferon action., Adenosine Deaminases Acting on RNA, RNA Editing, and Interferon Action. *J. Interferon Cytokine Res. Off. J. Int. Soc. Interferon Cytokine Res. J. Interferon Cytokine Res.* **31, 31**, 99–117 (2011).
148. McCormack, S. J. & Samuel, C. E. Mechanism of interferon action: RNA-binding activity of full-length and R-domain forms of the RNA-dependent protein kinase PKR — Determination of KD values for VAI and TAR RNAs. *Virology* **206**, 511–519 (1995).
149. Nekhai, S. & Jeang, K.-T. Transcriptional and post-transcriptional regulation of HIV-1 gene expression: role of cellular factors for Tat and Rev. *Future Microbiol.* **1**, 417–426 (2006).
150. Peruzzi, F. *The multiple functions of HIV-1 Tat: proliferation versus apoptosis.* **11**, (2006).

151. Lai, M.-C. *et al.* Human DDX3 Interacts with the HIV-1 Tat Protein to Facilitate Viral mRNA Translation. *PLOS ONE* **8**, e68665 (2013).
152. Braddock, M., Powell, R., Blanchard, A. D., Kingsman, A. J. & Kingsman, S. M. *HIV-1 TAR RNA-binding proteins control TAT activation of translation in Xenopus oocytes*. **7**, (1993).
153. Cullen, B. *Trans-activation of human immunodeficiency virus occurs via a bimodal mechanism*. **46**, (1986).
154. SenGupta, D. N., Berkhout, B., Gatignol, A., Zhou, A. M. & Silverman, R. H. Direct evidence for translational regulation by leader RNA and Tat protein of human immunodeficiency virus type 1. *Proc. Natl. Acad. Sci.* **87**, 7492–7496 (1990).
155. Wang, Y. & Samuel, C. E. Adenosine Deaminase ADAR1 Increases Gene Expression at the Translational Level by Decreasing Protein Kinase PKR-Dependent eIF-2 $\alpha$  Phosphorylation. *J. Mol. Biol.* **393**, 777–787 (2009).
156. Li, Z., Wolff, K. C. & Samuel, C. E. RNA adenosine deaminase ADAR1 deficiency leads to increased activation of protein kinase PKR and reduced vesicular stomatitis virus growth following interferon treatment. *Virology* **396**, 316–322 (2010).
157. Toth, A. M., Li, Z., Cattaneo, R. & Samuel, C. E. RNA-specific adenosine deaminase ADAR1 suppresses measles virus-induced apoptosis and activation of protein kinase PKR. *J. Biol. Chem.* **284**, 29350–29356 (2009).
158. Ward, S. V. *et al.* RNA editing enzyme adenosine deaminase is a restriction factor for controlling measles virus replication that also is required for embryogenesis. *Proc. Natl. Acad. Sci.* **108**, 331–336 (2011).



159. X George, C. & E Samuel, C. *Host response to polyomavirus infection is modulated by RNA adenosine deaminase ADAR1 but not by ADAR2.* **85**, (2011).
160. Schoggins, J. W. *et al.* A diverse range of gene products are effectors of the type I interferon antiviral response. *Nature* **472**, 481–485 (2011).
161. Kok, K.-H. & Jin, D.-Y. Balance of power in host-virus arms races. *Cell Host Microbe* **14**, 5–6 (2013).
162. Siu, K.-L. *et al.* Middle East Respiratory Syndrome Coronavirus 4a Protein Is a Double-Stranded RNA-Binding Protein That Suppresses PACT-Induced Activation of RIG-I and MDA5 in the Innate Antiviral Response. *J. Virol.* **88**, 4866–4876 (2014).
163. Kew, C. *et al.* Suppression of PACT-Induced Type I Interferon Production by Herpes Simplex Virus 1 Us11 Protein. *J. Virol.* **87**, 13141–13149 (2013).
164. Peters, G. A., Khoo, D., Mohr, I. & Sen, G. C. Inhibition of PACT-Mediated Activation of PKR by the Herpes Simplex Virus Type 1 Us11 Protein. *J. Virol.* **76**, 11054–11064 (2002).
165. Luthra, P. *et al.* Mutual Antagonism between the Ebola Virus VP35 Protein and the RIG-I Activator PACT Determines Infection Outcome. *Cell Host Microbe* **14**, 74–84 (2013).
166. Tawaratsumida, K. *et al.* Quantitative Proteomic Analysis of the Influenza A Virus Nonstructural Proteins NS1 and NS2 during Natural Cell Infection Identifies PACT as an NS1 Target Protein and Antiviral Host Factor. *J. Virol.* **88**, 9038–9048 (2014).

167. Tseng, Y.-Y., Liao, G.-R., Sen, G. C., Lin, F.-Y. & Hsu, W.-L. Regulation of PACT-Mediated Protein Kinase Activation by the OV20.0 Protein of Orf Virus. *J. Virol.* **89**, 11619–11629 (2015).
168. García, M. A. *et al.* Impact of Protein Kinase PKR in Cell Biology: from Antiviral to Antiproliferative Action. *Microbiol. Mol. Biol. Rev.* **70**, 1032–1060 (2006).
169. Sadler, A. & Williams, B. R. G. *Structure and function of the protein kinase R.* *Curr Top Microbiol Immunol.* **316**, (2007).
170. Samuel, C. E. The eIF-2 alpha protein kinases, regulators of translation in eukaryotes from yeasts to humans. *J. Biol. Chem.* **268**, 7603–7606 (1993).
171. Gil, J., Alcamí, J. & Esteban, M. Induction of apoptosis by double-stranded-RNA-dependent protein kinase (PKR) involves the alpha subunit of eukaryotic translation initiation factor 2 and NF-kappaB. *Mol. Cell. Biol.* **19**, 4653–4663 (1999).
172. Garcia, M., Meurs, E. & Esteban, M. *The dsRNA protein kinase PKR: Virus and cell control.* **89**, (2007).
173. Feng, G. S., Chong, K., Kumar, A. & Williams, B. R. Identification of double-stranded RNA-binding domains in the interferon-induced double-stranded RNA-activated p68 kinase. *Proc. Natl. Acad. Sci.* **89**, 5447–5451 (1992).
174. Katze, M. G. *et al.* Functional expression and RNA binding analysis of the interferon-induced, double-stranded RNA-activated, 68,000-Mr protein kinase in a cell-free system. *Mol. Cell. Biol.* **11**, 5497–5505 (1991).

175. Patel, R. C. & Sen, G. C. Identification of the double-stranded RNA-binding domain of the human interferon-inducible protein kinase. *J. Biol. Chem.* **267**, 7671–7676 (1992).
176. Chang, K.-Y. & Ramos, A. The double-stranded RNA-binding motif, a versatile macromolecular docking platform. *FEBS J.* **272**, 2109–2117 (2005).
177. Patel, R. C., Stanton, P., McMillan, N. M., Williams, B. R. & Sen, G. C. The interferon-inducible double-stranded RNA-activated protein kinase self-associates in vitro and in vivo. *Proc. Natl. Acad. Sci.* **92**, 8283–8287 (1995).
178. Laraki, G. *et al.* Interactions between the double-stranded RNA-binding proteins TRBP and PACT define the Medipal domain that mediates protein-protein interactions. **5**, (2008).
179. Vaughn, L. S. *et al.* Altered Activation of Protein Kinase PKR and Enhanced Apoptosis in Dystonia Cells Carrying a Mutation in PKR Activator Protein PACT. *J. Biol. Chem.* **290**, 22543–22557 (2015).
180. Daher, A. *et al.* TRBP control of PACT-induced phosphorylation of PKR is reversed by stress. *Mol Cell Biol* **29**, (2009).
181. Paroo, Z., Ye, X., Chen, S. & Liu, Q. Phosphorylation of the Human MicroRNA-Generating Complex Mediates MAPK/Erk Signaling. *Cell* **139**, 112–122 (2009).
182. Patel, R. C. & Sen, G. C. Requirement of PKR dimerization mediated by specific hydrophobic residues for its activation by double-stranded RNA and its antigrowth effects in yeast., Requirement of PKR Dimerization Mediated by Specific

- Hydrophobic Residues for Its Activation by Double-Stranded RNA and Its Antigrowth Effects in Yeast. *Mol. Cell. Biol. Mol. Cell. Biol.* **18, 18**, 7009, 7009–7019 (1998).
183. Nagata, S., Nagase, H., Kawane, K., Mukae, N. & Fukuyama, H. Degradation of chromosomal DNA during apoptosis. *Cell Death Differ.* **10**, 108–116 (2003).
184. Tewari, M. *et al.* Yama/CPP32 $\beta$ , a mammalian homolog of CED-3, is a CrmA-inhibitable protease that cleaves the death substrate poly(ADP-ribose) polymerase. *Cell* **81**, 801–809 (1995).
185. Peti, W. & Page, R. Molecular basis of MAP kinase regulation. *Protein Sci.* **22**, 1698–1710 (2013).
186. A McCubrey, J., M Lahair, M. & A Franklin, R. *McCubrey JA, Lahair MM, Franklin RA* Reactive oxygen species-induced activation of the MAP kinase signaling pathways. *Antioxid Redox Signal* **8**: 1775-1789. **8**, (2006).
187. Balachandran, S. *et al.* Activation of the dsRNA-dependent protein kinase, PKR, induces apoptosis through FADD-mediated death signaling. *EMBO J.* **17**, 6888–6902 (1998).
188. Srivastava, S. P., Kumar, K. U. & Kaufman, R. J. Phosphorylation of Eukaryotic Translation Initiation Factor 2 Mediates Apoptosis in Response to Activation of the Double-stranded RNA-dependent Protein Kinase. *J. Biol. Chem.* **273**, 2416–2423 (1998).
189. Takizawa, T., Tatematsu, C. & Nakanishi, Y. Double-stranded RNA-activated protein kinase (PKR) fused to green fluorescent protein induces apoptosis of human

- embryonic kidney cells: possible role in the Fas signaling pathway. *J. Biochem. (Tokyo)* **125**, 391–398 (1999).
190. G Smyth, P. & Berman, S. *Markers of apoptosis: Methods for elucidating the mechanism of apoptotic cell death from the nervous system.* **32**, (2002).
191. Elmore, S. Apoptosis: a review of programmed cell death. *Toxicol. Pathol.* **35**, 495–516 (2007).
192. Chong, K. L. *et al.* Human p68 kinase exhibits growth suppression in yeast and homology to the translational regulator GCN2. *EMBO J.* **11**, 1553–1562 (1992).
193. Kazemi, S. *et al.* Control of  $\alpha$  Subunit of Eukaryotic Translation Initiation Factor 2 (eIF2 $\alpha$ ) Phosphorylation by the Human Papillomavirus Type 18 E6 Oncoprotein: Implications for eIF2 $\alpha$ -Dependent Gene Expression and Cell Death. *Mol. Cell. Biol.* **24**, 3415–3429 (2004).
194. Rojas, M., Vasconcelos, G. & Dever, T. *An eIF2 $\alpha$ -binding motif in protein phosphatase 1 subunit GADD34 and its viral orthologs is required to promote dephosphorylation of eIF2 $\alpha$ .* **112**, (2015).
195. Singh, M., Castillo, D., Patel, C. V. & Patel, R. C. Stress-Induced Phosphorylation of PACT Reduces Its Interaction with TRBP and Leads to PKR Activation. *Biochemistry (Mosc.)* **50**, 4550–4560 (2011).
196. Fierro-Monti, I. & Mathews, M. B. Proteins binding to duplexed RNA: one motif, multiple functions. *Trends Biochem. Sci.* **25**, 241–246 (2000).
197. R Saunders, L. & Barber, G. *The dsRNA binding protein family: critical roles, diverse cellular functions.* **17**, (2003).

198. N Barber, G. *The NFAR's (Nuclear Factors Associated with dsRNA): Evolutionarily conserved members of the dsRNA binding protein family.* **6**, (2009).
199. Nakamura, T., Arduini, A., Baccaro, B., Furuhashi, M. & S Hotamisligil, G. *Small-Molecule Inhibitors of PKR Improve Glucose Homeostasis in Obese Diabetic Mice.* **63**, (2013).
200. McCormack, S., Thomis, D. & Samuel, C. Mechanism of interferon action: identification of a RNA binding domain within the N-terminal region of the human RNA-dependent P1/eIF-2 alpha protein kinase. *Virology* **188**, 47–56 (1992).
201. Laraki, G. *et al.* Interactions between the double-stranded RNA-binding proteins TRBP and PACT define the Medial domain that mediates protein-protein interactions. *RNA Biol* **5**, (2008).
202. Patel, R. C., Stanton, P. & Sen, G. C. Specific Mutations Near the Amino Terminus of Double-stranded RNA-dependent Protein Kinase (PKR) Differentially Affect Its Double-stranded RNA Binding and Dimerization Properties. *J. Biol. Chem.* **271**, 25657–25663 (1996).
203. Tian, B. & Mathews, M. B. Functional Characterization of and Cooperation between the Double-stranded RNA-binding Motifs of the Protein Kinase PKR. *J. Biol. Chem.* **276**, 9936–9944 (2001).
204. Heinicke, L. *et al.* *RNA Dimerization Promotes PKR Dimerization and Activation.* **390**, (2009).
205. A Lemaire, P., Anderson, E., Lary, J. & Cole, J. *Mechanism of PKR activation by dsRNA.* **381**, (2008).


206. Robertson, H. D. & Mathews, M. B. The regulation of the protein kinase PKR by RNA. *Biochimie* **78**, 909–914 (1996).
207. Vattem, K. M., Staschke, K. A., Zhu, S. & Wek, R. C. Inhibitory sequences in the N-terminus of the double-stranded-RNA-dependent protein kinase, PKR, are important for regulating phosphorylation of eukaryotic initiation factor 2 $\alpha$  (eIF2 $\alpha$ ). *Eur. J. Biochem.* **268**, 1143–1153 (2001).
208. Taylor, S. S., Haste, N. M. & Ghosh, G. PKR and eIF2 $\alpha$ : Integration of Kinase Dimerization, Activation, and Substrate Docking. *Cell* **122**, 823–825 (2005).
209. Lemaire, P. A., Lary, J. & Cole, J. L. Mechanism of PKR Activation: Dimerization and Kinase Activation in the Absence of Double-stranded RNA. *J. Mol. Biol.* **345**, 81–90 (2005).
210. Anderson, E. *et al.* Analysis of Monomeric and Dimeric Phosphorylated Forms of Protein Kinase R. *Biochemistry (Mosc.)* **49**, 1217–1225 (2010).
211. Roy, S., Delling, U., Chen, C.H., Rosen C.A. & Sonenberg, N. A bulge structure in HIV-1 TAR RNA is required for Tat binding and Tat-mediated trans-activation. *Genes Dev.* **4**, 1365 - 1373 (1990).
212. Daly, T.J., Cook, K.S., Gray, G.S., Maione, T.E., & Rusche J.R. Specific binding of HIV-1 recombinant Rev protein to the Rev-responsive element *in vitro*. *Nature* **342**, 816 - 819 (1989).
213. Olsen, H.S., Nelbock, P., Cochrane, A.W., & Rosen, C.A. Secondary structure is the major determinant for interaction of HIV rev protein with RNA *Science* **247**, 845–848 (1990).

214. Zapp, M.L. & Green, M.R. Sequence-specific RNA binding by the HIV-1 Rev protein. *Nature* **342**, 714 - 716 (1989).
215. Gabel, F. *et al.* Dynamic flexibility of double-stranded RNA activated PKR in solution. *J. Mol. Biol.* **359**, 610–623 (2006).



## APPENDIX A

### REPRINT PERMISSION FROM THE BIOCHEMICAL JOURNAL (PORTLAND PRESS)

[Search All Publications](#)

[Home](#) [For Authors](#) [For Librarians](#) [For Readers](#) [Editorial News](#) [Media Centre](#) [Our Journals](#)

## Rights and Permissions

- [Authors](#)
- [STM Publishers](#)
- [Non-commercial requests](#)
- [Commercial requests](#)
- [Archiving policy](#)
- [Copyright policy](#)
- [Data policy](#)
- [Sharing and public posting of articles](#)

## Authors

Authors do not usually need to contact Portland Press to request permission to reuse their own material, as long as the original work is properly credited. It is usual to provide the citation of (and where relevant a hyperlink to) the original publication:

"This extract/figure/table was originally published in [insert hyperlinked citation information, including Author(s), Journal Name, Year]."

As long as the original article, or portion of the article, is properly cited, and a link to the article is included, Authors retain the following non-exclusive rights:


1. To reproduce their article in whole or in part in any printed work (book or thesis) of which they are the Author
2. To reproduce their article in whole or in part at the Author's current academic institution for teaching purposes, including course packs
3. To re-use figures, tables, illustrations and excerpts of fewer than 300 words from their article in non-commercial works and/or works published by STM publishers where they are the author/creator
4. To include their article in whole or in part in their own dissertation or thesis in print or electronic format provided that the full-text article is not then shared in an open repository unless it is published via the [Gold Open Access route](#).
5. Authors are permitted to post a copy of their [Accepted Manuscript or AM\\*](#) to their Institutional Repository 12 months after final publication, provided this posting is labelled as a pre-publication manuscript, and provided the posting is hyperlinked (e.g. through the DOI) to the final published article, i.e. the [Version of Record or VoR\\*\\*](#) on the journal website.

Authors of Open Access (OA) articles may post the Version of Record (VoR) to their institutional repository. Portland Press will deposit the VoR in PubMed Central on behalf of the author in the case of Gold OA papers.

## APPENDIX B

# PROOF OF OPEN ACCESS PUBLICATION OF 'ADAR1 AND PACT CONTRIBUTE TO EFFICIENT TRANSLATION OF TRANSCRIPTS CONTAINING HIV-1 TRANS-ACTIVATING RESPONSE (TAR) ELEMENT'


Biochemical Journal (2017) 474 1241–1257  
DOI: 10.1042/BJCJ20160964

 PORTLAND PRESS

Research Article

### ADAR1 and PACT contribute to efficient translation of transcripts containing HIV-1 trans-activating response (TAR) element

Evelyn Chukwurah, Indhira Handy and Rekha C. Patel  
Department of Biological Sciences, University of South Carolina, Columbia, SC 29208, U.S.A.  
Correspondence: Rekha C. Patel (patelr@biol.sc.edu)

 OPEN ACCESS

Human immunodeficiency virus type 1 (HIV-1) has evolved various measures to counter the host cell's innate antiviral response during the course of infection. Interferon (IFN)-stimulated gene products are produced following HIV-1 infection to limit viral replication, but viral proteins and RNAs counteract their effect. One such mechanism is specifically directed against the IFN-induced Protein Kinase PKR, which is centrally important to the cellular antiviral response. In the presence of viral RNAs, PKR is activated and phosphorylates the translation initiation factor eIF2 $\alpha$ . This shuts down the synthesis of both host and viral proteins, allowing the cell to mount an effective antiviral response. PACT (protein activator of PKR) is a cellular protein activator of PKR, primarily functioning to activate PKR in response to cellular stress. Recent studies have indicated that during HIV-1 infection, PACT's normal cellular function is compromised and that PACT is unable to activate PKR. Using various reporter systems and *in vitro* kinase assays, we establish in this report that interactions between PACT, ADAR1 and HIV-1-encoded Tat protein diminish the activation of PKR in response to HIV-1 infection. Our results highlight an important pathway by which HIV-1 transcripts subvert the host cell's antiviral activities to enhance their translation.

#### Introduction

Cells infected with a virus employ a variety of mechanisms to counteract the negative impact of viral replication and promote cell survival [1]. The innate immune response to a viral infection is mediated by external and internal sensor molecules, which recognize the viral components as 'non-self' and trigger mechanisms leading to the production of interferons (IFNs) [2]. IFNs are secreted antiviral cytokines that bind in a paracrine and autocrine manner to cellular receptors and trigger signaling cascades culminating in the expression of IFN-stimulated genes (ISGs) [3]. Most ISGs have antiviral functions, although some ISGs with both antiviral and proviral functions have been previously described [4–6]. Viral and cellular factors regulate ISGs to promote or limit viral replication, respectively, and this regulatory interplay between the virus and the host cell is crucial in determining the outcome of a viral infection. Retroviruses such as the human immunodeficiency virus type 1 (HIV-1) produce viral factors that interact with various cellular proteins, including ISGs. As a result, the virus subverts their antiviral properties or co-opts them from their regular cellular activities to facilitate efficient viral replication within the infected host cell [7,8].

One of the ISG products is PKR (protein kinase, RNA-activated), a protein kinase that plays a central role in regulating the outcome of a viral infection [9–11]. In virally infected cells, PKR is activated by binding to dsRNA (double-stranded RNA), a product of several viral infections, including HIV-1 [12,13]. The interaction between PKR and dsRNA induces a conformational change that is essential for PKR's catalytic activation [14]. PKR then phosphorylates the translation initiation factor eIF2 $\alpha$  on serine 51, resulting in a decline of general protein synthesis, and consequent cessation of viral protein synthesis

Received: 26 October 2016  
Revised: 30 January 2017  
Accepted: 6 February 2017  
Accepted Manuscript online:  
6 February 2017  
Version of Record published:  
23 March 2017

© 2017 The Author(s). This is an open access article published by Portland Press Limited on behalf of the Biochemical Society and distributed under the Creative Commons Attribution License 4.0 (CC BY). 1241